TGF-β1-INDUCED CALCIFICATION OF VALVULAR MYOFIBROBLASTS: MECHANISMS AND THERAPEUTIC STRATEGIES

By

Joshua Daniel Hutcheson

Dissertation

Submitted to the Faculty of the

Graduate School of Vanderbilt University

in partial fulfillment of the requirements

for the degree of

DOCTOR OF PHILOSOPHY

in

Biomedical Engineering

December, 2012

Nashville, Tennessee

Approved:

W. David Merryman, PhD

Craig L. Duvall, PhD

Joey V. Barnett, PhD

Mark D. Does, PhD

Vincent Setola, PhD

TABLE OF CONTENTS

LIST OF TABLES

LIST OF FIGURES

Chapter 1

Introduction and Motivation

Aortic valve disease (AVD) is the third leading cause of cardiovascular disease and is especially prevalent among the elderly [1]. Studies have shown that AVD affects over 25% of people over 65 years of age, and currently, the only effective long-term treatment for advanced AVD is replacement surgery, a high risk procedure for elderly patients. For this reason, a non-invasive therapeutic to stop the development of AVD would greatly benefit those most at risk for developing severe AVD. Unfortunately, epidemiological studies have shown that promising drug candidates have not proven successful at slowing or reversing the end stages of AVD that necessitate valve replacement [2]. The lack of a therapeutic treatment limits the clinical options available to patients, and this often results in physicians opting to delay surgical intervention until aortic valve (AV) replacement is absolutely necessary leading to diminished AV function in the meantime. Thus, a novel therapy to prevent or slow the progression of AVD at the *earliest* possible stages may greatly increase patient quality of life.

The development of a suitable therapeutic for AVD depends on the ability to target the root cause of the disease, which ultimately manifests itself as a biomechanical problem where thickening and stiffening of the AV leaflets

diminishes its ability to maintain directionality in blood flow from the left ventricle to the aorta [3]. Thickened fibrotic, or sclerotic, AV leaflets may lose their ability to fully open and close, leading to reduced ejection of the blood out of the ventricle during when the heart pumps during systole and retrograde blood flow back into the ventricle when the heart rests during diastole. Progression of AVD is characterized by very stiff stenotic AV leaflets with bone-like calcific nodules that develop within the leaflets [4]. In order to develop a strategy to prevent AVD, a more thorough understanding of the cellular signaling and subsequent tissue level changes involved in the progression of AVD is needed to elucidate relevant therapeutic targets.

At the cellular level, AVD is believed to be caused by activation of AV interstitial cells (AVICs) to a myofibroblast phenotype [5]. This phenotype is characterized by increased expression of contractile, smooth muscle-like proteins such as smooth muscle α-actin (αSMA) and SM22α, and increased expression of these markers has been observed in excised AVD leaflets [6-8]. Once activated, AVICs increase extracellular matrix (ECM) deposition, directly leading to the decreased biomechanical compliance of the leaflets observed in AVD. The pro-fibrotic cytokine transforming growth factor-β1 (TGF-β1) has been the most extensively studied initiator of AVIC myofibroblast activation *in vitro*, and increased levels of TGF-β1 have been observed in AV leaflets from patients with AVD [9]. Additionally, mechanical strain has been observed to work in concert with TGF-β1 to induce fibrotic collagen accumulation [10] and calcific nodule formation [11] in *ex vivo* models of AVD. Unfortunately, due to the systemic

ubiquity of its signaling, TGF-β1 is not an ideal therapeutic target for the treatment of AVD. Therefore, we are interested in identifying other, more specific targets that interact with TGF-β1 signaling.

In addition to direct AV changes due to TGF-β1, serotonin (5-HT) and certain serotonergic receptor agonists have been shown to lead to AVD upstream of TGF-β1 through signaling at the serotonergic receptor 5-HT_{2B} [12]. Interestingly, 5-HT_{2B} has recently been shown to work in conjunction with angiotensin II (Ang II) type 1 receptor (AT_1) to mediate changes in cardiac fibroblasts that lead to ventricular hypertrophy [13]—pathology with ECM accumulation similar to AVD. Antagonists to these receptors also demonstrate anti-fibrotic effects in a variety of tissues [14-16]. Further, as evidence of the therapeutic relevance of these receptors, AT_1 receptor antagonists or blockers (ARBs) have been successfully utilized in a clinical setting to inhibit excessive TGF-β1 signaling observed in Marfan's syndrome [17], and 5-HT_{2B} antagonists have been shown to mitigate fibrotic changes that lead to pulmonary hypertension in a mouse model [15]. We believe that 5-HT_{2B} and/or AT_1 can be targeted to effectively modulate AVIC myofibroblast activation and may provide early time point druggable targets to prevent AVD progression.

The overall goal of the research presented in this dissertation is to understand how both biochemical and mechanical factors alter the biological state of the AVIC with an emphasis on elucidating the molecular mechanisms that lead to pathological differentiation of AVICs that is observed in AVD. We are also interested in how these mechanisms may be targeted therapeutically to treat

AVD. To do this, we must isolate the important signaling modalities and outcomes that lead to AVIC activation and understand the interactions between the various signaling pathways. This goal will be accomplished through the following three specific aims:

1. Determine the role of TGF-β1-induced changes in AVIC phenotype that lead to calcific nodule morphogenesis in a physiologically relevant, dynamic culture system.
2. Elucidate the mechanism associated with 5-HT_{2B} antagonist inhibition of TGF-β1-induced activation of AVICs.
3. Assess the ability of AT_1, a receptor similar to 5-HT_{2B}, in modulating TGF-β1-mediated changes in AVIC phenotype.

To begin, a detailed background on heart valve physiology and pathology will be given, and a primer on the role of serotonergic signaling in heart valves will be presented. Each specific aim will then be considered separately with each section offering a focused introduction and set of research methods that were used to complete the study. Finally, a discussion of the complete dissertation will be presented to highlight the potential impact of the results. Also, to aid the reader a table of reference has been provided to define uncommon abbreviations and terms, protein functions, antagonist/inhibitor descriptions, and metrics that will be used throughout the dissertation to assess AVIC signaling and differentiation (Table 1.1).

Table 1.1. Vocabulary and Assay Metrics

Category	Term or Abbreviation	Definition
General Terms	AV	Aortic valve - directs blood flow from left ventricle to aorta
	AVD	Aortic valve disease
	AVIC	Aortic valve interstitial cell - specialized fibroblast-like cell that maintains aortic valve architecture
	AVEC	Aortic valve endothelial cell - cells that line the surface of the aortic valve
	CAVD	Calcific aortic valve disease - late stage of aortic valve disease characterized by bone-like calcific nodules
	HVD	Heart valve disease
	Myofibroblast	Contractile fibroblast phenotype characterized by expression of smooth-muscle proteins and implicated in aortic valve disease
Marker of AVIC Phenotype	αSMA	Smooth muscle α-actin - a marker of myofibroblast differentiation
	Alizarin Red	Dye that stains calcium - used to identify calcific nodules
	Calcific nodule	Bone-like calcium phosphate structures formed by aortic valve interstitial cells
	SM22α	Common marker of smooth muscle cells and myofibroblasts
Cellular Signaling Proteins and Terms	5-HT_{2B}	Serotonin 2B receptor - G protein-coupled receptor implicated in drug-induced valve disease
	Alk5, TβRI	Activin-like kinase 5, TGF-β1 type 1 receptor - a serine-threonine kinase receptor
	AT_1	Angiotensin type 1 receptor - G protein-coupled receptor with known cardiovascular function
	cadherin-11	Intercellular adhesion protein that is expressed in myofibroblasts
	Canonical	Term used in cellular signaling to identify a common or traditional signaling pathway
	Cas, pCas	Protein that is a commonly phosphorylated by Src (pCas indicates phosphorylated Cas)
	Erk1/2, pErk1/2	Common cell signaling protein in the MAP kinase family (pErk1/2 indicates phosphorylated Erk1/2)
	GPCR	G protein-coupled receptor - a specialized cell surface receptor with 7 membrane-spanning regions
	MEK1/2	Kinase responsible for phosphorylating Erk1/2
	Non-canonical	Term used in cellular signaling to identify an uncommon or non-traditional signaling pathway
	p38, pp38	Common cell signaling protein in the MAP kinase family (pp38 indicates phosphorylated p38)
	PAI-1	Plasminogen activator inhibitor-1 - a common transcriptional target of the canonical TGF-β1 Smad signaling pathway
	Smad2/3, pSmad3	Cell signaling proteins and transcription factors that make up the canonical TGF-β1 signaling pathway (pSmad3 indicates phosphorylated Smad3
	Src, pSrc	Tyrosine kinase protein involved in many cellular signaling pathways (pSrc indicates phosphorylated Src)
	TGF-β1	Transforming growth factor-β1 - growth factor involved in many cellular signaling processes but implicated in fibrosis in a variety of tissues
	TβRII	TGF-β1 type 2 receptor - receptor to which TGF-β1 binds
Inhibitors and Antagonists	SB204741	Selective antagonist of 5-HT_{2B}
	SB228357	Antagonist of 5-HT_{2B}
	SIS3	Specific inhibitor of Smad3 signaling
	p38i, SB203580	Inhibitor of p38 phosphorylation
	U0126	Inhibitor of MEK1/2 - Inhibits Erk1/2 phosphorylation
	ZD7155	Selective antagonist of AT_1

Chapter 2

Background – Heart Valve Physiology and Pathology

Text for Chapter 2 taken from:

> Hutcheson, J.D., M.P. Nilo, and W.D. Merryman, *Mechanobiology of Heart Valves*, in Mechanobiology Handbook, J. Nagatomi, Editor. 2011, CRC Press: Boca Raton, FL.
>
> Hutcheson, J.D., et al., *Intracellular Ca(2+) accumulation is strain-dependent and correlates with apoptosis in aortic valve fibroblasts.* J Biomech, 2012. 45(5): p. 888-94.

2.1. Mechanobiology and Biomechanics of Heart Valves

Heart Valve Function

The heart acts as a pump to ensure that blood is distributed appropriately throughout the body. This is accomplished through a coordinated contraction of the heart muscles causing the blood to be pumped through four cardiac chambers. During the beginning of each cardiac cycle—a period known as diastole—deoxygenated blood from the body fills the right atrium and newly oxygenated blood from the lungs fills the left atrium. The flow of blood then proceeds through the tricuspid valve from the right atrium into the right ventricle or through the mitral valve from the left atrium into the left ventricle. Ventricular contraction—or systole—is the main impetus for moving blood out of the heart.

The contraction of the ventricles forces blood from the right ventricle into the pulmonary artery to be delivered to the lungs for oxygenation and delivery of blood to the systemic circulation from the left ventricle through the aortic valve. The cycle completes when blood returns to the heart during the next diastolic period. Within the heart, the four valves maintain unidirectional flow of blood (Fig. 2.1) by the coordinated action of leaflets that open and close during each cardiac cycle. In fact, the leaflets within each valve will open and close over 3 billion times in an average lifetime [18]. Therefore, the leaflets must be able to withstand dynamic, cyclic stresses while maintaining the structural integrity that is crucial to their function. The interplay between the forces caused by the fluid mechanics of blood flow and the biomechanical properties of the valve leaflets make the tissues that form the heart valve leaflets interesting subjects in mechanobiology. For introductory purposes, we will consider the two separate types of heart valves—the atrioventricular valves and the semilunar valves—and discuss the corresponding characteristics of each class.

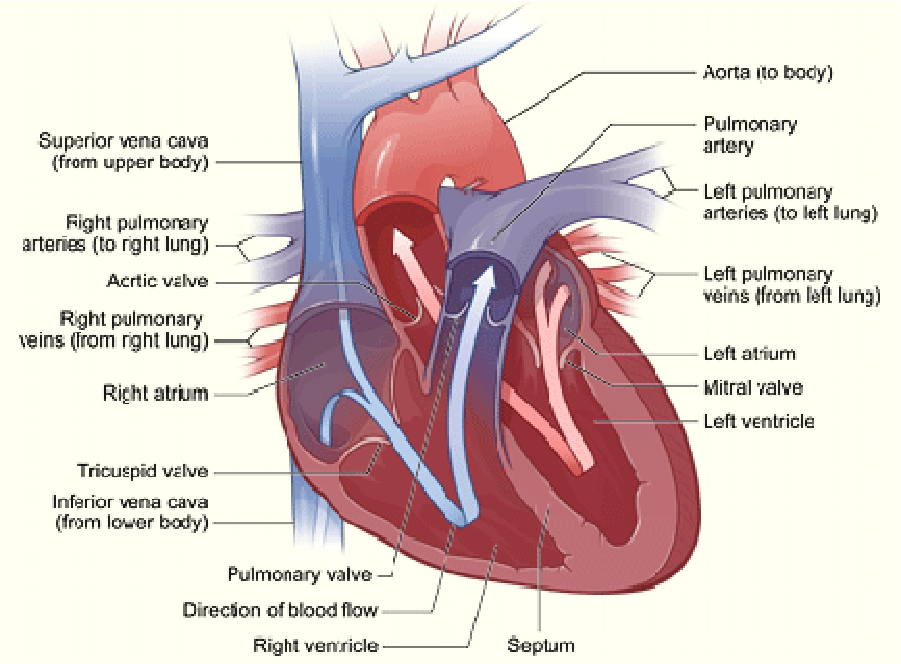

Fig 2.1. The general anatomy of the heart. All of the major components of the heart are depicted including the locations of the four heart valves and the direction of blood flow (reprinted with permissions from the National Heart, Lung, and Blood Institute, a part of the National Institutes of Health and the U.S. Department of Health and Human Services).

The atrioventricular valves (i.e., the tricuspid valve and mitral valve on the right and left side of the heart, respectively) remain open during ventricular diastole to allow blood to move from the atria into the ventricles. As the ventricles begin to contract during systole, the valve leaflets snap shut to prevent blood from returning into the atria for the duration of systolic contraction. This continual cycling between opening and closing of the atrioventricular valves is controlled by both hemodynamic pressure and chordae tendineae that tether the valve leaflets to papillary muscles within the ventricle walls. The structure of the two atrioventricular valves is similar, with the main difference being the number of leaflets. The mitral valve has two leaflets (Fig. 2.2); whereas, the tricuspid valve has three leaflets. During diastole, the pressure in the atria is higher than that in

the ventricles due to the influx of blood into the heart. This pressure difference causes the leaflets of the atrioventricular valves to extend outward into the ventricles; however, as the ventricles contract, the pressure gradient is reversed, causing the atrioventricular leaflets to be pushed back toward the atria. Tension from the chordae tendineae ensure that the leaflets come together to make a seal and do not prolapse—or protrude—back into the atria [19]. The interplay between the various components of these valves is more complicated when compared to the relatively simple semilunar valves directing blood flow out of the ventricles.

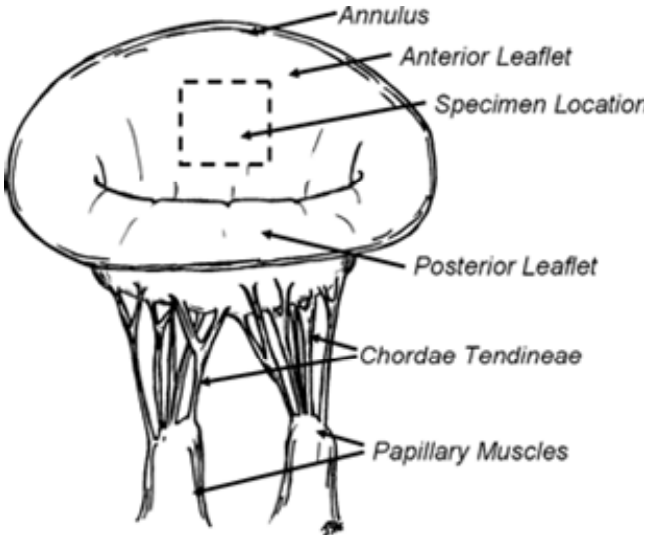

Fig 2.2. The anatomy of the mitral valve. All major portions of the tissue are shown. The dotted square indicates a portion of the anterior leaflet utilized in many of the studies discussed (reprinted with permissions from [20]).

The valves that direct blood flow from the heart to the body and lungs are known as semilunar valves due to the crescent shape of the leaflets (Fig. 2.3A, a view of the aortic valve from the perspective of the aorta). The pulmonary valve is situated between the right ventricle and pulmonary artery, and the aortic valve

directs flow from the left ventricle to the aorta. These two valves differ from the atrioventricular valves in that they lack chordae tendineae and rely solely on the hemodynamic forces of blood flow to direct opening and closing of their leaflets. Ventricular contraction during systole forces the leaflets of the semilunar valves open. During diastole, the leaflets coapt to prevent blood from flowing back into the ventricles. As we will discuss in much greater detail, the pressure of the blood on the leaflets of the closed semilunar valves during diastole introduces a high amount of stress on the tissues. This stress can lead to mechano-dependent signal transduction of pathologic responses at the cellular level within the leaflets that can greatly alter valve function.

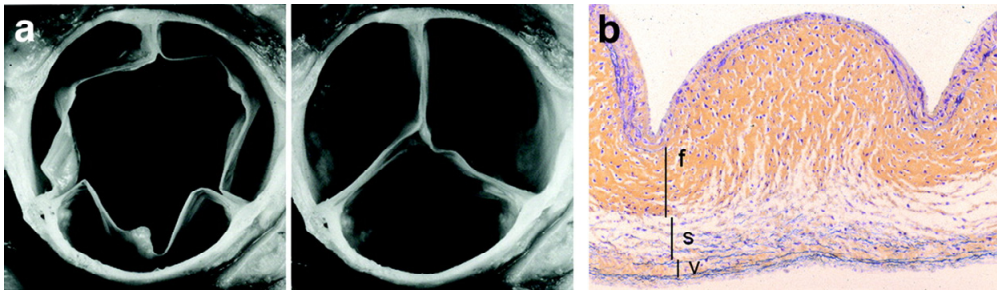

Fig 2.3. The anatomy of the aortic valve. (a) The aortic valve leaflets are pushed into the aorta during ventricular systole and coapt to form a seal during diastole. (b) A histological image of the layers of the aorta is shown. The ventricularis (v) is composed of elastin fibers. The spongiosa (s) provides a lubricating border between the ventricularis and the collagen-containing fibrosa (f) (reprinted with permissions from [21]).

The diminished ability of the valve to regulate blood flow can result in significantly altered cardiac function. Furthermore, heart valve disease (HVD) is one of the leading causes of cardiovascular disease, especially among the elderly. Studies have shown that HVD increases in prevalence from 0.7% in people between 18 and 44 years of age to over 13% of people over 75 years of

age. Moreover, early symptoms of aortic valve disease have been detected in 29% of patients over 65 years of age. These symptoms are associated with a 50% increase in cardiovascular related morbidity and a similar increase in the risk of myocardial infarction [22]. Currently, the only effective long-term treatment for advanced HVD is replacement surgery, an invasive, high risk procedure for elderly patients that requires substantial recovery time; therefore, understanding of HVD etiology is an important step in developing new, less invasive therapeutics or preventative strategies.

Global View of Heart Valve Mechanobiology

The importance of physiologic forces from normal cardiac function on cellular function has been extensively studied in recent years. In fact, the interrelationship between the mechanics and biological responses within the heart valves is evident from observing the differences between the biomechanical properties of the cells from the corresponding valves on each side of the heart. The pressures involved with systemic body circulation on the left side of the heart are dramatically higher than those of the pulmonary circulation on the right side of the heart; therefore, these pressure differences are transferred to the cells within the leaflets and produce dissimilarities that can be observed within cellular populations between the valves. The difference in mechanobiological response between the two sides was recently quantified by correlating transvalvular pressures (TVP) to heart valve interstitial cell (VIC)

stiffness [23]. VICs are the main cellular component of the valve leaflets and are thought to play a crucial role in maintaining the mechanical integrity of the valve tissues by regulating extracellular matrix biosynthesis [7, 24]. Isolated VICs from each of the four heart valves were analyzed for cellular stiffness using micropipette aspiration [25-26]. VICs isolated from the right-side valves—i.e., the tricuspid (TVIC) and pulmonary (PVIC) valves—displayed a significantly lower effective stiffness than the mitral (MVIC) and aortic (AVIC) valve cells isolated from the left-side valves (Fig. 2.4). Stiffness data correlated well with the level of collagen synthesis by the VICs, indicating that the AVICs and MVICs are responsible for producing more robust ECM proteins, which yields the higher overall stiffness seen in the left-side valves.

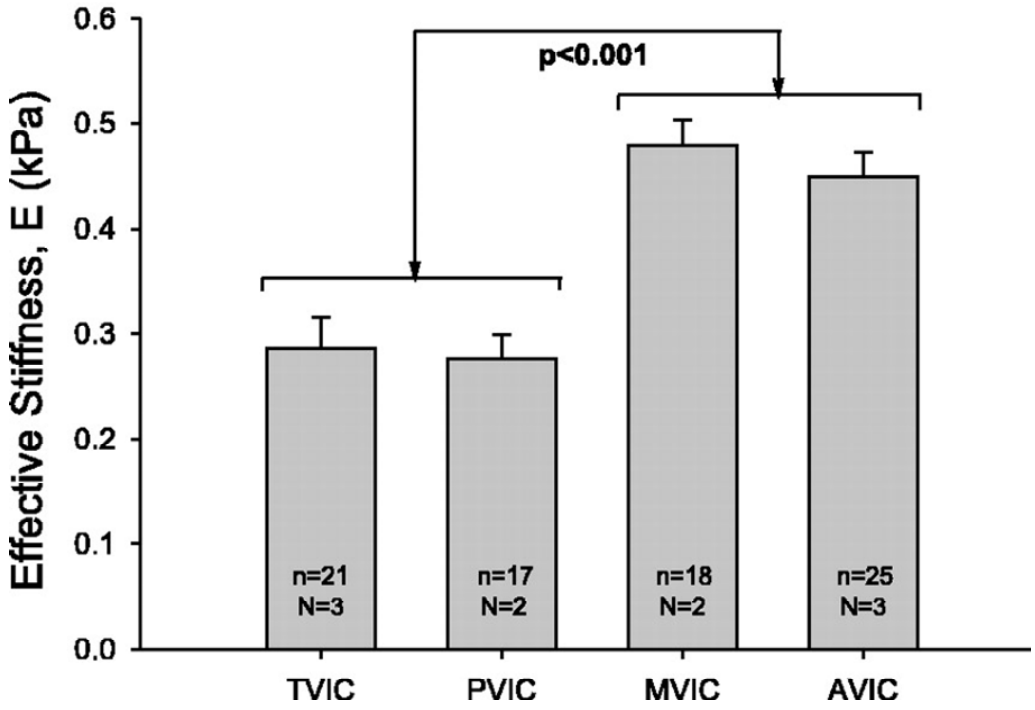

Fig 2.4. Comparison of interstitial cells from each side of the heart. The cells from the valves on the left side of the heart (MVICs and AVICs) exhibit a significantly higher stiffness than the cells from the valves on the right side of the heart (TVICs and PVICs) (reprinted with permissions from [23]).

All of the heart valves rely on their structural properties for correct function. This structural integrity is dictated by the material properties of the tissues comprising the valves. As mentioned above, the constant changes in TVP (due to contraction and relaxation of the cardiac chambers) place different stresses (i.e. force/area) across the heart and on different parts of the valves over the course of the cardiac cycle. The elevated pressures on the left-side of the heart lead to an increased importance on cellular mechanotransduction and also a heightened prevalence in disease for the aortic and mitral valves [27]. Therefore, for continued discussion, we will discuss the left-side valves only.

However, the reader should note that many of the valve properties mentioned here are also applicable to the right-side heart valves. In the following sections, we will review current understanding of how valves respond to demanding physical forces present in the heart and how improper cellular response results in altered tissue architecture, which leads to valve pathologies that are of clinical relevance.

2.2. Physiology and Pathology of the Aortic Valve

Biomechanics and Structure of Aortic Valve

As shown in Fig. 2.1, the AV is situated between the left ventricle and the aorta and functions to prevent regurgitation of blood into the left ventricle that has been pumped to the aorta for distribution throughout the body. The AV accomplishes this task using three adjacent leaflets that open during systole (Fig. 2.3A, left panel) and coapt (Fig. 2.3A, right panel) during diastole. Unlike the mitral valve (MV), which has papillary muscles and tendineae to help control movement of the leaflets, the AV relies solely on hemodynamic forces for opening and closing. Therefore, the function of the AV is heavily reliant on the mechanical properties of the leaflets [28].

Similar to the MV, each AV leaflet contains a layered ECM structure that is composed almost exclusively of collagen, elastin, and glycosaminoglycans (GAGs) [29]. These ECM components are organized into three distinct layers:

the ventricularis; the spongiosa; and the fibrosa (Fig. 2.3B). In the AV, the elastin layer is located on the ventricular side of the leaflets, and the collagen-rich fibrosa is on the aortic side. The spongiosa is situated between these two layers and is composed mainly of GAGs that help direct collagen orientation during opening and closing of the valve [30]. This structural alignment of the ECM within the leaflets allows them to withstand repeated cardiac strains caused by pressure of blood backflow during diastole.

To completely coapt during diastole and withstand the force of backflow, the leaflet must expand extensively in the radial direction, and have an almost immediate stress response at low strain levels in the circumferential direction [31]. The collagen fibers, which provide the greatest amount of structural support, align in the circumferential direction and this amounts to a cyclic, repeated strain of 10-20% in the circumferential direction with each diastolic cycle [28]. As with the MV during systole, the collagen in the AV quickly straightens during diastole, conferring structural rigidity to the leaflets. Leaflet deformation and straightening of the collagen causes the elastin of the ventricularis layer to stretch such that the three leaflets meet to seal the valve [32-33]. Once the diastolic pressure reaches 4 mm Hg, the collagen fibers completely align, and the valve closes completely at 20 mm Hg. Few leaflet changes are observed from 4 mm Hg to the peak diastolic pressure of 80 mm Hg [30]. During systolic opening of the valve, the TVP difference drops to zero causing the elongated elastin to recoil, which results in crimping of the collagen fibers and unloading of the AV leaflets.

Cellular Mechanobiology of Aortic Valves

In other parts of the vascular system, endothelial cells have been observed to play a crucial role in the transduction of mechanical signals such as changes in shear stress [34]. Because these cells are the first to experience any changes in outside forces that affect valve dynamics, they have received growing attention in their potential roles in regulating valve homeostasis. VECs are phenotypically distinct from other endothelia cells in the vasculature [35]. For instance, when subjected to the shear stresses of fluid flow, valve endothelial cells (VECs) align perpendicular to the flow [35]; whereas, endothelial cells from the aorta align parallel to the flow [34, 36]. This indicates that the VECs may play a distinct role in regulating the biomechanical properties of the valve through specially evolved mechanisms. Furthermore, AVECs have been observed to exhibit genotypic heterogeneity along the surface of each leaflet. Simmons et al. found that 584 genes were differentially expressed between AVECs from the aortic side and the ventricular side [37]. These genotypic differences may be important in regulating the differing biomechanical properties on each side of the valve, i.e., the collagen of the fibrosa and the elastin of the ventricularis, or conversely, the gene expression of these cells may be influenced by the differing shear stresses seen on each side of the leaflet. We will further discuss the implications of the AVEC heterogeneity in the section on AV pathologies.

Some have suggested that AVECs may regulate valve properties through complex paracrine signaling to the AVICs [37-41]. Butcher and Nerem showed that AVECs can prevent activation of the AVICs when the two cell types are

grown in co-culture [38]. In this study, porcine AVICs were seeded into leaflet model type I collagen hydrogels and subjected to 20 dynes/cm^2 of steady shear for up to 96 hours. The presence of the shear stress resulted in AVIC proliferation as well as an increase in αSMA and a decrease in GAGs—indicative of myofibroblast activation. When AVECs were introduced onto the surface of these gels in co-culture with the AVICs, these trends were completely reversed and the AVICs exhibited a more quiescent fibroblastic phenotype. This suggests that the AVECs may play a role in maintaining physiological homeostasis in the AV, and a loss or dysfunction of these cells may play a role in the onset and/or progression of AV disease.

Though the AVECs appear to play a crucial role in valve tissue maintenance, the tissue structure and mechanical properties of the valve seem to be regulated largely by the AVICs, the most abundant cell type in the AV. As mentioned before, these cells exhibit a plastic phenotype that alternates between a fibroblast-like state and a myofibroblast state depending on the needs of the tissue. Within the AV leaflets, AVICs are aligned with the collagen fibers in the circumferential direction, and studies have shown that they experience similar levels of strain, indicating that macro, tissue level deformations (strains) effectively transduce to the cellular level [42]. To continually respond to and monitor tissue level changes, AVICs are spread throughout the leaflet where they actively control and remodel the ECM to maintain its structural integrity. During times of tissue remodeling, AVICs become activated from their quiescent phenotype and gain smooth muscle cell characteristics [43-44]. This phenotypic

change results in increased cellular stiffness and contractility due to the formation of αSMA fibers within the AVICs. Once activated these cells also produce an excess of extracellular collagen that increases total tissue stiffness [45-46].

TGF-β1 signaling in AVD

The detailed cellular signaling pathways associated with AVIC myofibroblast activation are poorly understood; however, TGF-β1 activation and receptor binding has been identified as a major contributor to myofibroblast activation [10, 47-48] and was first studied in AVD as a potential mediator of AV leaflet thickening from carcinoid heart disease [49]. TGF-β1 is a member of the transforming growth factor superfamily of cytokines. In many tissues, TGF-β1 is secreted from cells as part of a latent complex and stored in the ECM. Various ECM cues such as mechanical strain [50], proteases [51], and pH changes [52] can result in the activation of TGF-β1, which then binds to the type II TGF-β1 serine/threonine kinase receptor (TβRII). Ligand binding at TβRII leads to recruitment and activation of the type I TβR, Alk5, which canonically elicits a wide variety of cellular processes by signaling through a family of transcription factors known as Smads [53]. For TGF-β1, specifically, phosphorylation of receptor Smads 2 and 3 (Smad2/3) by Alk5 leads to their association with co-Smad4. This Smad complex translocates to the nucleus and regulates transcription through interaction with CAGA-rich Smad binding elements on gene promoter regions. Plasminogen activator inhibitor-1 (PAI-1) is one example of a protein that can be expressed by Smad2/3 phosphorylation and nuclear translocation across many

cell types [54]. For this reason, plasmid constructs with the PAI-1 promoter region linked to expression of a reporter gene (e.g., luciferase) are commonly used to assay for canonical TGF-β1 signaling. Additionally, this canonical signaling has been shown to lead to diverse biologic responses that are both cell-type and environmental dependent.

Many studies have also focused on non-canonical signaling pathways to explain the myriad of cellular responses induced by TGF-β1 ligand binding, and p38 MAPK pathways have been identified as key mediators of cellular processes such as cell migration and mesenchymal transformations [55-57], which are characterized by upregulation of contractile elements similar to those identified in myofibroblastic activation. Recent studies have shown that TGF-β1-induced activation of p38 in epithelial cells is dependent upon phosphorylation of TβRII at tyrosine residue 284 (Y284) by Src tyrosine kinase (Src) [58]. Phenylalanine substitution at this residue (Y284F) of TβRII completely prevents p38 phosphorylation downstream of TGF-β1 ligand binding. Interestingly, activation of p130-Cas, the major substrate of Src, has been shown to lead to inhibition of Smad3 phosphorylation [59]. This indicates that Src phosphorylation may lead to activation of non-canonical p38 signaling while simultaneously suppressing canonical Smad3 signaling. The canonical and non-canonical TGF-β1 signaling pathways and interactions are summarized in Fig. 2.5.

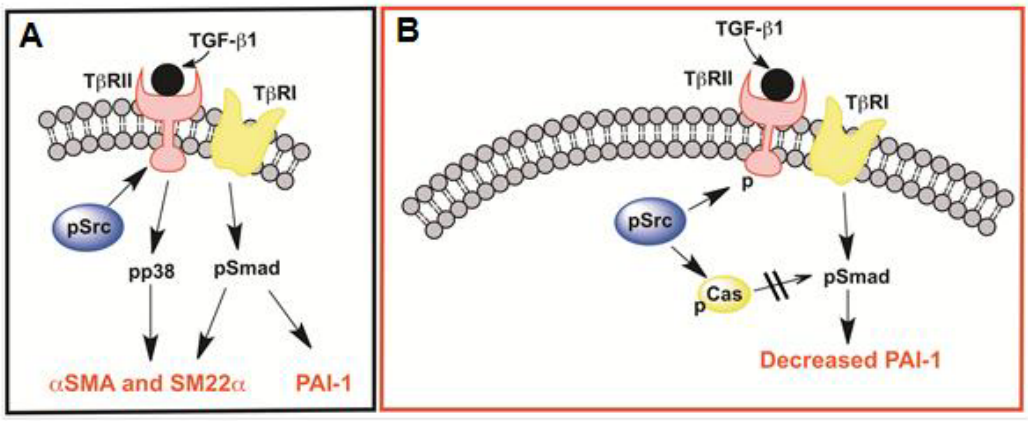

Fig. 2.5. TGF-β1 Signaling Pathways. (A) Canonically, TGF-β1 ligand binding to TβRII leads to recruitment and phosphorylation of TβRI (or Alk-5). This leads to phosphorylation and nuclear translocation of Smad transcription factors. Non-canonical TGF-β1 signaling has also been shown to be important in activating many cellular processes. One such pathway depends upon Src phosphorylation of TβRII and subsequent activation of p38. (B) Activated Src also leads to phosphorylation of Cas, which has been shown to inhibit Smad activity.

Using porcine AV leaflets in a tension bioreactor, the effects of TGF-β1 and cyclic stretch on myofibroblast activation were studied *in vitro* [10]. The measured outputs were αSMA, heat shock protein 47 (HSP47), type I collagen C-terminal propeptide (CICP), and TGF-β1. CICP and HSP47 are both surrogates for collagen biosynthesis [60-62]. The baseline control for this study was tissue in static culture that was not treated with active TGF-β1 (Null). Tissues receiving 15% stretch for two weeks (Tension) showed a significant increase in myofibroblast activation and collagen synthesis over the Null group and compared to day 0 controls (Fig. 2.6). This same trend was observed for tissue samples in the treated daily with 0.5 ng/ml active TGF-β1 for two weeks (TGF). Most interestingly, the combination of these two treatments (Tension+TGF) resulted in a very significant increase in myofibroblast activation and matrix remodeling than either independent treatment. This suggests a

synergism between TGF-β1 signaling and mechanical signal transduction. Furthermore, the large increase in TGF-β1 within the tissues indicates a feed-forward mechanism in which the AVICs respond to the combination of the two stimuli by producing even more TGF-β1. *In vivo*, this result may translate into an autocrine/paracrine signaling mechanism by which myofibroblasts produce TGF-β1 to remain activated in times of pathologic strain and signal for the activation of other AVICs to aid in tissue remodeling. In normal valves, the AVICs remain active until repair is complete and AV homeostasis is restored [43]. As discussed below, AV sclerosis may be a result of the over-activity of the AVICs resulting in a loss in AV compliance.

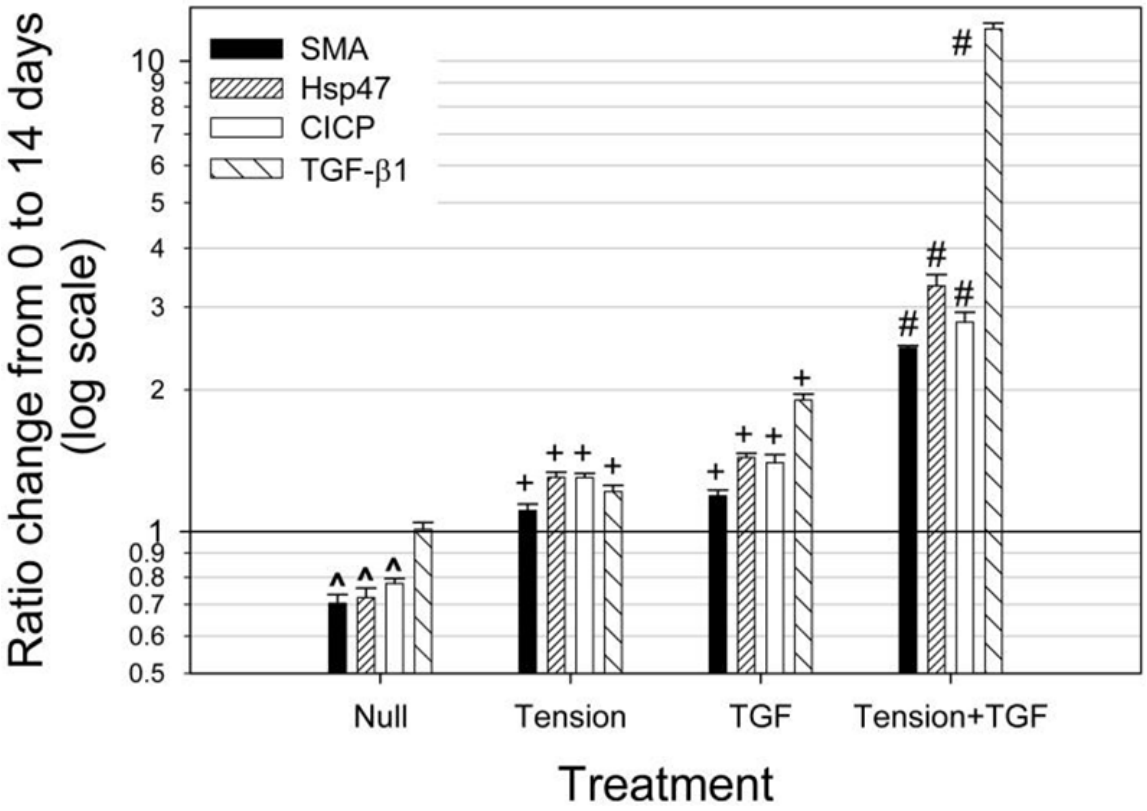

Fig 2.6. Effect of TGF-β1 and tension on AVICs. Both the presence of tension (Tension) and TGF-β1 (TGF) individually significantly increase markers of myofibroblast activation (SMA), ECM remodeling (Hsp47 and CICP), and the synthesis of native TGF-β1 (TGF-β1) over the non-treated controls (Null). A combined treatment of tension and TGF-β1 (Tension+TGF) showed a synergistic increase in all of the measured outcomes over either of the individual treatments (reprinted with permissions from [10]).

Early Effects of Strain on AVIC Homeostasis

Due to the synergistic effects of TGF-β1 and strain in altering AVIC behavior [10-11], we were interested in studying the short-term effects of strain in altering AVIC homeostasis. Changes in intracellular Ca^{2+} have been shown to play a significant role in the response of cultured myofibroblasts to mechanical stimuli. Specifically, mechanically-induced changes in intracellular Ca^{2+} lead to short term cellular contraction, allowing the cell to resist externally applied strains [63]. Previously, significant and sustained changes in AV leaflet mechanical

properties due to AVIC contraction have been observed due to addition of 90 mM KCl to the media, which results in a rapid Ca^{2+} influx into the cells [33, 64]. *In vivo*, AVICs are continuously subjected to a dynamic strain environment that has been shown to influence AVIC behavior [10, 65-66]; therefore, we investigated the role of strain-induced intracellular Ca^{2+} changes in AVICs. We believe that these changes may be important in normal AVIC function as well as disease progression. Correspondingly, mechanical strain has been shown to influence nodule formation in excised AV leaflets [11]. We assessed the role in intracellular Ca^{2+} accumulation in AVICs and the potential role of these changes in causing AVIC apoptosis.

The data indicate that extent of strain applied to AVICs is positively correlated with intracellular Ca^{2+} concentration and apoptosis. In real-time Ca^{2+} measurements, doubling the amount of strain applied to AVICs led to a significant 44% increase in the rate of Ca^{2+} accumulation over 5 min. The application of cyclic strain for 3 h also leads to a significant increase in AVIC intracellular Ca^{2+} over non-strained AVICs with a trending increase with increasing strain. Further, following the removal of strain, significantly more Ca^{2+} was retained in AVICs that were initially subjected to the higher strain. We believe that these accumulations may be important in directing AVIC behavior. A loss in Ca^{2+} homeostasis is known to lead to apoptosis in many cell types [67], and apoptosis has been shown to play a role in dystrophic calcification processes [11]. Indeed, our data indicate that AVIC apoptosis also increases with strain. Other studies have identified active osteogenic differentiation of AVICs that leads

to ossified nodules [68-69]. It is interesting to note that moderate increases in intracellular Ca^{2+} have been shown to be required for osteoblast activation in bone remodeling [70], and strain could play a role in inducing this differentiation in AVICs. Further, the data indicate that removal of Ca^{2+} is a biologically active process that occurs at a constant efflux rate independent of the amount of strain released and that higher strain leads to significantly more retention of intracellular Ca^{2+} over time in AVICs. Therefore, we speculate that increased strain could lead to small but gradual accumulations of intracellular Ca^{2+} and pathologic disruption to AVIC homeostasis.

The influx of extracellular Ca^{2+} could be due to either stretch-activated ion channels [71] or non-specific openings in the plasma membrane due to strain [72]. $GdCl_3$ treated AVIC data indicate that strain-induced intracellular Ca^{2+} accumulation occurs through stretch-activated channels in AVICs. One potential important characteristic of these channels lies in their increased sensitivity to small changes in strain [71, 73]. For the case in which Ca^{2+} diffusion is dictated by the concentration gradient across non-specific pores in the plasma membrane, the rate of accumulating intracellular Ca^{2+} is:

$$\frac{d[Ca^{2+}]_i}{dt} = A_{pore} N_{Ca^{2+}}, \qquad (1)$$

where $[Ca^{2+}]_i$ is the concentration of intracellular Ca^{2+}, A_{pore} is the total area of all open pores, and N_{Ca2+} is the molar flux of Ca^{2+} through the open pores A_{pore} cannot be determined directly; however, if a constant flux is assumed for any

given strain, the ratio of Ca^{2+} accumulation rates between two different strains should be proportional to the ratio of pore area for each strain. If an elliptical pore is assumed,

$$A_{pore} = \frac{\pi d_1 d_2}{4}, \qquad (2)$$

where d_1 and d_2 are the diameters of the elliptical axes. Therefore, the ratio of two pore areas is equivalent to the ratio of the products of the diameters of each ellipse, or

$$\frac{(A_{pore})_{\varepsilon=20\%}}{(A_{pore})_{\varepsilon=10\%}} = \frac{(d_1 d_2)_{\varepsilon=20}}{(d_1 d_2)_{\varepsilon=10}}, \qquad (3)$$

where the subscripts outside the parentheses denote the strain magnitudes. A change in uniaxial strain from 10% to 20% and a plasma membrane Poisson ratio of 0.49 [71], results in an off axis strain of -4.9%. The strains in each axis can then be used to relate change in the length of each axis for an applied uniaxial strain from 10% to 20%. Substituting these relations into Equation 3 yields a 4.6% increase in total pore area, which would correspond to a 4.6% increase in the rate of intracellular Ca^{2+} accumulation. However, the ratio of slopes from the data gives a 44% increase in the rate of intracellular Ca^{2+} accumulation from 10% to 20% strain. This indicates an increased sensitivity to intracellular Ca^{2+} accumulation at higher strains previously reported for mechanosensitive ion channels [71, 73]. The probability of opening mechanosensitive channels has been observed to have a sigmoidal dependence

on strain, whereby a relatively small change in strain can lead to a higher number of open channels and a large Ca^{2+} influx [71]. This sensitivity could have pathological consequences whereby small increases in AV strain lead to significant increases in intracellular Ca^{2+}. A graphic illustration of a proposed Ca^{2+} accumulation mechanism in AVICs is shown in Fig. 2.7. In this model, heightened strain leads to increased Ca^{2+} influx through an increased number of opened channels. This Ca^{2+} then accumulates over time as the rate of efflux from AVICs is constant and cannot counteract the increased load, resulting in a loss of AVIC homeostasis.

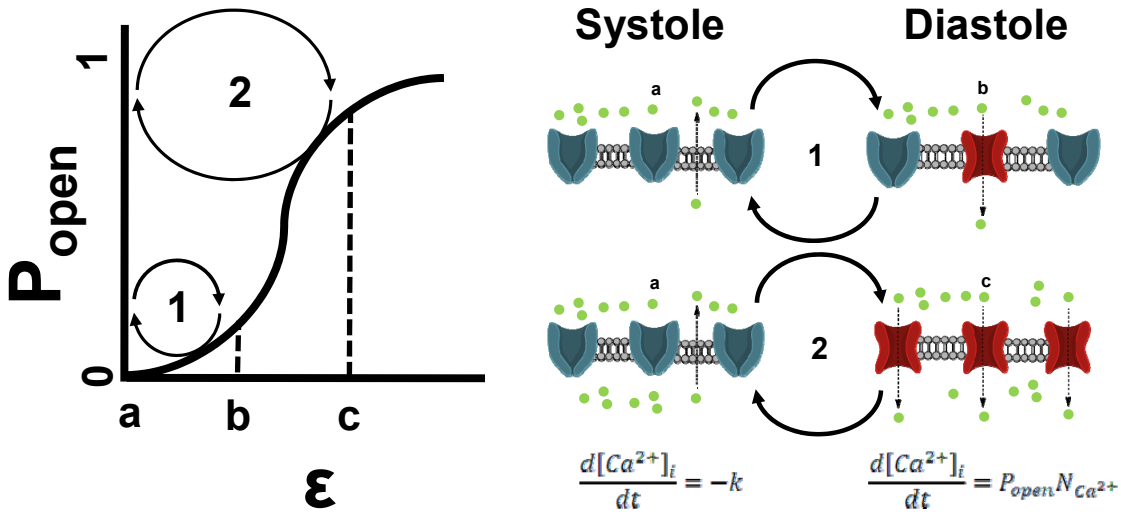

Fig. 2.7. Proposed mechanism of Ca^{2+} handling in AVICs. (A) The probability of opening (P_{open}) a stretch activated channel is a sigmoidal function of strain. When no strain is applied (case a, x-axis), no channels are open. When low strain is applied (case b), the P_{open} increases and some channels open. When a larger strain is applied (case c), P_{open} increases dramatically and a large number of channels open. (B) Physiologic strain during diastole therefore may open some channels, causing a small influx of Ca^{2+} into AVICs. This Ca^{2+} is pumped back out of AVICs during systole (cycle 1). Increased diastolic loading under pathologic conditions may lead to greater strain on AVICs, more open channels, and a greater influx of Ca^{2+} (cycle 2). Assuming a constant efflux independent of strain, AVICs are not able to sufficiently remove the accumulated intracellular Ca^{2+}, which leads to apoptosis after multiple cycles.

The results of this study provide insight into AVIC responses to mechanical strain and early mechanotransductive events that may contribute to AV calcification. Studies are needed to clarify the molecular mechanisms associated with both the strain-mediated intracellular Ca^{2+} increase and the active cellular-mediated decrease. Finally, identification of important pathways and downstream consequences of increased intracellular Ca^{2+} may reveal therapeutic targets for AV disease.

Aortic Valve Pathologies and Current Research

AV disease can be classified as an inflammatory, congenital, or degenerative disease [74]. Until the mid-1980s, inflammatory valve pathologies such as those caused by rheumatic heart disease were much more common than degenerative diseases; however, with the eradication of such diseases as scarlet fever in the Western world, degenerative AV disease has become more prevalent in the United States, but inflammatory valve disease remains a major problem in developing countries [75]. Though a recent study has suggested that pathogen infections may also play a role in modulating the activity of AVICs and thus could lead to the development of AV disease, this is still an area of ongoing research [76]. Therefore, for continued discussion we will mainly focus on better-established AV pathologies with congenital and degenerative etiologies.

Congenital diseases are those of a genetic origin and are inherited at birth. The most frequent congenital valvular defect is the bicuspid AV (with a

prevalence of approximately 1%) [77]. This defect occurs due to the fusion of two of the three AV leaflets, leaving the individual with two functional leaflets. Early in life, this genetic malfunction does not cause problems in the majority of individuals; however, adults with this malformation are at much greater risk of developing degenerative valve pathologies [30]. The mechanisms through which this defect results in valve dysfunction is still largely unknown. Current theories associate the failing of the bicuspid valve to AV-mediated alterations of the aortic wall. The changes in aortic stress may then be transferred to the AV leaflets, which could exacerbate deleterious AV alterations—a theory explained in more detail below. High levels of MMPs have been observed in the aortic walls of patients with bicuspid AVs [78]. MMPs work by degrading ECM structural components and, in these cases, cause dilatation of the aortic wall. One study has also implicated changes in endothelial expression of nitric oxide in inducing alterations of the aortic wall [79]. Nitric oxide signaling causes smooth muscle cell relaxation, which also results in aortic dilatation. The link between the bicuspid leaflets and these signaling mechanisms are unclear. Regardless of the mechanism, however, the expanded aorta results in a higher volume of blood being forced back onto the leaflets during diastole. Accordingly, this increased pressure is transferred from the aorta to the cells within the AV leaflet, which mediate tissue remodeling.

For many years, the prevailing view among many researchers and clinicians was that AV degeneration was similar in nature to—if not identical to—the progression of atherosclerosis [74]. More recently, this view has been the

subject of some controversy in the field. Both diseases involve the same risk factors and exhibit similar histological morphology; however, the AV leaflets lack smooth muscle cells, which play a significant role in atherosclerosis. Also, recent findings have shown that AV disease progression is more highly dependent on the interplay between the mechanical factors and inflammatory cytokines than the immunological processes that seem to mediate atherosclerosis. In fact, Robicsek et al. have observed that changes in the mechanical compliance of the aorta can lead to changes in AV function [74], similar to the observations in the bicuspid AV studies. The reduced aortic compliance can lead to a significant stress-overload on the AV leaflets, and thus result in increased matrix remodeling in the absence of other internal or external cues. Furthermore, this hyper-stressed diastolic state of the leaflets and resulting over-activity of the ECM remodeling mechanisms leads to a loss in the biomechanical integrity and functionality of the AV.

The most common degenerative AV pathology is known as AV sclerosis, which is characterized by thickening and stiffening of the valve leaflets. Changes in AV stiffness can lead to improper opening of the valve or insufficient coaptation of the AV leaflets to prevent backflow from the aorta to the LV [80]. The progression of this degenerative disease seems to occur over the course of years, and can lead to valve stenosis in the most serious cases. Stenosis occurs when the leaflets become so rigid that they are unable to coapt during diastole, resulting in partial occlusion of the valve. This pathology represents the most

extreme case of AV degeneration and may be largely mediated by improper activity of the AVICs [48, 81-83].

Again, under normal physiological conditions AVICs exhibit a fibroblastic phenotype; however, the initiation of VHD has been found to be caused by the activation of AVICs to a myofibroblast phenotype [7]. As discussed above, AVICs can be activated in times of tissue development and repair. During these physiological circumstances, activated myofibroblasts remodel the ECM and return the tissue to homeostasis after which many of the myofibroblasts return to a quiescent state. The characteristic thickening observed in AV sclerosis occurs when these cells remain activated, creating an excess amount of collagen. This over activation may occur due to a chronic physical change in the systemic circulation such as the stress transduction caused by the lost aortic compliance as observed by Robicsek et al. [74] (see above). The constant increased diastolic pressure on the tissue is transferred to the AVICs within the leaflets. As discussed before, this heightened mechanical stimulation may lead to AVIC activation and release of important signaling cytokines such as TGF-β1. The combination of a sustained pathological mechanical load and a constant increase in the production of TGF-β1 may lie at the root of the cellular cause of degenerative AV disease [84].

VECs have also been shown to play a role in the etiology and progression of valve disease. In diseased or injured vascular tissues, endothelial cells direct the appropriate immune response by upregulating cell adhesion molecules (CAMs) that mediate platelet attachment and activation as well as by secreting

cytokines that are recognized by specialized inflammatory cells [85-88]. Similarly, AVECs have been observed to increase expression of CAMs (ICAM-1 and VCAM-1) and secretion of inflammatory cytokines such as IL-8, IL-1β and IFN-γ in response to oscillatory, turbulent fluid flows and pathological mechanical strains [39]. The exact mechanisms by which the AVECs may contribute to pathogenesis in heart valves remain unclear; however, these cells may mediate tissue changes through paracrine signaling to the AVICs within the valve. In support of this theory, IL-1β has also been found in the cells within the valvular interstitium and may be an important in modulating the overall disease progression [81].

It is also important to note that the decreased leaflet compliance that is associated with degenerative AV disease occurs due to an increase in type I collagen and the formation of calcium deposits on the aortic side of the valve leaflets [69, 89]. This is intuitive because the mechanical load placed on the leaflets during diastole occurs due to a backflow in blood from the ascending aorta; therefore, this stress would be transferred to the AVICs on the aortic side of the valve. However, the AVECs may also play an important, though lesser known, function in the degenerative effects. The spatial heterogeneity of these cells may cause side-specific susceptibility to AV calcification [37]. The AVECs directly adjacent to the fibrosa have been found to express much lower levels of anti-calcification enzymes when compared to the AVECs on the ventricular side of the leaflets [39]. This suggests that the AVECs may also play an important role in sensing and responding to the various stresses on each side of the leaflets.

Though the AVICs may be more directly involved in the tissue changes that are observed in AV degeneration, signaling from the AVECs may direct AVIC phenotype in vivo through the differential expression of signaling cytokines.

Concluding Remarks on AV Physiology

The heart is the most dynamic organ in the human body. It relies on a coordinated action of chemical and electrical stimuli to produce the necessary mechanical responses needed to provide blood to the outermost regions of the body. Within the heart, the four valves work to direct blood flow and these heart valves rely heavily on their biomechanical properties to ensure proper function; therefore, the cells that compose these valves are extremely interesting case studies in the field of mechanobiology. Recent studies have begun to connect the effects of changes in the mechanical load on the valves to the biological response of the cells within the tissues. Throughout this chapter, we have focused on the important biomechanical features of the ECM of the valve tissues. We have also highlighted how the mechanical forces placed on the valve tissues can be transduced to the cellular level, which can lead to a feedback mechanism by which the cells actively work to remodel the tissues. In all valves, VECs likely play an important role in recruiting inflammatory cells to the surface of the leaflet and translating shear stress on the tissue into signaling cytokines that can modulate the activity of the VICs. The VICs themselves regulate tissue properties through secretion of ECM components in response to changes in tissue strain

and signaling cytokines (Fig. 2.8). Under normal conditions, these processes would persist until valve remodeling is complete; whereupon, the valve would return to its physiologic state. However, the over-activity of these signaling mechanisms has been shown to affect a variety of HVDs. A better understanding of this complex interplay between mechanical stimulation as the signaling mechanisms utilized by the various cells that compose the valves may lead to the development of less invasive therapies and preventative techniques for heart valve disease.

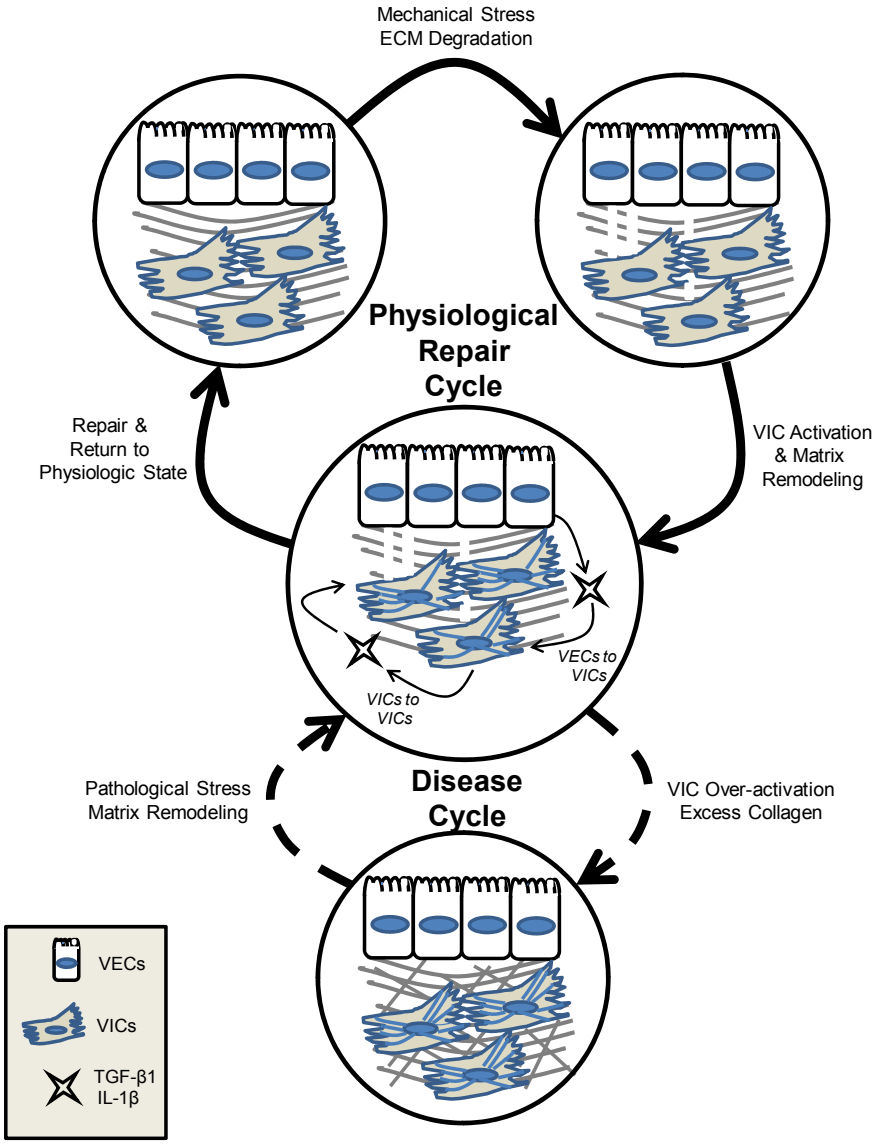

Fig 2.8. Summary of the valve response to increased mechanical stress. The valve leaflets are composed of a layer of VECs with an underlying layer of VICs that maintain the ECM components. Heightened mechanical stresses that lead to changes in the ECM result in paracrine signaling from the VECs to the VICs and between different VICs. This causes the VICs to become activated, whereupon they begin the process of remodeling the ECM within the valve tissues. Under normal conditions, the valve tissues return to homeostasis after the ECM has been repaired (Physiological Repair Cycle); however, in disease state, the VICs remain constitutively active resulting in an accumulation in extracellular collagen (Disease Cycle).

2.4. Treatments for HVD

Currently, the only viable long-term treatment option for HVD is valve replacement surgery. Typically, the native diseased HV is either replaced by a decellularized HV of bovine or porcine origin or supplanted by a mechanical HV. While the techniques and resultant risks associated with HV replacement procedures have dramatically improved, surgery still remains a poor option for the two patient populations most affected by HVD: children and elderly.

In pediatric patients, the main concern is the integration of replacement HVs within tissues that are rapidly growing and changing. Compounding the problem in children, replacement HVs tend to wear quickly and typically need to be replaced within 20 years [90]. To circumvent these problems, many surgeons elect to perform the Ross procedure whereby the pulmonic HV is resected and placed in the aortic position. The replacement HV is then placed in the position formerly occupied by the pulmonic HV. The advantage of this procedure is that the pulmonic HV is able to incorporate within native tissue in the aortic position, and the replacement HV wears more slowly due to the lower pressures associated with the pulmonic circulation. The major disadvantage of the Ross procedure is that it requires two very invasive surgical procedures (i.e., resection of both the aortic and pulmonic HVs), and often, the pulmonic HV is not able to adapt to the increased pressure associated with systemic circulation. For these reasons, the Ross procedure is rarely performed in elderly patients. Faced with the problems associated with HV replacement, physicians often delay surgical options until they are absolutely necessary; therefore, many patients would

greatly benefit from an early treatment to delay or prevent the onset of HVD. Elderly patients face a difficult recovery following open-chest surgery that, while improving their cardiac function, their quality of life declines for a prolonged period of time (up to a year). Thus, elderly patients would benefit greatly from a pharmacological strategy against HVD.

The hopeful story in recent years has been that lipid-lowering drugs (*i.e.*, statins) might prevent HVD [91-93], similarly to their promise against atherosclerosis. In 2001, two retrospective studies indicated that statins may inhibit the progression of aortic valve stenosis [94-95], and it was suggested that large prospective studies be conducted. When these prospective studies were finally completed, the efficacy of statins proved disappointing. In 2005, a small double-blind, placebo controlled study showed no benefit of statins to reduce HVD [96]. Moreover, a recent report of a large clinical study demonstrated, rather conclusively, that statins do not reduce major cardiovascular outcomes, including aortic valve replacement, in patients with aortic valve stenosis [97]. In light of these findings, the enthusiasm for statin therapy as a potential preventive treatment for HVD has been severely dampened. Thus, there is no pharmacological strategy currently available or being developed (to our knowledge) that has the potential to prevent or delay HVD progression.

Chapter 3

Serotonergic Signaling and Heart Valve Disease

Text for Chapter 3 taken from:

Hutcheson, J.D., et al., *Serotonin receptors and heart valve disease--it was meant 2B.* Pharmacol Ther, 2011. 132(2): p. 146-57.

3.1. Serotonin

Serotonin or 5-hydroxytryptamine (5-HT; Fig. 3.1) is enzymatically transformed from the essential amino acid tryptophan following hydroxylation and decarboxylation. Serotonin was discovered and isolated from serum 60 years ago [98], and shortly after, the molecule was determined to originate from the enterochromaffin (or Kulchitsky) cells that are found throughout the gastrointestinal and bronchopulmonary system [99]. High concentrations of 5-HT are found in blood platelets and enterochrommaffin cells of the gut; lesser amounts are found around neurons located along the raphé nuclei of the brainstem. The human brain has evolved a sophisticated arrangement of axons stemming from the raphé nuclei to innervate nearly every brain region.

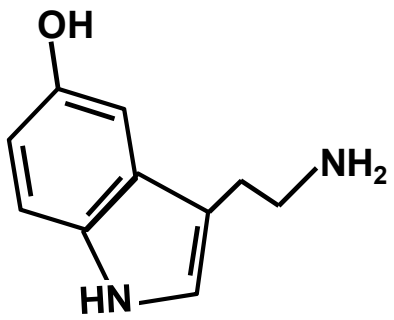

Fig. 3.1. Molecular structure of serotonin.

5-HT is involved in a diverse array of physiologic and biologic processes. In the brain, 5-HT has been found to affect mood, appetite, anxiety, aggression, perception, pain, and cognition [100-102]. Systemically, 5-HT contributes to vascular and non-vascular smooth muscle contraction and platelet aggregation. Serotonin released from neurons is recaptured by an active reuptake pump (serotonin transporter), and is then inactivated by monoamine oxidase and converted to 5-hydroxyindoleacetic acid [103]. *In vivo*, the rate of urinary 5-hydroxyindoleacetic acid output is commonly used as an index of 5-HT metabolism.

3.2. Serotonin receptors

Signaling of 5-HT is mediated by receptors that are located on the cell membrane of neurons and most other cells in the body [101-102]. There are six classes of G protein-coupled 5-HT receptors ($5\text{-}HT_{1,2,4,5,6,7}$) that can be subdivided into 14 unique subtypes. The $5\text{-}HT_3$ receptor is unique among 5-HT receptors in that it is a ligand gated ion channel [101, 104]. Heterotrimeric

guanine nucleotide-binding protein G protein-coupled receptors (GPCRs) are well characterized and have been described extensively [105-106]. Briefly, GPCRs are transmembrane proteins consisting of seven membrane-spanning α-helical segments with an extracellular N-terminus and an intracellular C-terminus. The binding of 5-HT to one of its receptors is thought to elicit a conformational change that activates associated heterotrimeric G proteins and recruits other downstream signaling/scaffolding molecules, such as GPCR kinases and β-arrestins [107-108]. Upon activation by an agonist-occupied GPCR, G proteins release guanosine diphosphate, which is constituitively bound to the α subunit of the heterotrimer, and bind guanosine triphosphate (GTP). Binding of GTP to the α subunit causes it to dissociate from the βγ subunits (which remain associated to each other); free Gα then interacts with nearby, downstream effectors (*e.g.*, adenylate cyclase for Gαs/olf- and Gαi/o/z-types or phospholipase C for Gαq/11-types), generating second messengers (*e.g.*, cAMP produced by adenylate cyclase or inositol 1,4,5-trisphosphate and diacylglycerol produced by phospholipase C) that modulate downstream effectors inside the cell (*e.g.*, protein kinases A and C activated by cAMP and diacylglycerol) [see [109] for review of 5-HT signaling pathways]

Because of the systemic presence of 5-HT and the multitude of receptor types found throughout the body that can elicit a myriad of cellular responses, drugs targeting 5-HT receptors are effective treatments for a variety of conditions. Each 5-HT receptor subtype contains at least one important therapeutic target. For instance, antimigraine medications (*e.g.*, ergotamine,

sumatriptan) activate 5-$HT_{1B/D}$ receptors. Clinically effective antipsychotics block the activation of 5-HT_{2A}, 5-HT_{2C} (Roth et al, 1992), 5-HT_6 [110], and 5-HT_7 [110-111] receptors [see [112] for review]. Acid reflux can be managed with drugs that activate 5-HT_4 receptors [113], while drugs that block the activation of 5-HT_4 receptors are used to treat cardiac arrhythmias [114]. Antagonism of 5-HT_6 receptors has been postulated to enhance memory and learning in healthy individuals [115]. There are many pharmaceuticals used to target the multitude of serotonergic GPCRs; however the 5-HT_2 receptors are among the most frequently targeted, highlighting their important role in physiological and pathophysiological processes (see Roth *in press* for recent review).

5-HT_2 receptors

The 5-HT_2 family consists of three GPCRs: 5-HT_{2A}, 5-HT_{2B}, and 5-HT_{2C}. 5-HT induces an increase in inositol 1,4,5-trisphosphate (which leads to release of intracellular calcium stores and diacylgycerol [116-118]. In addition to these known signaling mechanisms, 5-HT_2 receptors also generate second messenger signaling that leads to cell-type specific responses depending on the organ under consideration. Some of the most notable effects of 5-HT_2 receptor-preferring drugs involve the brain, and these activities are exploited therapeutically. Two important, common examples are atypical antipsychotics and anorexigens. These drugs—and/or their metabolites—display activity at 5-HT_{2A} (viz: atypical antipsychotics are inverse agonists) [119-120] and 5-HT_{2C} receptors (anorexigens and putative atypical antipsychotic drugs are agonists) [121]. 5-

HT_{2A} and 5-HT_{2C} receptors are highly abundant in various human brain regions with 5-HT_{2A} being highly concentrated in cortical regions and 5-HT_{2C} more broadly distributed [122-123]. The 5-HT_{2B} receptor subtype displays a lower expression in the brain [116], and its role in the effects of psychoactive agents is less. Nevertheless, recent genetic and pharmacologic studies have implicated 5-HT_{2B} receptors in the biological activities of the recreational psychostimulant 3,4-methylenedioxymethamphetamine (MDMA, ecstasy) [124-125] and the anorexigen fenfluramine [126].

In fact, many clinically used agents, particularly antipsychotics and anorexigens, display some activity at all three subtypes. One reason for low selectivity among 5-HT_2 receptor-active compounds is the high degree of amino acid sequence homology among the three subtypes [100, 127] with a structural similarity of 45-50% between the receptors [128]. This homology is of significant consequence as drugs intended for the 5-HT_{2A} or 5-HT_{2C} receptors located in the brain may also bind to the 5-HT_{2B} receptors expressed in the brain or in other tissues.

5-HT_{2B} receptors

What is now called the 5-HT_{2B} receptor (Fig. 3.2) was first recognized 50 years ago relating to the putative role of a specific 5-HT receptor subtype in the contraction of the gastric fundus from rat stomach [129]. Although there was controversy prior to the cloning of the 5-HT_{2B} receptor whether the stomach fundus receptor was pharmacologically distinct from the 5-HT_{2A} and 5-HT_{2C} [130], this disappeared once all three were cloned and their tissue distribution

illuminated. Since then, 5-HT_{2B} receptors have been found to be present in both rodent and human tissues, particularly in the cardiovascular system, gastrointestinal tract, bone, and central nervous system [131-133]. Importantly, the tissue distribution of 5-HT_{2B} receptor protein in rodents and humans is similar, as are their pharmacologies [134]; this observation facilitates the extrapolation of physiological and pharmacological results from rodent studies of the 5-HT_{2B} receptor to humans.

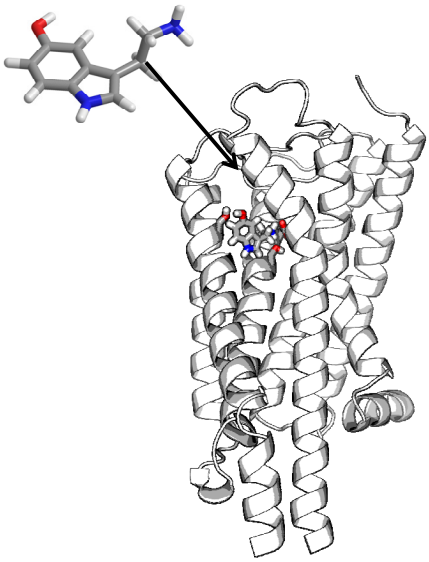

Fig. 3.2. A three-dimensional homology model of the 5-HT2B receptor. The model is based on the crystal structure of squid rhodopsin, which has a high degree of homology with the 5-HT2B receptor. Shown are two TM3 residues and one TM6 residue known to interact with serotonin.

The complexity and variety of 5-HT_{2B} receptor expression is paralleled by its signal transduction. Activation of 5-HT_{2B} has been found to stimulate phospholipase C [135] and phospholipase A2 [136], both of which increase intracellular calcium levels. Activation of 5-HT_{2B} receptors in some cell types has also been shown to stimulate nitric oxide synthase [137]. In fibroblasts and

smooth muscle cells, the biological result of activating 5-HT_{2B} receptors is mitosis ([133, 138-140] and secretion of inflammatory cytokines and extracellular matrix (ECM) components [13, 141]. As such, 5-HT_{2B} receptors appear to play a crucial role in allowing these cells to maintain the structural homeostasis of the tissues comprising them (*e.g.*, myocardium, heart valves, blood vessels). For example, over-expression of 5-HT_{2B} receptors in hearts of transgenic mice results in cardiac hypertrophy and decreased ventricular function due to enhanced ECM and remodeling [141-142]. Likewise, genetic deletion of 5-HT_{2B} receptors was shown to lead to ventricular dilation and incomplete cardiac development [138].

The molecular signaling pathways associated with these matrix remodeling responses appears to involve typical mitogenic signal transduction as well as coordination between the signaling of 5-HT_{2B} receptors and various growth factor and cytokine receptors [138-139, 143]. Specifically, 5-HT_{2B} activation in mouse fibroblasts was initially shown to lead to the $p21^{Ras}$- and heterotrimeric G protein-dependent activation of mitogen activated protein kinase (MAPK) [144]. Further studies in fibroblasts revealed that 5-HT_{2B} activation also leads to phosphorylation of the cytoplasmic tyrosine kinase Src [139]. Src phosphorylation appears to enhance signaling of the platelet derived growth factor and epidermal growth factor [139, 145]; Src inhibitors have been found to negatively affect signaling at both these receptors [139, 146]. A more recent study connected these 5-HT_{2B} signaling pathways using pharmacological agents to selectively inhibit key signal transduction proteins in cardiac fibroblasts [13]. Accordingly, 5-HT_{2B} receptor-mediated Src activation was found to lead to an

increase in matrix metaloproteinase activity, which leads to a release of heparin-bound epidermal growth factor. In turn, epidermal growth factor signaling leads to MAPK activation and subsequent upregulation of various cytokines. In addition, Jaffré et al. [13] demonstrated that 5-HT_{2B} receptors work in concert with the angiontensin II type 1 receptor (AT_1) to mediate hypertrophic signaling in cardiac fibroblasts. These results indicate that, in cardiac fibroblasts at least, the function of both GPCRs is required for the activity of either one. Consequently, by inhibiting one receptor the action of the other receptor is likewise inhibited.

Many of the cardiac-related studies into the molecular signaling pathways of the 5-HT_{2B} receptors have focused on the role of this receptor in ventricular fibroblasts. In this review, we will highlight the role 5-HT_{2B} receptors may play in mediating changes in heart valves. Therefore, to make the connection between these cardiac tissues, it is interesting to note that the signaling pathways discussed previously seem to play a major role in both regulating and responding to the biomechanical properties of tissue, which, as noted below, is crucial to the appropriate function of heart valves. Thus, both AT_1 and 5-HT_{2B} receptors demonstrate a mechano-dependent upregulation and signaling activation during ventricular pressure overload that results in an increase in tissue stress levels [147-148]. Moreover, agonist signaling at these GPCRs has been shown to lead to an increase in expression of the cytokine transforming growth factor-β1 (TGF-β1) [12, 147], which has also been shown to exhibit mechano-responsive signaling [50] and seems to be a key mediator in the tissue changes that lead to heart valve disease [10, 48].

Carcinoid syndrome

Carcinoid syndrome occurs as a result of the formation of neuroendocrine tumors arising from oncogenic enterochromaffin cells. These cells are reservoirs of 5-HT and normally deliver 5-HT to platelets for controlled systemic distribution; however, when tumor-forming enterochromaffin cells metastasize to the liver, 5-HT can more readily reach systemic circulation leading to the cardiac changes associated with carcinoid heart disease (CHD). CHD was first noted 80 years ago by the Dutch pathologist A.J. Scholte, who observed that a patient with a carcinoid tumor also had thickened tricuspid valve leaflets [149]. Interestingly, CHD differs from most forms of HVD in that it mostly affects right-side HVs (*i.e.*, the pre-lung tricuspid and pulmonary valves). Elevated blood levels of 5-HT are carried to the right side of the heart through the inferior vena cava, where it is believed that interaction with 5-HT_{2B} receptors on cells in the tricuspid and pulmonic HVs leads to the extracellular matrix secretion and the thickening of the HV leaflets that characterize HVD. As the blood continues into pulmonary circulation, the 5-HT is inactivated by monoaminoxigenase in the lungs and, therefore, does not induce HV changes when the blood returns to the left side of the heart. For many years, the serotonergic receptor subtype responsible for CHD was not known due to the fact that serotonin has a similar affinity for many of its receptors, and several of the subtypes are expressed throughout the cardiovascular system. The current hypotheses identifying 5-HT_{2B} receptor as the major HV target came about only as a result of inadvertant targeting of the 5-HT_{2B} receptors with Fen-Phen.

Fen-Phen

Among all the serotonergic drugs on the market, there may be none more recognizable to the general public than fenfluramine, one of the components of the 'Fen-Phen' anorexigen combination. This popular diet drug regimen consisting of *fen*fluramine and *phen*teramine was shown to be better tolerated than either alone in 1984 and the drug combination was subsequently and widely prescribed [150]. However, a study published in late 1997 identified both right-sided and left-sided HV defects in a number of patients who had been taking Fen-Phen for an average of 12 months [151]. Soon thereafter, the drugs (including other fenfluramine formulations) were voluntarily withdrawn from the market based upon recommendations by the FDA. In a retrospective study, the highest incidence of HVD development from Fen-Phen was found to be 25.2% among patients treated for an average of 20 months [152].

Early histological analyses of diseased tissue from Fen-Phen patients indicated a pathophysiology similar to that observed in carcinoid patients and from tissues of subjects who had taken specific ergot-derived formulations. In this regard, in the mid-1960s, researchers and physicians noticed a strong connection between the ergot agents methysergide and ergotamine and the development of fibrotic pathologies including HVD [153-155]. Some even went as far as to note that the "similarities in chemical structure of serotonin, methysergide, and ergotamine" may "suggest a common pathophysiologic mechanism for ergot alkaloid-associated valve disease and carcinoid valve

disease" [156]. Much like with CHD, however, the exact molecular cause of the tissue changes that lead to HVD remained undetermined.

The Fen-Phen episodes sparked new interest in identifying the specific 5-HT receptor subtype involved in drug-induced HVD. Due to the known mitogenic roles of the 5-HT_2 subfamily, Fitzgerald et al. [133] examined the interaction of fenfluramine, norfenfluramine (the main metabolite of fenfluramine), ergotamine, and methysergide on human 5-HT_{2A}, 5-HT_{2B}, and 5-HT_{2C} receptors. The ergot-derived compounds were found to possess high affinity for all three receptor subtypes. In contrast, fenfluramine rotamers demonstrated weak affinities for the 5-HT_2 receptors; however, the norfenfluramine rotamers exhibited relatively high affinity for both 5-HT_{2B} and 5-HT_{2C} receptors (Table 3.1) and slightly lower affinity for 5-HT_{2A} receptors. These results suggested that norfenfluramine, the main metabolite of fenfluramine, was chiefly responsible for 5-HT_2 receptor activation, and thus, the most likely candidate for causing Fen-Phen-mediated HVD. Furthermore, norfenfluramine was found to be two orders of magnitude more potent at 5-HT_{2B} and 5-HT_{2C} receptors compared with 5-HT_{2A} receptors (Table 3.2), and 5-HT_{2C} receptors, which are restricted to the central nervous system, were found to be expressed at exceedingly low levels within HV tissues (Fig. 3.3). Simultaneously, Rothman et al. (2000) compared the *in vitro* pharmacology of norfenfluramine with that of known inducers of HVD (5-HT, methysergide), as well as with that of serotonergic drugs not associated with HVD (negative controls), and found that the HVD-associated compounds were, unlike the negative controls, potent 5-HT_{2B} receptor agonists (see below). Taken together

with the expression of 5-HT_{2B} receptors in heart valve tissue [133] and the mitogenic effect of 5-HT_{2B} receptors in cardiac and other cell types [138-139], these results pointed to the 5-HT_{2B} receptor as the serotonergic target leading to HVD.

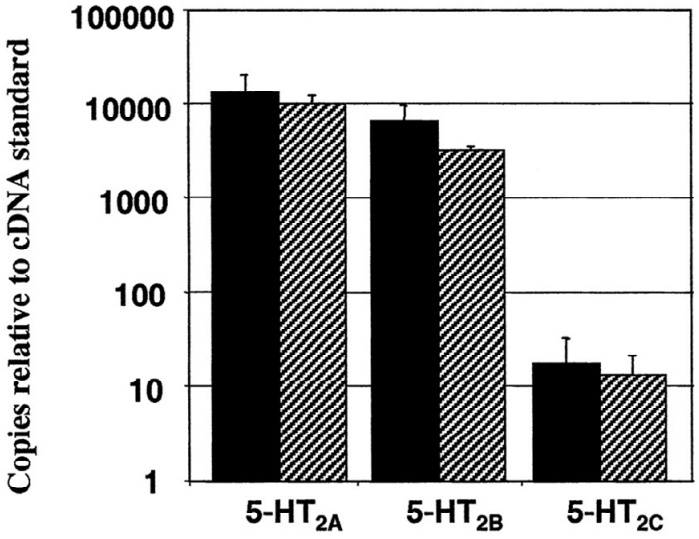

Fig. 3.3. 5-HT_2 receptor subtype expression in the aortic valve. 5-HT_{2A} and 5-HT_{2B} receptors are expressed in much greater numbers than 5-HT_{2C} as shown by random primed cDNA (solid bars) or oligo(dT) data (hatched bars). Reprinted with permissions from [133].

As noted above, the results of the Fitzgerald et al. study were supported in a seminal report published simultaneously by Rothman et al. [157] in which the affinities and potencies of 15 different molecules were tested at 11 different 5-HT receptor subtypes: 5-HT_{1A}, 5-HT_{1B}, 5-HT_{1D}, 5-HT_{1E}, 5-HT_{2A}, 5-HT_{2B}, 5-HT_{2C}, 5-HT_{5A}, 5-HT_6, and 5-HT_7. In this study, all but the 5-HT_{2B} receptor subtypes were systematically ruled out based on pharmacological similarity with HVD-associated molecules and pharmacological differences from negative control molecules that were not suspected mediators of HVD (*e.g.*, fluoxetine and its

metabolite norfluoxetine). The 5-HT_2 receptor subtypes were the only receptors to display relatively high affinity (Table 3.1) and high potency (Table 3.2) for both the norfenfluramine rotamers and for the HVD-associted ergot-derived compounds (Tables 3.1 and 3.2, italicized).

Table 3.1. Comparison of Receptor Subtype Affinity (K_i in nM)

	Receptor Subtype		
Drug	**5-HT_{2A}**	**5-HT_{2B}**	**5-HT_{2C}**
5-HT[1]	614*	4.0	12.2
(+)-Fenfluramine[2]	2470	2080	3920
(-)-Fenfluramine[2]	1430	1620	680
(+)-Norfenfluramine[2]	187	56	27
(-)-Norfenfluramine[2]	267	99	65
Cabergoline[4]	7.8	2.6	190
Pergolide[3,4]	1.6	14	45
Ergotamine[1]	*9.0**	*3.0*	*12.0*
Methysergide[1]	*15.0**	*9.1*	*1.8*
Methylergonovine[1]	*12.6**	*0.49*	*12.4*
Phenteramine[1]	>10,000*	>10,000	>10,000

*from rat 5-HT_{2A}

[1] [157] [2] [133]

[3] [140] [4] [158]

Similar to the Fitzgerald et al study, the data indicate both high affinity (K_i) and potency (shown by phosphatidylinositol hydrolysis, K_{act}) at 5-HT_{2B} over 5-HT_{2A} for norfenfluramines and the known inducers of HVD. It is important to note that in both the Fitzgerald et al. (2000) and Rothman et al. (2000) studies, phenteramine did not exhibit high affinity agonism of 5-HT_{2B} receptors (Table 3.1); correspondingly, formulations consisting of phenteramine alone (*i.e.*, in the absence of fenfluramine)—in use for decades prior to the Fen-Phen HVD outbreak—have not been associated with the disease [157].

Table 3.2. Comparison of Receptor Subtype Potency (K_{act} or EC_{50} for phosphoinositide hydrolysis in nM)

	Receptor Subtype		
Drug	**5-HT_{2A}**	**5-HT_{2B}**	**5-HT_{2C}**
5-HT[1]	66	2.4	0.6
(+)-Fenfluramine[1]	>10,000	379	362
(-)-Fenfluramine[1]	5,279	1,248	360
(+)-Norfenfluramine[2]	3,100	24	190
(-)-Norfenfluramine[2]	26,600	292	727
Cabergoline[3]	7.76	2.57	2.40
Pergolide[3]	1.62	6.03	4.47
Ergotamine[1]	*16*	*9.8*	*5*
Methysergide[1]	*3.5*	*150*	*2.9*
Methylergonovine[1]	*1.3*	*0.8*	*2.5*
Lisuride[3]	8.13	0*	7.76

*Lisuride exhibits antagonist signaling at the 5-HT_{2B} receptor.[3]

[1] [157] [2] [133]

[3] Adapted from: [158]

Pergolide and Cabergoline

Following the Fen-Phen episode, a number of additional HVD-inducing drugs have been identified. First among these were the non-specific dopamine agonists pergolide and cabergoline, prescribed for Parkinson's disease [159-160]. The stories of pergolide and cabergoline are similar to that of fenfluramine. The first preliminary account of potential pergolide-mediated HVD was reported in 2002 [161]. Dopamine agonists had become popular anti-Parkinsonian therapeutics, and many feared that these drugs would suffer the same fate as fenfluramine. Around the same period of time, many drugs were beginning to be profiled at 5-HT_{2B} receptors including anti-Parkinsonian drugs, amphetamine derivatives and other medications receptors [140, 158]. Of the large number of drugs tested, pergolide, cabergoline, MDMA and its active N-demethylated

metabolite 3,4-methylenedioxyamphetamine (MDA) were found to exhibit potent agonist activity at 5-HT_{2B} [140, 158]. It is interesting to note in this regard that Newman-Tancredi and colleagues were solely interested in differentiating activity of several Parkinsonian drugs at various serotonergic receptor subtypes and suggested that 5-HT_{2B} activity might be associated with some sort of therapeutic action of pergolide and cabergoline rather than a potentiator of side-effects. On the other hand, Setola et al. predicted that pergolide and other drugs which were 5-HT_{2B} agonists (including MDMA and MDA) would be associated with a high incidence of HVD. Accordingly, the incidence of HVD from pergolide and cabergoline has been found to be 23.4% and 28.6%, respectively [160]; no significant increase in HVD incidence has been associated with any of the other dopamine agonists. Further, three of the other drugs (lisuride, bromocripine, and terguride) were found to be potent agonists at 5-HT_{2A} receptors [158], but have little to no activity at 5-HT_{2B} receptors [162]. None of these drugs has been subsequently reported to be associated with HVD. These findings lend further credence to the theory that the 5-HT_{2B} receptor is the molecular culprit for drug-mediated HVD. Tables 3.1 and 3.2 contain partial compilation of the results from these early studies and offer a representative view of the data that first indicated agonist activity at 5-HT_{2B} receptors leads to the development of HVD.

A search for others

Following the Fen-Phen and pergoline/cabergolide findings, many other drugs have been tested for agonist activity at 5-HT_{2B}. Specifically, the NIMH

Psychoactive Drug Screening Progam has sought to screen large numbers of FDA-approved drugs and drug-like compounds for agonist activity at 5-HT_{2B} receptors in order to identify drugs/chemotypes with HVD liability [162-164]. The most recent findings in this effort identified 27 5-HT_{2B} receptor agonists among 2200 drugs and drug-like compounds (Table 3.3; [162]).

Table 3.3. Agonist efficacies and potencies at 5-HT_{2B} (E_{max} given as % of 5-HT, EC_{50} for calcium flux in nM)[1]

Drug	E_{max}	EC_{50}
5-HT	100.0	1.78
BW 723C86	92.9	1.41
DOI	88.2	1.45
Norfenfluramine	107.4	2.45
Cabergoline	98.5	398
Pergolide	88.5	74.1
Methylergonovine	49.5	21.4
Roprinirole	*73*	*2570*
Guanfacine	*93*	*123*
Oxymetazoline	*70.9*	*45.7*
Quinidine	*55.9*	*186*
Xylometazoline	*55.7*	*240*
Fenoldopam	*92.5*	*77.6*

[1] Adapted from: [162]

Of these, 14 had previously been identified as 5-HT_{2B} receptor agonists, including 7 known HVD-associated drugs (Table 3.3). Six of the compounds that had not previously been identified as 5-HT_{2B} receptor agonists are currently approved medications (Table 3.3, italics), with five of these acting as potent agonists: guanfacine, oxymetazoline, quinidine, xylometazoline, and fenoldopam. Guanfacine and quinidine were noted to be of particular concern. Guanfacine is often prescribed as an antihypertensive agent, and quinidine is used to treat

arrhythmia. As such, both tend to be prescribed for sustained periods and could potentially lead to valvular problems. The recent indication of guanfacine to treat attention deficit hyperactivity disorder in pediatric patients is of particular concern [162]. Of less concern (perhaps) are xylometazoline, oxymetazoline, and fenoldopam, which are typically prescribed for relatively short time periods. However, all of these compounds should be studied closely to ensure that there is no link to HVD.

One of the identified agonists, ropinirole, was found to be much less potent than the other compounds (active only at 1 μM) and therefore may not be associated with inducing HVD. Indeed, ropinirole, which has been used for several years to treat restless legs syndrome, has been considered 'safe' vis-à-vis HVD. However, a very recent study documented a case of retroperitoneal fibrosis in a patient using ropinirole [165]. Additionally, at least four other cases of HVD have been reported in patients using ropinirole [165]. While these relatively few reports may not indicate a statistically increased risk of HVD with ropinirole use, these types of cases should be continuously monitored to ensure that no causal link exists.

Learning from previous mistakes

Though unfortunate in terms of human and economic loss, the fenfluramine case has led to some important insights. The first and most impactful of these is that screening drugs for 5-HT_{2B} receptor agonist activity is the best *in vitro* method for identifying potential drug-inducing HVD candidates

[140, 157, 163]. The case of MDMA supports this recommendation. In 2003, the NIMH Psychoactive Drug Screening Program, in collaboration with Richard Rothman's group NIDA, profiled the serotonergic amphetamine derivative MDMA to identify targets other than the monoamine plasmalemmal transporters. The screening campaign revealed that MDMA and MDA were both moderately potent 5-HT_{2B} receptor agonists, and that they stimulated the proliferation of primary human VIC cultures in a 5-HT_{2B} receptor-dependent manner [140]. These findings led us to predict that MDMA use may be a risk factor for HVD. In 2007, a clinical study reported an increased prevalence of HVD in MDMA users [166]. Thus, the aforementioned studies support the claim that *in vitro* screening of drugs at 5-HT_{2B} receptors can identify previously unknown drug-inducing HVD candidates.

Another lesson that can be learned from the role of 5-HT_{2B} receptors in HVD is that 5-HT_{2B} receptor antagonists may be potential prophylactics and/or treatments. Indeed, if the activation of 5-HT_{2B} receptors (on heart valve interstitial cells and/or other cells) contributes to HVD, it is likely that blockade of 5-HT_{2B} receptors may antagonize the onset and/or progression of the disease [163]. Furthermore, there are a number of 5-HT_{2B} receptor antagonists that are FDA-approved medications (e.g., antidepressants, antipsychotics, antihistamines) with established records of safety and tolerability [140, 157, 162-163]. Along these lines, Droogmans and colleagues recently reported that the antihistamine cyproheptadine—which is also a potent 5-HT_{2B} receptor antagonist [167]—mitigated pergolide-induced HVD in rats [168], as predicted by Roth (2007).

Similar experiments using other 5-HT_{2B} receptor antagonists, and analyses of HVD prevalence among large numbers of patients taking medactions with 5-HT_{2B} receptor antagonist activity (e.g., antihistamines, antidepressants, antipsychotics), will be informative in terms of HVD prevention/treatment strategies.

3.3. 5-HT_{2B} receptor as a novel treatment strategy

The development of a suitable therapeutic to prevent/retard HVD depends on the ability to target the root cause of the disease, which ultimately manifests itself as thickening and stiffening of HV leaflets, which diminishes the ability of the HV to maintain directionality in blood flow. At a cellular level, HV stiffening is believed to be caused by activation of VICs to a myofibroblast phenotype [7, 81, 169-170]. Once activated, these cells increase ECM deposition, which directly leads to the decreased compliance of the leaflets observed in HVD. Additionally, increased mechanical strain has been shown to exacerbate VIC activation [10-11, 171-172]. In order to develop a strategy to prevent or treat HVD, a more thorough understanding of the cellular signaling and subsequent tissue-level changes involved in the progression of HVD is needed to elucidate the relevant molecular targets. Given the large number of currently-approved medications that exhibit antagonist/inverse agonist activity at 5-HT_{2B} receptors [162], we believe that the 5-HT_{2B} receptor is a tractable target to achieve these therapeutic goals.

Given its negative history, the idea of targeting 5-HT_{2B} for therapeutic gain may initially seem counter-intuitive; however, studies have begun to explore the potential benefits of controlling 5-HT_{2B} receptor signaling [15, 173-174]. Just as agonists of the 5-HT_{2B} receptor have been observed to lead to HVD, many of these agonists have also been implicated in fibrotic responses and ECM alterations that lead to other pathologies such as ventricular hypertrophy [13, 143] and pulmonary arterial fibrosis and hypertension [175]. Correspondingly, genetic deletion of 5-HT_{2B} receptor expression in mice has been shown to lead to incomplete cardiac development characterized by ventricular dilation and a lack of tissue integrity [138, 176]. Taken together, these results indicate that 5-HT_{2B} receptors play a crucial role in the maintenance of ECM homeostasis in cardiac tissues, and with a better understanding of the downstream effectors of these receptors, the pathways may be able to be manipulated to therapeutically target cardiac fibrotic diseases [177].

As an illustration of this, studies in pulmonary fibrosis have shown that 5-HT_{2B} receptor antagonists can effectively reduce fibrotic lesions in a mouse model [15], and the selective 5-HT_{2B} receptor antagonist PRX-08066 has been shown to increase ventricular ejection fraction and reduce hypertrophy and vascular remodeling in a rat model of pulmonary arterial hypertension [173]. A 5-HT_{2B} receptor antagonist may be able to function similarly in preventing HVD by blocking the fibrotic response of VICs to other, non-serotonergic stimuli.

As mentioned previously, TGF-β1 is believed to be a key mediator of the cellular changes that lead to HVD. Unfortunately, the ubiquity of TGF-β1 signaling makes this molecule a poor therapeutic target. A more appropriate therapeutic goal would be to interrupt TGF-β1 signaling through a separate pathway that is more localized to HV tissues, and the 5-HT_{2B} receptor signaling pathway may be a promising candidate to achieve this goal. Evidence suggests that the signaling pathway from 5-HT_{2B} receptors may crosstalk with TGF-β1 signaling pathways [12], which may be mediated in part by the tyrosine kinase Src. Src is known to play an important role in both 5-HT_{2B} and TGF-β1 receptor signaling pathways and has been shown to be involved in the 5-HT_{2B} receptor-dependent regulation of the platelet derived growth factor receptor [139, 178-182]. Therefore, 5-HT_{2B} receptor blockade has the potential to function in two ways: 1) preventing proliferation and fibrotic ECM accumulation by VICs directly, and 2) interacting with TGF-β1 signaling pathways to prevent VIC myofibroblastic differentiation.

Additionally, AT_1 antagonists have been observed to inhibit TGF-β1 signaling in Marfan's syndrome [17, 183-184], and as such, the AT_1 antagonist losartan has shown tremendous clinical promise in treating afflicted patients. Given that AT_1 and 5-HT_{2B} receptors may be functionally linked in other cell types [13], 5-HT_{2B} receptor antagonists may work in a similar manner to mitigate TGF-β1 signaling. Therefore, 5-HT_{2B} receptors may provide a localized pharmacological target to prevent the VIC-mediated fibrotic changes that characterize HVD. As noted above, many 5-HT_{2B} receptor antagonists are

currently FDA-approved and used clinically to treat other diseases, with acceptable tolerance. Furthermore, it is interesting to note that lisuride has been shown to be an antagonist at 5-HT_{2B} receptors [158] and was prescribed for more than 30 years without a single known report of HVD [185]. While the absence of documented cases does not necessarily lead to the conclusion that lisuride prevented HVD in these patients, it does seem reasonable to believe that given the large population of patients that received lisuride and its known serotonergic activity, even background levels (i.e., not significantly higher than the total population) would have been reported. In conclusion, we believe that these types of molecules should be tested for efficacy in preventing or treating HVD, as has been suggested [163].

Chapter 4

Aim 1 – TGF-β1 Induces Pathologic Differentiation of AVICs

Text for Chapter 4 taken from:

> Hutcheson, J.D., et al., *Cadherin-11 regulates cell-cell tension necessary for calcific nodule formation by valvular myofibroblasts.* In preparation, 2012.

4.1. Introduction

The differentiation of quiescent fibroblasts to activated myofibroblasts represents a normal physiological response to injury *in vivo*; however, persistence of the myofibroblast population contributes to a spectrum of fibrotic disease [186-189]. Activated myofibroblasts are characterized by increased contractility due to smooth muscle alpha-actin (αSMA), and in normal physiology, these cells remodel the extracellular matrix (ECM) by secreting proteases for matrix breakdown and *de novo* ECM components such as collagen [186-187]. Failure of the myofibroblasts to apoptose or return to quiescence in pathological cases causes impairment of organ systems due to elevated contractions and accumulation of ECM components. One disease in which the myofibroblast is thought to play a crucial role is calcific aortic valve disease (CAVD) [190-195].

Increased αSMA expression in aortic valve interstitial cells (AVICs), the resident fibroblast population in the aortic valve, has been observed in excised fibrotic leaflets [196]. Increased expression of the profibrotic cytokine transforming growth factor β1 (TGF-β1) has also been observed in these leaflets, and accordingly, TGF-β1 has been shown to lead to myofibroblast activation of AVICs *in vitro* [48, 196-197]. Additionally, in *ex vivo* models of CAVD, TGF-β1 works synergistically with mechanical strain to lead to collagen accumulation, characteristic of early CAVD, and formation of bone-like calcific nodules, an endpoint of CAVD [10, 198]. Two distinct calcific nodule morphologies have been observed: dystrophic calcification driven by myofibroblastic phenotypes [9, 93, 199] and ossification driven by osteogenic phenotypes [200-201]. In diseased explants, dystrophic calcification and ossification has been observed in 83% and 13% of explanted diseased valves, respectively [202].

In vitro, dystrophic nodule formation involves myofibroblast differentation of AVICs. Upregulation of αSMA during myofibroblast differentiation by TGF-β1 leads to an increase in mechanical tension between AVICs leading to subsequent aggregation into nodules, which calcify through apoptotic processes [48, 203]. When αSMA expression is suppressed, calcific nodules are unable to develop thereby revealing the essential role of acquired contractility within AVICs in calcific nodule formation [93]. Confoundingly, preventing phosphorylation of Erk1/2 with a MEK1/2 inhibitor leads to increased αSMA expression [204] yet prevents calcific nodule formation [205], suggesting the requirement of another essential component of nodule formation that has yet to be ascertained.

Along with increased αSMA expression, myofibroblast differentiation has been associated with changes in cadherin expression. Specifically, in lung fibroblasts, TGF-β1 induced myofibroblast differentiation leads to an increase of cadherin-11 and a decrease of N-cadherin [206]. Increased cadherin-11 expression has been implicated in various pathologies including pulmonary fibrosis and arthritis [207-208]. Functionally, the transition to cadherin-11 yields stronger intercellular connections that improve force development in myofibroblast populations. Recent works have shown that elevated intercellular tension along with increased contractility drive calcific nodule formation of AVICs *in vitro* [93, 199]. Therefore, we hypothesize that cadherin-11 is essential for robust cell-cell connections necessary for generating intercellular tension required for calcific nodule formation.

To test this hypothesis, we quantified the expression and contributions of cadherin-11 in calcific nodule formation of AVICs. Here, we show that TGF-β1 induced myofibroblast differentiation of AVICs leads to upregulation of αSMA and cadherin-11 expression in an Erk1/2 dependent fashion, corresponding to increased functional contractility and cell-cell connection strength, respectively. Subsequent knockdown of cadherin-11 inhibits the ability of AVICs to generate calcific nodules similar to knockdown of αSMA [93], demonstrating that both proteins are necessary for dystrophic calcific nodule morphogenesis.

4.2. Methods

AVIC isolation and culture

Porcine aortic valve leaflets were excised from sacrificed animals within 10 minutes of slaughter at a local abattoir. Leaflets were stored in phosphate buffered saline (PBS) at 4°C to ensure survival. Within 3 hours (h) of sacrifice, AVICs were isolated as previously described [209]. Briefly, after the removal of the endothelium, the leaflet was minced into 1 mm^2 pieces and digested in a 1 mg/ml collagenase solution (Worthington Biochemical Corp., Lakewood, NJ) for 1 h at 37° C and 5% CO_2. The collagenase solution with the remaining tissue was passed through a cell strainer to collect a cell solution which was centrifuged at 1500 RPM for 5 min to obtain the cell pellet. The pellet was resuspended in Dulbecco's Modified Eagle Medium (DMEM) supplemented with 10% fetal bovine serum (FBS) (Atlanta Biological; Lawrenceville, GA), and 1% Antibiotic-Antimycotic (Gibco; Grand Island, NY). The cells were seeded on tissue culture dishes and incubated at 37° C and 5% CO_2 with media changes every three days. AVICs were cyropreserved after the second passage and all experiments in this study were performed using AVICs between passages 3-6.

Calcific Nodule Treatments and Analyses

AVICs were seeded onto BioFlex Pronectin culture plates (Flexcell International Corporation) at a density of 60,000 cells/cm^2 in 3 ml of media. After reaching confluence (~48 h), AVICs were treated with 1 ng/mL TGF-β1, 10 μM

U0126, a MEK1/2 inhibitor that prevents Erk1/2 phosphorylation, or U0126 + TGF-β1 for 24 h, after which they were subjected to 15% cyclic equibiaxial strain via the Flexcell-4000 tension system (Flexcell International Corporation) at a frequency of 0.75 Hz for 24 h. The specific sequence of TGF-β1 for 24 h followed by 15% cyclic strain results in the formation of dystrophic calcific nodules [199].

To quantify nodule counts following treatments, AVICs were rinsed twice with PBS and fixed in 3.7% neutral buffered formaldehyde for 15 min. AVICs were rinsed with PBS and, unless immediately stained, stored at 4^{o}C for up to several days. Each 35 mm well was rinsed with deionized water (dH_2O) and stained with 1 ml of 14 mM Alizarin red S (Sigma) (in dH_2O, pH 4.1, where undissolved particulates were removed with a 0.45μm filter) for 30 min with agitation to determine calcium deposition. After staining, the cells were washed 4 times with dH_2O to remove excess dye. Positively stained nodules were manually counted under the microscope.

To examine the morphology of the nodules formed following treatments, wells were rinsed with PBS and stained with Annexin V conjugated with Alexa fluor 488 (5% solution in Annexin binding buffer; Invitrogen) for 15 minutes to detect apoptotic cells. Propidium Iodide (0.4% solution in Annexin binding buffer; Invitrogen) was used as a counter-stain for necrotic cells. Images were taken with a Nikon TE300 inverted tissue culture fluorescence microscope.

Wound Assay

A wound assay to quantify the level of intercellular tension was performed as described previously [199]. Briefly, AVICs were seeded on tissue culture polystyrene 6-well plates at 60,000 cells/cm^2 and allowed to adhere overnight. AVICs were treated with either 1 ng/ml TGF-β1, 10 μM U0126, or a combination of these treatments for 24 h. Prior to the introduction of a wound to the monolayer with a pipet tip, the extracellular growth media was washed away and replaced with media containing 1.8 mM Ca^{2+} or 0.45 mM Ca^{2+} in order to select for function of different cadherins. All cadherins require extracellular Ca^{2+} for function; however, cadherin-11 functions at lower Ca^{2+} concentrations than normal cadherins such as N-cadherin. Previous studies have identified 0.3 – 0.8 mM as a threshold concentration range in which cadherin-11 is functional but N-cadherins display reduced functionality in this range [210]. Immediately after wounding, each well was imaged, and wound areas were calculated using ImageJ analysis software.

Protein and mRNA Assays

AVIC activation was quantified by assaying for αSMA protein expression using an indirect ELISA as described previously [199, 211]. AVIC mRNA was isolated per manufacturer protocol using RNeasy isolation kit (Qiagen). A cDNA library using forward (CAAGTTAGTGTACAGTATCCTGG) and reverse (GTCTTTAGCCTTCACTCT TCC) primers was then created with Oligo d(T) and RNAse inhibitor (Applied Biosystems) using M-MLV reverse transcriptase

enzyme (Promega). Finally, qPCR was performed on a HT7900 sequence detection system (Applied Biosystems, VUMC DNA Resource Core).

Immunofluorescence

AVICs were plated on fibronectin functionalized coverslips and treated with 1 ng/mL TGF-β1, 10 μM U0126, or U0126 + TGF-β1 for 24 h. The cells were then fixed in 3.7% formaldehyde, permeabilized with 0.1% Triton X-100, and blocked with 1% bovine serum albumin for 1 h at room temperature. A primary antibody to cadherin-11 (2 μg/ml, Santa Cruz) was added to the coverslips for 3 h at room temperature. After thorough washing in PBS, a fluorescently labeled secondary antibody (Alexa Fluor 488, Invitrogen) was added to the coverslip for 1 h. The coverslips were then washed and sealed with ProLong Gold antifade reagent (Invitrogen) overnight prior to imaging with a Nikon Eclipse E800 equipped with a Spot RT3 camera.

siRNA Knockdown

The necessity of cadherin-11 expression in calcific nodule morphogenesis was assessed using siRNA knockdown. Cadherin-11 specific siRNA was designed using specialized algorithms, and 40 pM each of three different siRNA plasmids (CCAAGTTAGTGTACAGTAT, GGGATGGATTGTTGAA, CCTTATGACTCCATCCAAA, Sigma) were pooled and transfected into AVICs using Lipofectamine 2000 (Invitrogen) for 6 h. AVICs were allowed to recover

overnight prior to the addition of TGF-β1 and strain as described above. Western blotting was used to confirm knockdown efficiency.

4.3. Results

αSMA Expression is Not Sufficient for Calcific Nodule Formation

Consistent with previous results [204], treating AVICs with either 1 ng/ml TGF-β1 or 10 μM U0126 leads to a significant increase in αSMA mRNA and protein expression (Fig. 4.1A). A combination of these treatments also significantly increases αSMA expression compared to non-treated controls. As shown previously [199], AVICs treated with TGF-β1 prior to the addition of strain form significantly more calcific nodules compared to non-treated, strained control AVICs (Fig. 4.1B), and calcific nodules were determined to be dystrophic with an apoptotic ring surrounding a necrotic core (Fig. 4.1C). The addition of U0126 to the TGF-β1 treatment prevents this increase in calcific nodule formation.

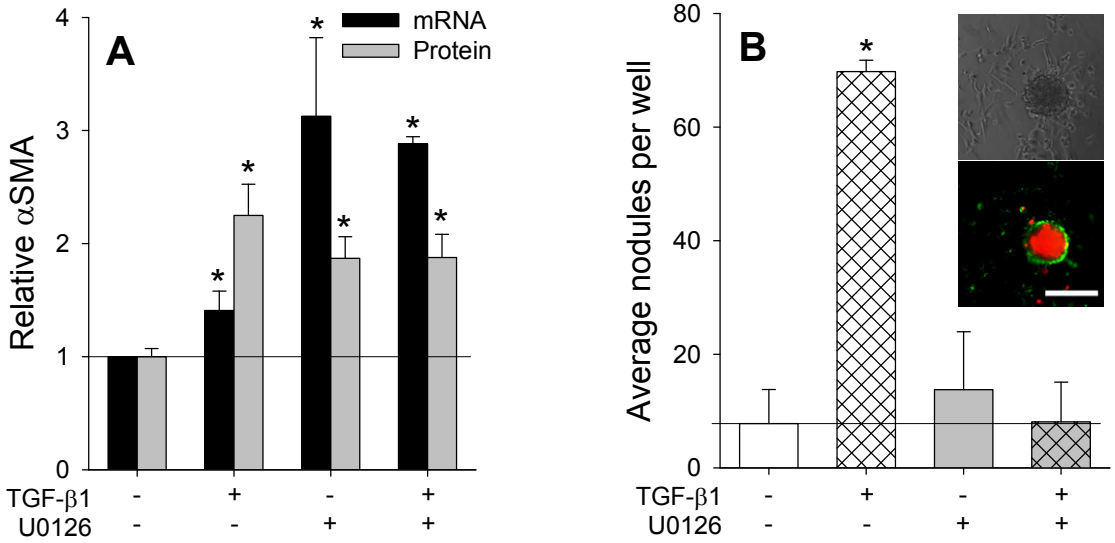

Fig. 4.1. The effect of MEK1/2 inhibition on hallmarks of dystrophic calcification. AVICs were treated TGF-β1, U0126, U0126 + TGF-β1 and assayed for αSMA and calcific nodule formation. MEK1/2 inhibition suppresses αSMA expression (A) and dystrophic calcific formation (B) of AVICs in the presence and absence of TGF-β1. Scalebar = 250 μm. All error bars indicate standard error of the mean. * indicates significant difference ($p < 0.005$) versus control.

Erk1/2 Inhibition Does Not Effect Canonical TGF-β1 Signaling

U0126 is designed to be a specific inhibitor to MEK1/2, the kinase directly upstream of the MAPK Erk1/2. Therefore, we were interested in assessing the effect of TGF-β1 and U0126 treatments on Erk1/2 phosphorylation in AVICs. Treating AVICs with TGF-β1 for 1 h significantly increased Erk1/2 phosphorylation (Fig. 4.2A), and this phosphorylation is completely inhibited by the U0126 treatment. We were next interested in determining potential off target effects of U0126 treatment at other common TGF-β1 signaling proteins. TGF-β1 treatment for 1 h induces significant phosphorylation of its canonical transcription factor Smad3 (pSmad3) in a manner that is not inhibited by U0126 treatment as

indicated by Western blotting (Fig. 4.2A). In addition to Smad3, we have previously shown that 1 h of TGF-β1 treatment leads to phosphorylation of the MAPK p38 that is necessary for TGF-β1-induced αSMA expression in AVICs [211]. Treating AVICs with U0126 does not inhibit TGF-β1 p38 phosphorylation (Fig. 4.2A). Consistent with the pSmad3 results, treating AVICs with TGF-β1 for 24 h leads to a significant increase in PAI-1 promoter luciferase activity that is not inhibited by U0126 treatment (Fig. 4.2B).

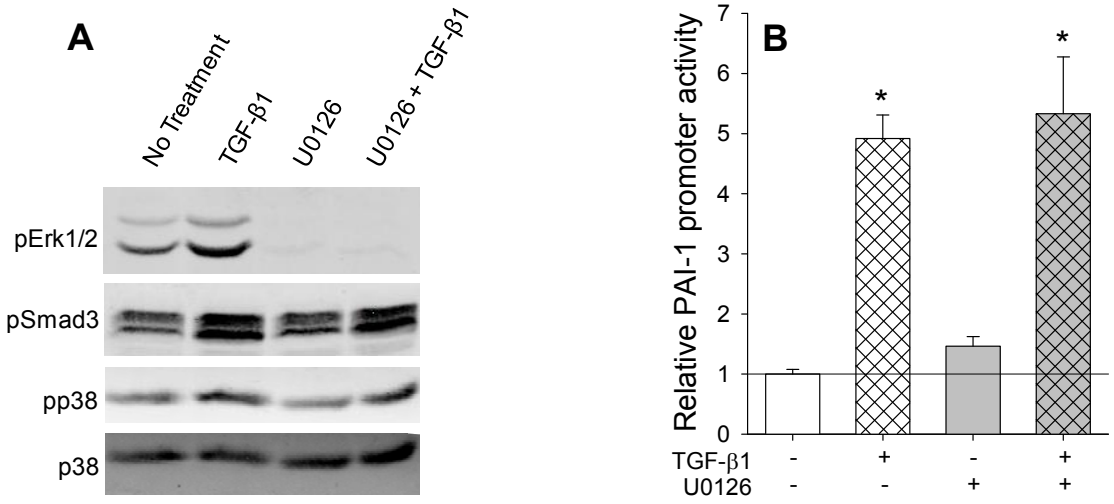

Fig. 4.2. U0126 does not interfere with canonical TGF-β1 signaling. (A) U0126 is a specific MEK1/2 inhibitor as indicated by the complete inhibition of pErk1/2 but no change in pSmad3 or pp38. (B) Similar to the pSmad3 results, U0126 does not inhibit PAI-1 promoter activity following TGF-β1 treatment. All error bars indicate standard error of the mean. * indicates significant difference ($p < 0.005$) versus control.

Erk1/2 Inhibition Suppresses TGF-β1 Induced Expression of Cadherin-11

AVICs treated with TGF-β1 for 24 h exhibit a significant increase in cadherin-11 mRNA compared to non-treated controls (Fig. 4.3A). This mRNA increase is completely inhibited by treating AVICs with U0126. Immunofluorescence images also indicate changes in cadherin-11 expression and cellular localization following the TGF-β1 and U0126 treatments (Fig. 4.3B). TGF-β1 treated AVICs exhibit cadherin-11 expression as indicated by FITC fluorescence between adjacent cells (with nuclei indicated by DAPI staining). Expression of cadherin-11 was not observed in AVICs treated with U0126 or in non-treated controls.

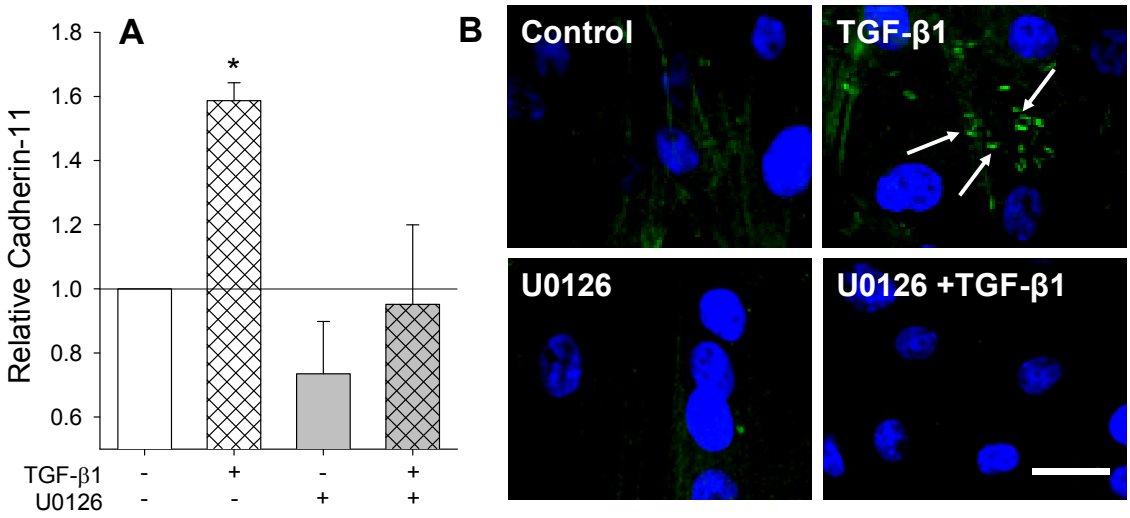

Fig. 4.3. TGF-β1 incubation for 24 h increases cadherin-11 expression in AVICs. (A) RT-PCR reveal a 1.58 fold increase in cadherin-11 mRNA in samples treated with TGF-β1 and a decrease in cadherin-11 mRNA with inhibition of MEK1/2. (B) Immunostaining show strong presence of cadherin-11 in TGF-β1 groups with minimal to no stain in other treatment groups. Scalebar = 10 μm. All error bars indicate standard error of the mean. * indicates significant difference ($p < 0.005$) versus control.

Cadherin-11 is Required for Elevated Intercellular and Calcific Nodules

Given that TGF-β1 induces expression of cadherin-11 in a manner that is inhibited by U0126, we were next interested in determining if upregulation of this protein plays a role in increased intercellular tension that is believed to lead to the formation of dystrophic calcific nodules *in vitro*. When a wound is introduced to statically cultured AVICs in 1.8 mM Ca^{2+}, a concentration that allows all cadherins to function, all treatment groups display increased intercellular tension as shown by larger wound areas compared to non-treated controls (Fig. 4.4A). However, when a wound is applied to AVICs in 0.45 mM Ca^{2+} media, a concentration that permits functionality of cadherin-11 but below the functional concentration for typical cadherins, only TGF-β1 treated AVICs exhibit a significantly increased wound area.

To determine if cadherin-11 expression is necessary for calcific nodule formation, we used siRNA to knockdown cadherin-11 in AVICs. AVICs treated with lipofectamine transfection reagent alone or in combination with a non-specific scramble siRNA construct generated robust calcific nodules following TGF-β1 treatment for 24 h and mechanical strain for an additional 24 h; however, AVICs transfected with siRNA specific to cadherin-11 exhibit dramatically reduced calcific nodule morphogenesis (Fig. 4.4B).

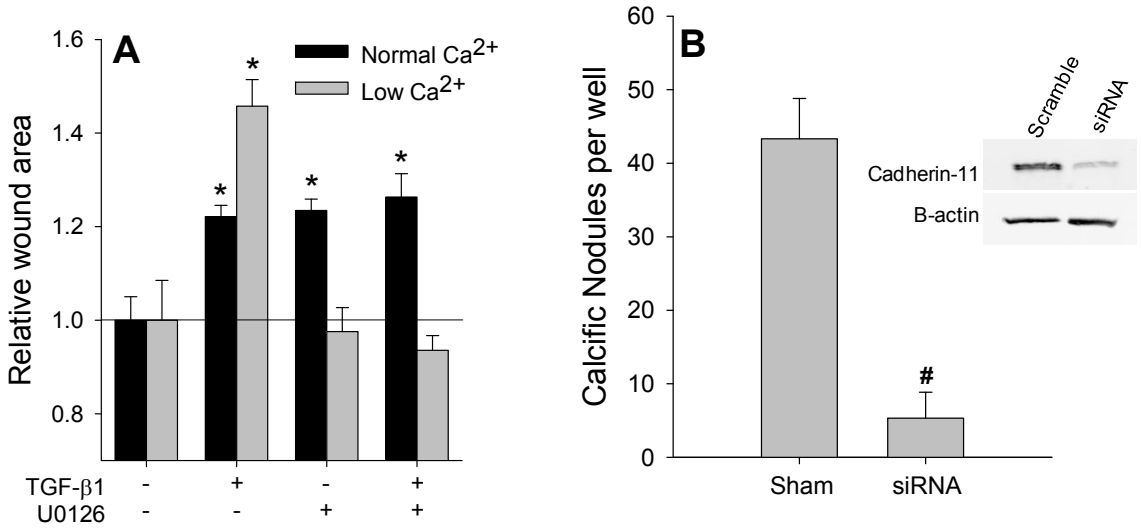

Fig. 4.4. Cadherin-11 generates intercellular tension through αSMA that enables calcific nodule morphogenesis. (A) Wound assay reveals strength of intercellular connection which correlates to wound area. At normal Ca^{2+} levels, with all cadherins functional, TGF-β1, U0126, and U0126 + TGF-β1 treatments all increased wound area size due to increased αSMA expression. However, at low Ca^{2+} levels, where cadherin-11 is still functional and others are not, TGF- β1 treated cells created a large wound. (B) siRNA knockdown of cadherin-11 reveal a sharp decline the calcific nodules generated. All error bars indicate standard error of the mean. * indicates significant difference ($p < 0.005$) versus control. # indicates significant difference ($p < 0.005$) versus Sham.

4.4. Discussion

Dystrophic calcification in CAVD has been associated with the pathological differentiation of AVICs to myofibroblasts, which is characterized by increased αSMA expression. Treating AVICs with U0126, however, indicates that the presence of αSMA is not sufficient to drive dystrophic calcification, leading to the hypothesis that there exist other relevant mechanisms that have not been elucidated. Here, we present data indicating that TGF-β1 treatment of AVICs leads to expression of the atypical cadherin, cadherin-11, and expression of this

intercellular adhesion protein is necessary for the development of dystrophic calcific nodules *in vitro* (Fig. 4.5).

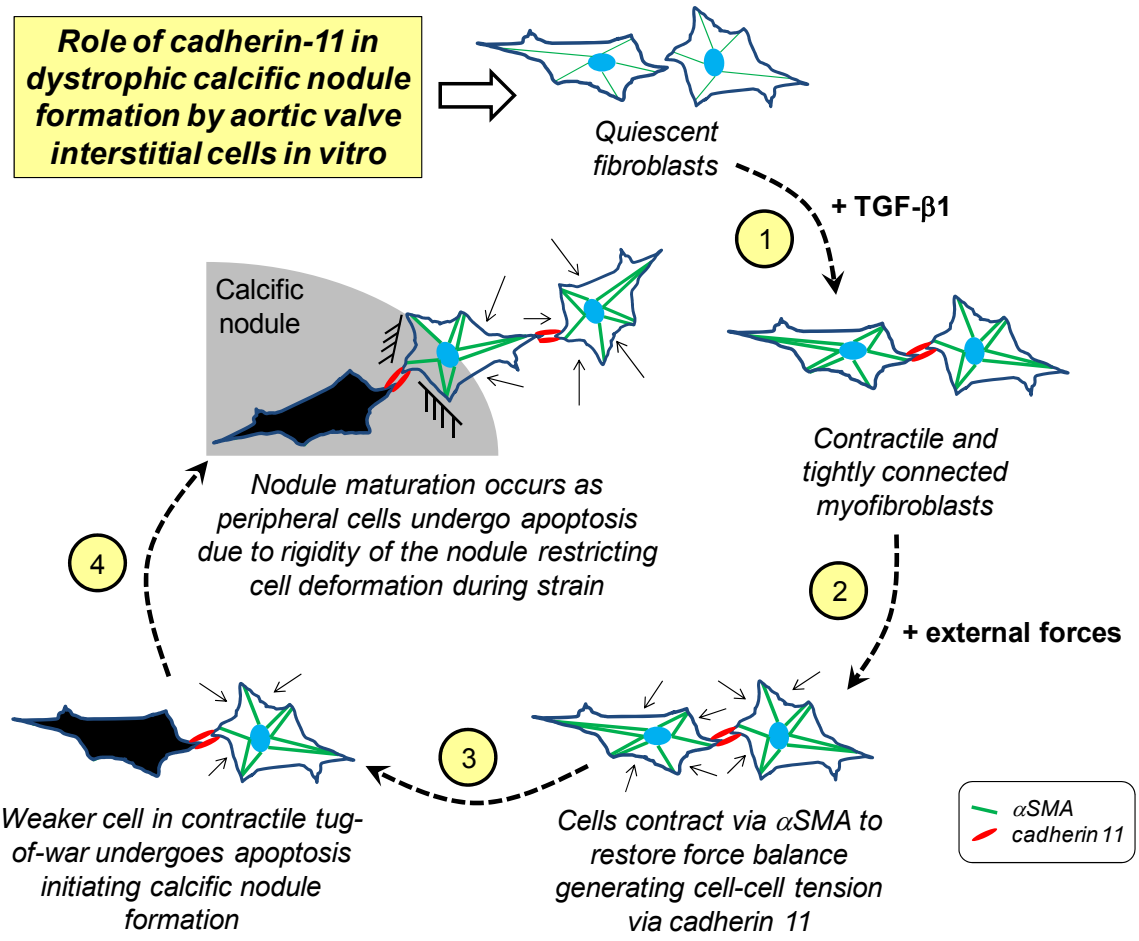

Fig. 4.5. Process of calcific nodule formation. Intercellular tension builds as contractile myofibroblastic AVICs become tightly connected through expression of cadherin-11. Release of this tension leads to cell aggregates that calcify through an apoptotic process.

Previous *in vitro* studies on dystrophic calcific nodule formation revealed the importance of αSMA as a mediator of the process. TGF-β1 treatment of AVICs led to increased expression of αSMA, which reinforces stress fibers and produces a more contractile cell. Benton et al. showed this increased contractility leads to contraction events that pull groups of cells from their neighboring cells resulting in cell aggregates that develop into calcific nodules through an

apoptosis driven pathway [93]. Recently, we found that mechanical strain exacerbated the formation of these aggregates by introducing a force imbalance on the monolayer whereby increased intercellular tension is overcome by the addition of externally applied strain [199]. This led us to theorize that TGF-β1 induced myofibroblast populations possessed higher intercellular tension than quiescent fibroblasts, thus making them more sensitive to mechanical strain and subsequent nodule formation.

Interestingly, distinct differences in cadherin expression have been observed in fibroblast and myofibroblastic populations with fibroblasts expressing N-cadherin and myofibroblasts expressing cadherin-11 [206]. Cadherin-11 junctions withstand twofold higher forces when compared to connections formed with N-cadherin [212]. Furthermore, upon application of forces, cadherin-11 expressing cells will continue to hold on and eventually rip at the plasma membrane while N-cadherin expressing cells release from each other [206]. These stronger intercellular contacts work synergistically with increased αSMA expression leading to the accumulation of tension within myofibroblast populations. To test the effect of cadherin-11 on elevated intercellular tension, we utilized a wound assay as described previously [199]; however, in this study we varied the concentration of extracellular Ca^{2+} to select for function of different cadherins. All cadherins require the presence of extracellular Ca^{2+} in order to function, but atypical cadherins such as cadherin-11 have a higher Ca^{2+} affinity (K_D ~ 0.2 mM) than normal cadherins [210]. Therefore, cadherin-11 functions at lower Ca^{2+} concentrations than normal cadherins such as N-cadherin (K_D =

0.7mM). This difference in cadherin Ca^{2+} affinity is reflected in the wound assay results. At the higher Ca^{2+} concentration, all cadherins are functional. TGF-β1 and U0126 treatments both lead to an increase in αSMA, thus an increase in AVIC contractility; therefore, these two treatment groups cause significant tension builds as the AVICs pull on each other in the monolayer, ultimately leading to large increases in wound area. When the extracellular Ca^{2+} is lowered such that only cadherin-11 is functional, intercellular tension does not build in the U0126 treated AVICs, and the wound area for this treatment group is not significantly different than non-treated controls. However, for TGF-β1 treated AVICs in the low Ca^{2+} case, the presence of cadherin-11 in AVICs treated with TGF-β1 alone allows intercellular tension to build in the monolayer, leading to a significant increase in wound area. Similarly, when siRNA is used to knockdown the expression of cadherin-11, calcific nodules failed to form after TGF-β1 treatment and mechanical strain. This indicates that robust cell-cell connectivity in conjunction with contraction events are both necessary for calcific nodule formation.

Expression of cadherin-11 by TGF-β1 is blocked by pre-treating AVICs with U0126, an inhibitor to MEK1/2. MEK1/2 is a MAPK kinase that when activated leads to phosphorylation of the MAPK Erk1/2. TGF-β1-induced phosphorylation of Erk1/2 has been observed in a wide-variety of cell types and has been shown to be necessary for numerous cellular responses [213-215]. Activation of Erk1/2 has also been shown to suppress αSMA expression in mouse embryonic fibroblasts [216]. Consistently, U0126 treatment leads to a

significant increase in αSMA expression in AVICs. Our previous results indicate that TGF-β1-induced expression of αSMA in AVICs requires phosphorylation of a different non-canonical MAPK p38 [211]. Therefore, it seems that these two non-canonical pathways may independently lead to expression of proteins that are characteristic of pathological differentiation of AVICs. In contrast, canonical TGF-β1 signaling leads to increased expression of PAI-1, and we have hypothesized that upregulation of PAI-1 through activation of the canonical Smad2/3 pathway may be involved a negative feedback of TGF-β1 signaling [211]. Therefore, the results of these studies suggest a divergence in TGF-β1 signaling that leads to AVIC myofibroblastic differentiation through activation of non-canonical pathways (p38 and Erk1/2) that each lead to a different cellular outcome that may be very important in CAVD, while canonical Smad pathways may not be directly involved in pathological signaling for CAVD. We believe that the results of this study may suggest a therapeutic approach for CAVD by targeting either of these non-canonical pathways or direct inhibition of cadherin-11 function.

In order for the current work to realize a larger clinical impact, the *in vitro* mechanisms and AVIC outcomes identified in this study should be further studied *in vivo*. Unfortunately, *in vivo* research into the mechanisms of CAVD is currently limited by the lack of an animal model that accurately recapitulates human pathology. However, we believe that identification of cadherin-11 may provide a useful tool for better understanding the pathogenesis of CAVD, and our results may have implications beyond solely elucidating mechanisms of calcific nodule formation. AVIC myofibroblast activation is believed to be one the earliest

processes in CAVD; however, early valvular changes are difficult to detect in patients. Very few markers of this differentiation are known, and the most commonly used ones such as αSMA do not lend themselves to imaging techniques due to their cytosolic expression. Since cadherin-11 is a transmembrane protein, it allows for targeting via molecular imaging tracers and may provide a molecular fingerprint for the onset of CAVD.

Chapter 5

Aim 2 – 5-HT_{2B} antagonism arrests non-canonical TGF-β1 signaling and prevents AVIC activation

Text for Chapter 5 taken from:

> Hutcheson, J.D., et al., *5-HT2B antagonism arrests non-canonical TGF-β1-induced valvular myofibroblast differentiation.* J Mol Cell Cardiol, 2012. In press.

5.1. Introduction

The lack of a therapeutic treatment for calcific aortic valve disease (CAVD) limits the clinical options available to patients, and this often results in physicians opting to delay surgical intervention until aortic valve (AV) replacement is absolutely necessary, leading to diminished AV function in the meantime. The development of a suitable therapeutic for CAVD depends on the ability to target the root etiology of the disease, which at the cellular level, is believed to be caused by activation of AV interstitial cells (AVICs) from a quiescent fibroblastic phenotype to a contractile myofibroblast phenotype characterized by the expression of smooth muscle α-actin (αSMA) and SM22α [48, 217]. Once activated, AVICs increase extracellular matrix deposition, leading to the fibrotic changes characteristic of the onset of CAVD [218]. End-stage CAVD is

characterized by the formation of bone-like calcific nodules within stenotic leaflets, severely compromising the biomechanical integrity of the AV [9]. In order to develop a strategy to prevent CAVD, a more thorough understanding of the cellular signaling that leads to the subsequent tissue level changes involved in the progression of CAVD is needed to elucidate relevant therapeutic targets.

Transforming growth factor-β1 (TGF-β1) is highly expressed in diseased AV leaflets and has been the most extensively studied cytokine initiator of AVIC activation and CAVD [9-10, 48]. TGF-β1 ligand binding at its type II receptor (TβRII) leads to recruitment and activation of the type I TβR, Alk5, which canonically elicits a wide variety of cellular processes by signaling through the transcription factors Smads 2 and 3 [53]. Many studies have also focused on non-canonical signaling pathways to explain the myriad of cellular responses induced by TGF-β1 ligand binding, and p38 MAPK pathways have been identified as key mediators of cellular processes such as cell migration and mesenchymal transformations [55-57], which are characterized by upregulation of contractile elements similar to those identified in myofibroblast activation. In addition, recent studies have demonstrated that TGF-β1-induced phosphorylation of p38 in epithelial cells is dependent upon phosphorylation of TβRII by Src tyrosine kinase [58].

Unfortunately, the ubiquity associated with its signaling makes direct inhibition of TGF-β1 a poor therapeutic strategy for CAVD. Further, the relative contributions of canonical and non-canonical TGF-β1 signaling in leading to myofibroblast activation of AVICs are unknown. Here, we were interested in

studying the interaction between a specific G protein-coupled receptor (GPCR) highly localized to cardiopulmonary tissues, the serotonin 2B receptor (5-HT_{2B}), with TGF-β1 signaling, and assessing the potential of targeting this receptor for prevention of CAVD. The motivation for this study stems from the finding that agonism of 5-HT_{2B} was the major culprit in the development of pathologic AV alterations that led to the recall of norfenfluramine, a popular drug used to treat obesity, and pergolide, a drug used to treat Parkinson's disease [133, 157]. 5-HT_{2B} agonists were found to lead to AVIC myofibroblast activation in a TGF-β1-dependent manner [12, 219]; therefore, we hypothesized that antagonism of 5-HT_{2B} opposes TGF-β1-mediated myofibroblast activation of AVICs. In support of our hypothesis, antagonism of 5-HT_{2B} has been shown to induce anti-fibrotic responses in animal models of cardiac hypertrophy and pulmonary fibrosis [13, 15]; however, the molecular mechanisms of this action remain unclear, and the ability of 5-HT_{2B} antagonism to directly inhibit TGF-β1-mediated myofibroblast activation of AVICs has not been examined. We believe that the results of this study may lead to novel therapeutic strategies for CAVD and should be studied further.

5.2. Methods

AVIC Isolation and Culture

AVICs were isolated from porcine valves obtained from a local abattoir by dissecting the valve cusps from the surrounding muscle and digested with

collagenase. Isolated AVICs were then cultured at 37^{o}C and 5% CO_2 on T-75 tissue culture treated flasks in cell growth media consisting of DMEM supplemented with 10% fetal bovine serum (FBS), 1% penicillin/streptomycin antibiotic, and 1% amphotericin B antifungal. Previous studies have shown that AVICs retain phenotypic plasticity up to 10 passages after initial harvest [220]. We have observed phenotypic changes as early as 7 passages after harvest; therefore, we did not exceed this maximum limit and for this study, when AVICs ceased to respond to TGF-β1 treatment, as indicated by αSMA expression, they were excluded.

Antagonist and Inhibitor Treatments

For all assays of AVIC activation (αSMA and SM22α), AVICs were cultured in DMEM with 1% serum. For all assays of phosphorylation events, treatments were given in serum free DMEM. Unless otherwise noted, 1 μM 5-HT_{2B} antagonists (SB204741 and SB228357, both from Tocris) were added 30 min prior to the addition of 1 ng/ml active TGF-β1 (R&D Systems). SB204741 was chosen due to its high selectivity to 5-HT_{2B} (pK_i = 7.95) compared to the closely related 5-HT_{2A} (pK_i < 5.2) and 5-HT_{2C} (pK_i = 5.82) receptors [221]. SB228357 is a mixed 5-$HT_{2B/2C}$ antagonist that is orally active and has been shown to display inverse agonist properties [222] at 5-HT_{2C}. Given that 5-HT_{2C} receptors have been shown to be minimally expressed in AVICs [133] (supported by PCR data in our lab), we chose to use this as an additional 5-HT_{2B} antagonist in the present study. Concentrations of the antagonists were chosen to ensure

maximum receptor binding based upon the pK_i values given by the manufacturer and crude dose response analyses performed in our laboratory to determine efficacy and potency of TGF-β1 inhibition. Small molecule inhibitors of Alk5 (2 μM SB431542, Tocris), p38 (10 μM SB203580, Tocris), or Smad3 (10 μM SIS3, Sigma) were also added 30 min prior to TGF-β1 in appropriate samples.

AVIC Viability and Proliferation Assay

AVIC viability was assessed using Calcein AM (Invitrogen) and propidium iodide (Invitrogen) stains. Calcein AM is cleaved by esterases within viable cells to exhibit a green fluorescence, and propidium iodide emits red fluorescence only after traversing the compromised plasma membrane of non-viable cells and binding to DNA. Therefore, viable cells were identified by green, but not red, fluorescence, and non-viable cells were identified by red, but not green fluorescence. A positive control was utilized to ensure efficacy of the viability assay by fixing AVICs with 3.7% formaldehyde to render them non-viable. To assess proliferation, AVICs were seeded at the same density and treated with one of the two 5-HT_{2B} antagonists. After 24 h, AVICs were harvested and counted. The harvested cell counts were then compared to non-treated controls to determine changes in proliferation.

Electroporation Transfection Protocol

AVICs were harvested via trypsinization and resuspended at 2 x 10^6 cells/ml in cytomix buffer supplemented with ATP and glutathione. This buffer is designed to mimic cytosolic composition in order to maintain cellular homeostasis during poration. This AVIC suspension was loaded into 4 mm electroporation cuvettes along with 20 µg of the plasmid to be delivered. AVICs were then subjected to an exponential decay electroporation protocol using a capacitance of 500 µF and a peak voltage of 350 V. Following electroporation, the cuvettes were placed on ice for 10 min to allow the AVICs to recover. After this recovery incubation, AVICs were resuspended in culture media and reseeded onto the appropriate growth surface.

Quantification of Myofibroblast Activation

AVICs were lysed with Cell Lytic M lysis buffer (Sigma) supplemented with protease inhibitor cocktail (Roche) and centrifuged to remove membrane components. The collected cell lysates were frozen at -80^{o}C for storage; each frozen cell lysate was thawed and assayed for total protein content using a standard Bradford Assay. αSMA was quantified using indirect ELISA after verifying antibody specificity by Western blotting. Briefly, 100 µl of 5 µg/ml cell lysate solution was adsorbed onto the bottom of 96 well plates by overnight incubation in a carbonate/bicarbonate buffer (pH 9.6). The high pH buffer reduces inter-protein interactions to give an even distribution of proteins within the wells. Non-specific binding sites on the well were blocked using 5% milk in phosphate-buffered saline (PBS) for at least 1.5 h at room temperature.

Following this step, 100 µl of polyclonal antibody to αSMA (1:200 in blocking solution) was added to each well and allowed to incubate at room temperature for 1.5 h. After washing the wells 3 times with PBS, each plate was incubated for 1 h with a secondary antibody linked to a peroxidase enzyme. Subsequently, the plates were washed thoroughly with PBS to remove unbound secondary antibodies and each well will receive 100 µl of a detection substrate that reacts in the presence of peroxidase to give a product with a characteristic absorbance. The absorbance of each well was detected using a plate reader, and the αSMA content of each sample was compared to a standard curve created using αSMA peptide to calculate the concentration of αSMA in each sample.

SM22α has also been shown to be an early marker of smooth muscle-like differentiation [223], and has been detected in diseased AV leaflets [217]. Therefore, we utilized a partial promoter to SM22α that was subcloned into a luciferase reporter plasmid (p-441SM22luc) as a measure of SM22α promoter activity [224]. This vector was introduced into AVICs via electroporation prior to the addition of GPCR antagonist or TGF-β1 treatments. Following electroporation, AVICs were seeded into 12-well plates and allowed to recover for 24 h. After 24 h of the prescribed treatment, AVICs were lysed using 200 µl reporter lysis buffer, and 20 µl of this lysate solution was added to a well of a 96-well plate. Luciferase activity was detected by adding 100 µl luciferase substrate to each well and recording the luminescent product using a plate reader.

Calcific Nodule Formation and Detection

To study the effects of 5-HT_{2B} antagonism on calcific nodule morphogenesis as in [199], AVICs were cultured in BioFlex® culture plates to 100% confluence on the growth surface. After reaching confluence, AVICs were treated with either 1 ng/ml TGF-β1 alone or in combination with 1 μM 5-HT_{2B} antagonist for 24 h. After this incubation period, the treatments were replaced with cell culture media and subjected to 15% cyclic strain at 0.75 Hz for 24 h. Following this strain regimen, calcific nodules were identified using Alizarin Red staining to assay for calcium phosphate deposition. AVICs were fixed in 3.7% formalin and 1 ml of Alizarin solution was added to each well for 30 min. The wells were then washed thoroughly with PBS and imaged with conventional microscopy. To ensure that the calcific nodules formed were due to an apoptosis-driven dystrophic process, we utilized an Annexin V/propidium iodide apoptosis assay as described previously [199]. Briefly, AVICs were rinsed with PBS and stained with Annexin V conjugated with Alexa fluor 488 (5% solution in Annexin binding buffer; Invitrogen) for 15 minutes to detect apoptotic cells. Propidium Iodide (0.4% solution in Annexin binding buffer; Invitrogen) was used as a counter-stain for necrotic cells. Apoptosis and necrosis images were taken after 24 h of mechanical strain using a fluorescence microscope (Nikon TE300 Inverted Tissue Culture Microscope).

Assays for Canonical and Non-canonical TGF-β1 Signaling

AVICs were lysed in RIPA buffer either 15 min or 1 h after AVICs were treated with the prescribed treatment. Lysate solutions were centrifuged to remove lipid components, and total protein concentration was determined using a BCA protein analysis. All proteins were denatured by boiling the samples with β-mercaptoethanol, and gel electrophoresis was used to separate the proteins based upon size. Western blotting was then used to assay for pSmad3, pp38, pSrc, and pCas, and antibodies to the total protein of interest (i.e., both phosphorylated and unphosphorylated forms) were used to establish proper protein loading. PAI-1 promoter activity was also used to assay for canonical TGF-β1 signaling after 24 h of treatment. To assay for this activity, we utilized a partial PAI-1 promoter (p3TP-lux) subcloned into a luciferase reporter plasmid [54]. This plasmid was transfected into AVICs using the electroporation methods described above, and luciferase activity was assayed according to the methods detailed for SM22α promoter activity.

Src Plasmids for AVIC Transfection

To examine the effects of Src activity on AVIC phenotype, AVICs were transfected via electroporation with a vector to express a constitutively active version of Src whereby the autoinhibitory site, tyrosine 527, was mutated to express a phenylalanine residue [225]. Transfection of this mutated Src was verified using Western blotting. For real-time fluorescence imaging of Src

trafficking within the cell, a wild-type Src plasmid fused to a mCherry fluorescent reporter was transfected into AVICs. Time-lapse images were collected using a spinning disk Nikon Eclipse TE-2000 confocal microcope equipped with a Photometrics Cascade 512B camera. Both Src plasmids were generous gifts from the laboratory of Irina Kaverina.

Statistical Analyses

The data are reported as the mean of all replicates, and error is given as standard error of the mean (sample sizes < 30). For each experiment the reported n value indicates independent biological replicates. Statistical significance between treatments was determined by one-way ANOVA, and pairwise differences were identified using post-hoc Holm-Sidak testing.

5.3. Results

5-HT_{2B} antagonism inhibits AVIC activation and calcific nodule formation

Two structurally dissimilar antagonists to 5-HT_{2B}, SB204741 and SB228357, were examined for their ability to inhibit TGF-β1-induced myofibroblast activation in isolated porcine AVICs. Consistent with previous studies [48], AVIC activation was induced by incubation with 1 ng/ml TGF-β1 for 24 h, exhibiting a two-fold increase in both αSMA protein expression and SM22α promoter activity (Fig. 5.1A). Treating AVICs with 1 μM of either SB204741 or

SB228357 for 30 min prior to and continuing during TGF-β1 incubation abrogates TGF-β1-induced myofibroblast activation of AVICs in the same manner as a direct inhibitor of Alk5.

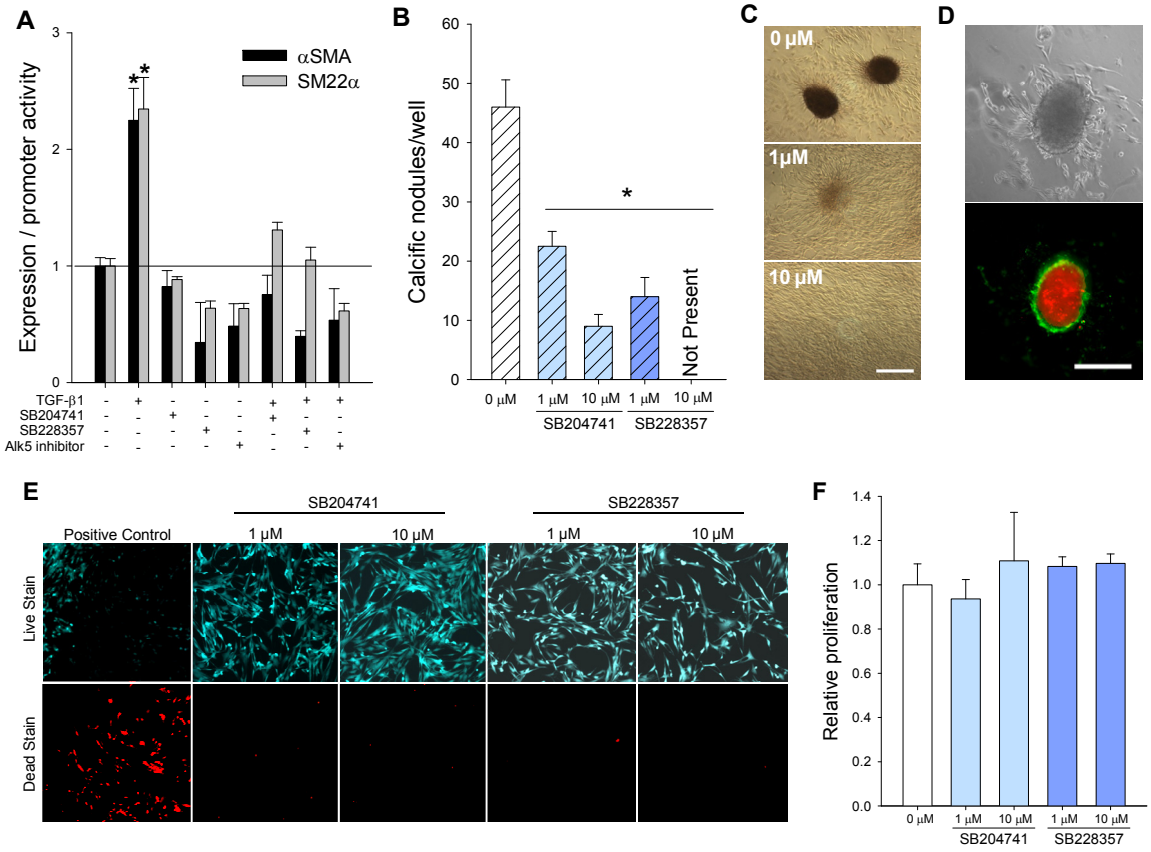

Fig. 5.1. 5-HT$_{2B}$ antagonism prevents TGF-β1-induced myofibroblast activation and calcific nodule morphogenesis in AVICs. A, Treating AVICs with 1 ng/ml TGF-β1 for 24 h leads to a significant increase in markers for myofibroblast activation, αSMA expression and SM22α promoter activity. Both of these myofibroblast activation markers are reduced to basal levels by pretreating AVICs with either of two 5-HT$_{2B}$ antagonists, SB204741 or SB228357, or an inhibitor of Alk5 (n ≥ 3). **B,** Adding 15% strain to TGF-β1 treated AVICs leads to calcific nodule morphogenesis that is decreased in a dose dependent manner by treatment with SB228357 ($p < 0.005$, n = 3). **C,** Calcific nodules were identified using Alizarin Red staining to identify regions with high calcium content. **D,** Calcific nodules were found to be dystrophic with an apoptotic ring (green) of AVICs surrounding a necrotic core (red). Images shown indicate bright field and fluorescence of a single calcific nodule. **E,** Live AVICs were stained green with Calcein AM and dead AVICs were stained red with propidium iodide. Neither 5-HT$_{2B}$ antagonist appear to have a deleterious effect. **F,** The 5-HT$_{2B}$ antagonists do affect AVIC proliferation over 24 h. All error bars indicate standard error of the mean. * indicates significant difference ($p < 0.005$) versus control. Scale bar = 250 μm.

The data indicate that 5-HT_{2B} antagonism can prevent AVIC myofibroblast activation, an early event in CAVD, so we were also interested in assessing changes in calcific nodule formation, an endpoint in CAVD. Studies indicate that 83% of excised calcific AV leaflets from human patients are dystrophic [202] and appear to be driven by a TGF-β1-induced apoptotic mechanism [9]. Our lab has recently developed a model system that recapitulates the formation of dystrophic calcific nodules *in vitro* [199]; AVICs treated with TGF-β1 for 24 h prior to the addition of 15% cyclic strain for 24 h form robust calcific nodules that are correlated with αSMA expression. These results are consistent with previous studies that have shown that αSMA expression is necessary for nodule formation by AVICs in static culture [93] and that TGF-β1 is required for the formation of nodules in mechanically strained excised aortic valve leaflets [11]. Here, AVICs were treated with either 1 ng/ml TGF-β1 or a combination of TGF-β1 and 5-HT_{2B} antagonist for 24 h prior to the addition of strain (Fig. 5.1B). Calcific nodules were identified using Alizarin Red staining to detect calcium accumulations (Fig. 5.1C), and as shown previously [199], these nodules form via a dystrophic mechanism as indicated by an outer ring of apoptotic AVICs, as indicated by green fluorescent Annexin V, surrounding a red fluorescent propidium iodide stained necrotic core (Fig. 5.1D). AVICs treated with 1 μM SB228357 or SB204741 form significantly fewer and less mature calcific nodules than the TGF-β1 treated positive control, and 10 μM SB204741 further reduces nodules while SB228357 completely inhibits the formation of any calcific nodules. It should be noted that

the antagonist treatments did not affect AVIC viability (Fig. 5.1E) or proliferation (Fig. 5.1F).

5-HT$_{2B}$ antagonism prevents TGF-β1-induced p38 phosphorylation

The data indicate that antagonism of 5-HT$_{2B}$ inhibits both myofibroblast activation of AVICs as well as calcific nodule morphogenesis *in vitro*. We were next interested in assessing the effects of 5-HT$_{2B}$ antagonism on canonical TGF-β1 Smad signaling. Specifically, Smad3 signaling has been shown to direct a wide variety of TGF-β1-induced cellular responses through direct binding of these transcription factors to gene regulatory elements. Plasminogen activator inhibitor-1 (PAI-1) is one example of a protein that is expressed by Smad3 phosphorylation (pSmad3) and nuclear translocation across many cell types [54]. Thus, we used a plasmid construct with a partial PAI-1 promoter region (p3TP-lux) linked to expression of a luciferase reporter gene to assay for canonical TGF-β1 signaling. Interestingly, 5-HT$_{2B}$ antagonism does not inhibit canonical TGF-β1 signaling as indicated by pSmad3 and PAI-1 promoter activity (Fig. 5.2A-B).

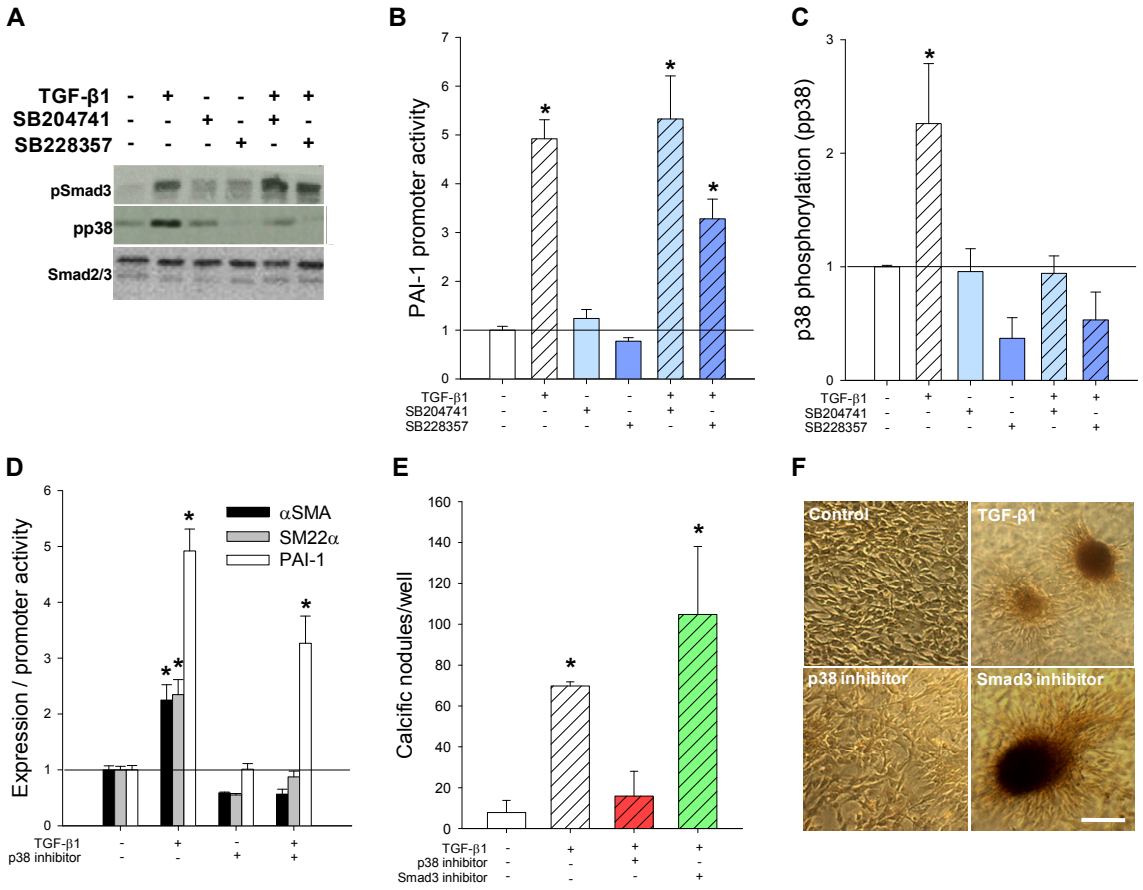

Fig. 5.2. 5-HT$_{2B}$ antagonism prevents non-canonical p38 MAPK but not canonical Smad3 signaling. A, TGF-β1 treatment leads to increased Smad3 phosphorylation (pSmad3) after 15 min and p38 phosphorylation (pp38) after 1 h. 5-HT$_{2B}$ antagonism inhibits TGF-β1-induced pp38 but not pSmad3. **B,** 24 h of TGF-β1 treatment leads to a five-fold increase in canonical PAI-1 promoter activity that is not inhibited by either of the 5-HT$_{2B}$ antagonists (n ≥ 3). **C,** Average densitometry (n = 5) reveals a two-fold increase in pp38 after TGF-β1 treatment that is completely inhibited by 5-HT$_{2B}$ antagonism. **D,** p38 inhibitor blocks TGF-β1-induced αSMA expression and SM22α promoter activity but not PAI-1 promoter activity. **e,** p38 inhibition blocks TGF-β1-induced calcific nodule morphogenesis but Smad3 inhibitor did not. **d,** Representative images indicate the presence of calcific nodules in AVICs treated with TGF-β1 alone or in combination with Smad3 or p38 inhibitors. All error bars indicate standard error of the mean. * indicates significant difference ($p < 0.005$) versus control. Scale bar = 250 mm.

Due to the lack of canonical changes, we next assessed possible non-canonical interactions. Many studies have focused on non-canonical signaling pathways to explain the myriad of cellular responses induced by TGF-β1 ligand binding. Particularly, p38 MAPK pathways have been identified as key mediators of cellular processes such as cell migration and mesenchymal transformation [58, 226-227], which are characterized by upregulation of contractile elements similar to those identified in myofibroblast activation. TGF-β1 treated AVICs exhibit a 2.3-fold increase in p38 phosphorylation (pp38), which is completely inhibited by both 5-HT_{2B} antagonists (Fig. 5.2A,C). Additionally, a p38 inhibitor mitigates TGF-β1-induced αSMA expression and SM22α promoter activity but does not significantly inhibit canonical PAI-1 promoter activity (Fig. 5.2D). Similarly, p38 inhibition also prevents TGF-β1-mediated calcific nodule formation, while a specific inhibitor of Smad3 does not reduce the formation of calcific nodules by AVICs (Fig. 5.2E-F).

Function and spatial location of Src tyrosine kinase are altered by 5-HT_{2B} antagonism

TGF-β1-mediated phosphorylation of p38 has recently been shown to be dependent upon phosphorylation of TβRII at tyrosine 284 by Src tyrosine kinase [58]. In addition, 5-HT_{2B} has been shown to activate platelet-derived growth factor receptors intracellularly via Src activation [139]. Given that 5-HT_{2B} antagonism prevents TGF-β1-mediated p38 phosphorylation, we expected an upstream inhibition of Src phosphorylation, which would prevent its interaction

with TβRII. Therefore, we assessed the effect of TGF-β1 treatment and 5-HT_{2B} antagonism on Src phosphorylation at its active site, tyrosine 418 (pSrc). Treating AVICs with TGF-β1 leads to increased levels of pSrc in a manner that is abrogated by treatment with an Alk5 inhibitor, indicating that pSrc induction is downstream of Alk5 activation by TβRII after TGF-β1 ligand binding (Fig. 5.3A).

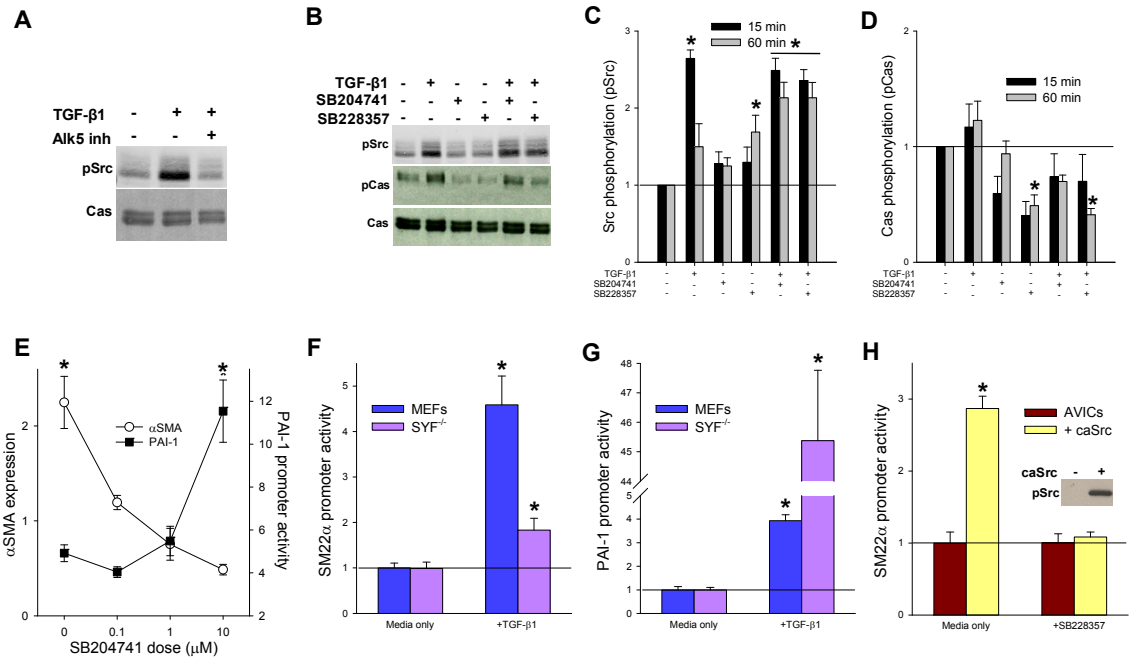

Fig. 5.3. 5-HT_{2B} antagonism inhibits Src function. A, TGF-β1 induces Src phosphorylation (pSrc) after 15 min of incubation that is inhibited by an Alk5 inhibitor. **B,** Neither 5-HT_{2B} antagonist inhibit TGF-β1-induced pSrc; however, pCas is reduced with antagonist treatment in the presence of TGF-β1. **C,** Average densitometry (n = 6) reveal a 2.5-fold increase in pSrc by TGF-β1 at 15 min that return to near basal levels after 1 h. pSrc levels remain elevated in AVICs treated with TGF-β1 and either 5-HT_{2B} antagonist after 1 h. **D,** Average densitometry (n = 4) reveals that TGF-β1 treatment leads to a trending increase in Cas phosphorylation (pCas); however, 5-HT_{2B} antagonists reduce pCas to sub-basal levels. **E,** Increasing doses of SB204741 lead to decreasing αSMA but increasing PAI promoter activity in AVICs treated with TGF-β1 (n = 3). **F,** $SYF^{-/-}$ MEFs exhibit significantly less SM22α promoter activity compared to wild-type MEFs following 24 h of TGF-β1 treatment. **G,** $SYF^{-/-}$ genetically modified MEFs exhibit a 45-fold increase in PAI-1 promoter activity due to TGF-β1, whereas wild-type MEFs exhibit a four-fold increase in PAI-1 promoter activity. **H,** AVICs transfected to express constitutively active Src (caSrc) exhibit significantly greater SM22α promoter activity independent of TGF-β1, and SB228357 abrogates this increase. * indicates significant difference ($p < 0.005$) versus control.

TGF-β1-induced pSrc peaks at 15 min post-stimulation and returns to near control levels after 1 h. Surprisingly, 5-HT_{2B} antagonism does not affect pSrc induction after 15 min of TGF-β1 stimulation (Fig. 5.3B-C). In fact, 1 h treatment with SB228357 alone leads to a significant increase in pSrc, and the combination of either 5-HT_{2B} antagonist with TGF-β1 leads to a sustained activation of Src at 1 h. To assess changes in the downstream function of pSrc, we assayed for phosphorylation within the substrate domain of Crk associated substrate (pCas), a major downstream target of pSrc [228]. Interestingly, 5-HT_{2B} antagonism reduces pCas to below basal levels even in cases where pSrc is significantly increased (Fig. 5.3B, D). This finding is unusual since increased Src phosphorylation typically results in increased pCas.

Previous studies have shown that pCas serves as a negative regulator of canonical TGF-β1 signaling by inhibiting phosphorylation of Smad3 [59]. Therefore, we hypothesized that since 5-HT_{2B} antagonism appears to inhibit pCas, pSmad3 is not inhibited and canonical signaling is subsequently enhanced. This can be seen with increasing doses of 5-HT_{2B} antagonist in the presence of TGF-β1, which lead to progressive decreases in αSMA expression after 24 h, while canonical TGF-β1 signaling, as shown by PAI-1 promoter activity, is increased in response to the non-canonical inhibition (Fig. 5.3E). To verify this counterintuitive response, we examined wild type mouse embryonic fibroblasts (MEFs) and MEFs with genetically deleted Src family kinases (Src, Yes, Fyn; $SYF^{-/-}$) when exposed to TGF-β1. As expected, $SYF^{-/-}$ MEFs exhibit significantly less SM22α promoter activity and significantly higher PAI-1 promoter

activity compared to wild type MEFs (Fig. 5.3F-G), indicating that Src function is important in non-canonical TGF-β1 signaling and is also involved in the suppression of canonical signaling. In AVICs, 5-HT_{2B} antagonism may alter the functionality of Src without directly affecting Src phosphorylation to decrease non-canonical but increase canonical TGF-β1 signaling. To examine this hypothesis, AVICs were transfected to express a constitutively active Src (caSrc), whereby tyrosine 527, the autoinhibitory Src phosphorylation site, is mutated to phenylalanine, thereby preventing phosphorylation at this site and the subsequent conformational change that inhibits Src kinase activity. Expression of caSrc significantly increases SM22α promoter activity in AVICs after 24 h independent of TGF-β1 ligand in the media and in a manner that is completely inhibited by 5-HT_{2B} antagonism (Fig. 5.3H).

Thus far, the data indicate that 5-HT_{2B} antagonism leads to a change in Src functionality, independent of Src phosphorylation. This subsequently prevents association with downstream substrates resulting in decreased Cas and p38 phosphorylation, thereby preventing TGF-β1-induced myofibroblast activation in AVICs. Recent studies suggest that endosomal trafficking and changes in the cellular localization of Src may affect its downstream signaling [229]. Therefore, we used confocal microscopy to assess changes in Src trafficking dynamics before and after 5-HT_{2B} antagonism.

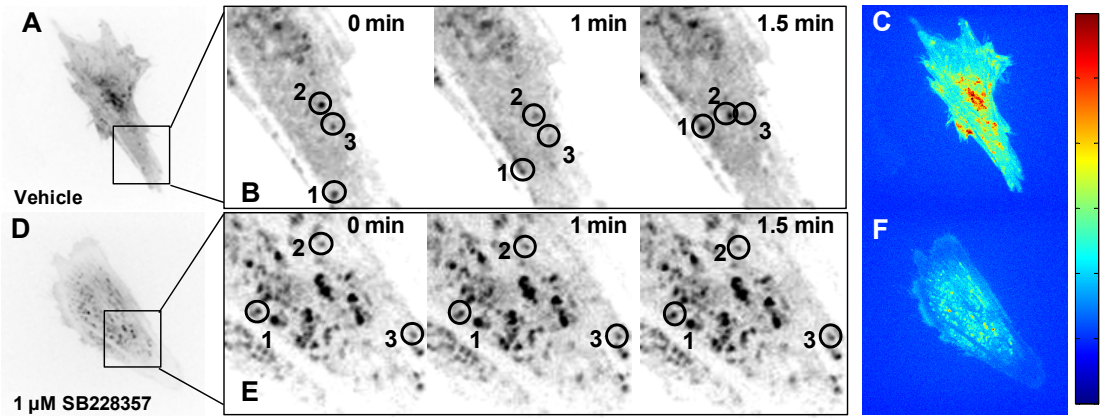

Fig. 5.4. 5-HT$_{2B}$ antagonism arrests Src motility within AVICs. A, AVICs transfected with mCherry-N$_1$-Src and treated with DMSO vehicle for 1 h were imaged by time-lapse microscopy using a spinning disk Nikon Eclipse TE-2000 confocal microcope equipped with a Photometrics Cascade 512B camera. Images were taken every 15 s for a total of 15 min. **B,** A subsection of a DMSO vehicle treated AVIC allows for clear identification of Src movement at t = 0, 1, and 1.5 min. **C,** Eulerian based analysis of pixel intensity changes within the image over the course of 15 min represents Src kinematics. Red indicates a high degree of movement, and blue indicates little movement within a pixel. **D, E,** AVICs treated with 1 μM SB228357 for 1 h exhibit little to no movement at t = 0, 1, and 1.5 min. **F,** 5-HT$_{2B}$ antagonism arrests Src movement over the 15 min imaging time.

AVICs were transfected to express fluorescently-labeled wild-type Src (Fig. 5.4A-F), and images were captured after 1 h of treatment once every 15 s for a total of 15 min. AVICs treated with dimethyl sulfoxide (DMSO) vehicle alone indicate free and rapid movement of the fluorescently labeled Src proteins within the cell. A representative section of a DMSO-treated AVIC (Fig. 5.4B) exhibits altered spatial localization of three labeled Src proteins at 1 min and 1.5 min of imaging. To capture the overall Src kinematics across the entire cell an Eulerian approach was used whereby the change in intensity for each pixel is calculated over time as a representative measure of the movement of Src both within and out of the plane of focus. These values were then used to create a heat map of the image with red indicating a high degree of pixel intensity variation (i.e. Src

movement) during the 15 min of imaging and blue indicating little variation over time (Fig. 5.4C). AVICs treated with 1 μM SB228357 for 1 h (Fig. 5.4D) exhibit little change in spatial localization of fluorescently-labeled Src proteins over the course of 1.5 min (Fig. 5.4E). Similarly, the Eulerian analysis of the 5-HT_{2B} antagonist treated AVIC (Fig. 5.4F) indicates little fluctuation in pixel intensity over the 15 min imaging interval compared to the DMSO-treated control AVIC. The entire time-lapse sequence shows the clear effect of the antagonist over 15 min.

5.4. Discussion

The major impact of this study is three-fold: 1) non-canonical p38, but not canonical Smad3, signaling is required for TGF-β1-mediated myofibroblast activation in AVICs, 2) non-canonical TGF-β1 signaling, and thus myofibroblast activation of AVICs, can be arrested by 5-HT_{2B} antagonism, and 3) 5-HT_{2B} antagonism physically restricts Src, preventing downstream signaling. The relative contributions of Smad3 and p38 signaling in AVICs were previously unknown. These data indicate that TGF-β1 signaling activates both canonical Smad and non-canonical p38 MAPK pathways, and in AVICs, both appear to depend on activation of Alk5 after ligand binding (Fig. 5.5A). Previous studies have demonstrated that activation of Src and non-canonical signaling actually suppresses canonical TGF-β1 signaling [59]. Our results indicate that non-canonical signaling may play a more substantial role in driving myofibroblast

activation of AVICs than canonical signaling. Inhibition of p38 was found to completely inhibit TGF-β1-induced upregulation of myofibroblast markers. Additionally, p38 inhibition prevented the formation of calcific nodules by AVICs, whereas inhibition of the canonical Smad3 pathway did not prevent TGF-β1-induced nodule morphogenesis. These results may elucidate new therapeutic targets (in addition to 5-HT_{2B} antagonists) that interact with p38 MAPK signaling to inhibit myofibroblast activation of AVICs by TGF-β1.

This study is also the first to indicate a direct interaction between a specific GPCR, 5-HT_{2B}, and non-canonical TGF-β1 signaling. Further, we have identified a novel signaling mechanism wherein a physical arrest of Src tyrosine kinase trafficking by 5-HT_{2B} antagonism prevents its association with the downstream substrate Cas (Fig. 5.5B) and likely TβRII, which prevents pp38 [58]. This action results in an inhibition of non-canonical p38 activation, which is necessary to induce AVIC myofibroblast differentiation, while simultaneously stimulating canonical Smad3 activation and resultant PAI-1 expression, which may be involved in the negative regulation of TGF-β1 activity [230]. PAI-1 inhibits the activation of the protease plasmin from plasminogen. Active plasmin degrades fibrin (a component of the ECM), and has been shown to lead to the activation of latent TGF-β1 [51, 230]. The major physiological purpose of TGF-β1-induced myofibroblast differentiation is ECM secretion and remodeling. PAI-1 may then work to inhibit further plasmin activation, thus preventing continued breakdown of the ECM and further activation of TGF-β1 and effectively turning off the ECM repair process. Therefore, enhanced canonical signaling due to 5-

HT_{2B} antagonism may not be detrimental *in vivo* given the inhibition of non-canonical signaling and resulting decrease in cellular differentiation.

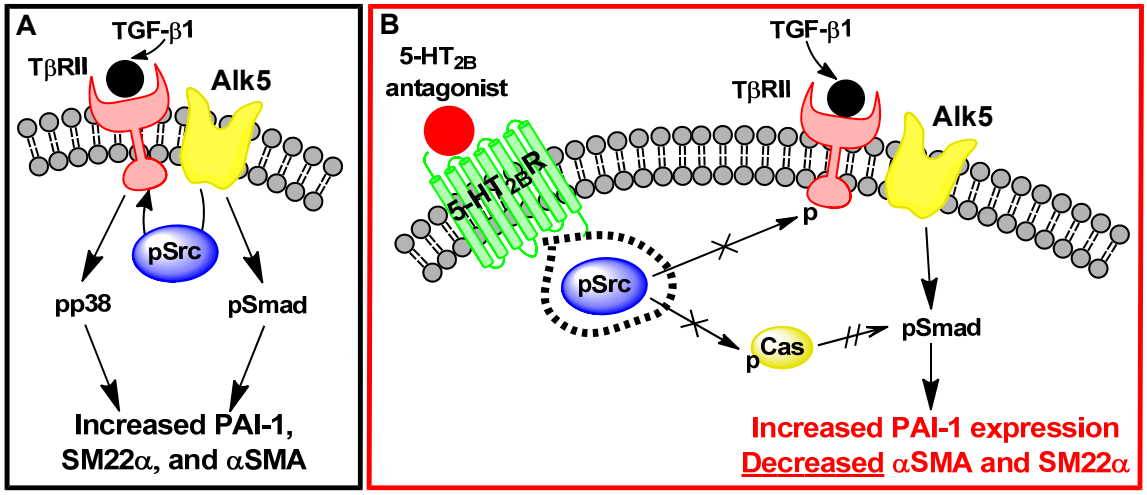

Fig. 5.5. Proposed mechanism of 5-HT_{2B} antagonist inhibition of TGF-β1 signaling. A, TGF-β1 ligand binding to TβRII leads to Alk5-dependent canonical signaling through Smad phosphorylation (pSmad) and non-canonical signaling through Src phosphorylation (pSrc) and subsequent p38 phosphorylation (pp38). **B,** Treatment with a 5-HT_{2B} antagonist physically sequesters pSrc preventing non-canonical TGF-β1 signaling by restricting Src's ability to phosphorylate TβRII and Cas (indicated with x on arrows), but enhancing canonical signaling by suppressing Cas phosphorylation (pCas), which prevents pCas inhibition of pSmad (shown by double hatched arrow).

The action of physically arresting Src is most likely due to the stimulation of GPCR endocytosis — a process often involving pSrc [231-232] — due to antagonist binding. These results also provide another potential example of interactions between G proteins and focal adhesion proteins such as Src to alter cytoskeletal function similar to recent reports [233]. We believe that the clinical implications of this study demonstrate the potential for 5-HT_{2B} as a druggable target for prevention of CAVD, and may also indicate the potential of targeting other GPCRs that are members of the Gαq family in a tissue-specific manner to prevent fibrosis. Interestingly, antagonists to another Gαq GPCR localized to

cardiopulmonary tissues – namely, angiotensin II type 1 (AT_1) receptor blockers (ARBs) – have been successfully utilized in a clinical setting to inhibit excessive TGF-β1 signaling observed in Marfan's syndrome [17, 184]. Also of note, AT_1 and 5-HT_{2B} have been found to display a functional co-dependence in cardiac fibroblasts, whereby antagonism of one of these GPCRs completely inhibits the other GPCR [13]. Therefore, 5-HT_{2B} and AT_1 receptors may also share similar functionality in AVICs. Thus far, however, retrospective epidemiological studies have proven inconclusive on the effectiveness of ARB treatment in reducing CAVD outcomes. Early reports indicated that ARBs were ineffective in preventing the progression of CAVD in high-risk elderly patients [234], but recent studies have presented a more optimistic view on the therapeutic impact of ARBs with patients exhibiting lower scores of AV remodeling [235] and decreased overall cardiovascular outcomes due to AV stenosis [236]. The discrepancy may be one of timing, as it may be important to begin therapeutic intervention at the earliest possible time to prevent the development of CAVD. As indicated in this study, 5-HT_{2B} antagonism prevents TGF-β1 myofibroblast activation of AVICs, which we believe to be one of the earliest events in the progression of CAVD. Future studies should consider the relative efficacy of 5-HT_{2B} antagonism and ARB treatments in preventing TGF-β1 effects in AVICs.

The impact of the current study and future studies with ARBs would be greatly enhanced by *in vivo* validation; however, at this time there is no ideal animal model for CAVD that recapitulates human pathology. Therefore, to establish a more conclusive understanding of the therapeutic potential of Gαq

antagonists, randomized controlled studies should be conducted to measure CAVD outcomes in patients taking already approved ARBs or 5-HT_{2B} antagonists.

Chapter 6

Aim 3 – Comparing Efficacy of 5-HT_{2B} and AT_1 Antagonist Inhibition of TGF-β1 in AVICs

6.1. Introduction

Calcific aortic valve disease (CAVD) is the third leading cause of cardiovascular disease and is especially prevalent among the elderly. Studies have shown that CAVD affects over 25% of people over 65 years of age [1], and currently, the only effective long-term treatment for advanced CAVD is replacement surgery, a high risk procedure for elderly patients. For this reason, a non-invasive therapeutic to stop the development of CAVD would greatly benefit those most at risk for developing severe CAVD. Unfortunately, epidemiological studies have shown that promising drug candidates such as statins have not proven successful at slowing or reversing the end stages of CAVD that necessitate valve replacement [218].

Transforming growth factor-β1 (TGF-β1) has been the most extensively studied initiator of CAVD through myofibroblast activation of aortic valve interstitial cells (AVICs); however, serotonin (5-hydroxytryptamine, 5-HT) and certain serotonergic receptor agonists have been shown to lead to CAVD upstream of TGF-β1 through signaling at the serotonergic G protein-coupled receptor (GPCR) 5-HT_{2B}. Further, we have recently shown that 5-HT_{2B} antagonism inhibits TGF-β1-induced activation of AVICs by physically arresting

non-canonical TGF-β1 signaling and preventing the subsequent upregulation of myofibroblast markers such as smooth muscle α-actin (αSMA) [211]. Since 5-HT_{2B} expression and signaling is far less ubiquitous that that of TGF-β1, we proposed that the 5-HT_{2B} receptor may be targeted in a therapeutic manner to prevent or treat CAVD progression.

Recently, Jaffre et al. [13] demonstrated that 5-HT_{2B} works in concert with another GPCR, AT_1, to mediate hypertrophic signaling in cardiac fibroblasts. Angiotensin II (ang II) demonstrates a mechano-dependent signaling activation during ventricular pressure overload similar to that noted above for 5-HT_{2B} [147], and increased ang II signaling at AT_1 results in an increase in TGF-β1 secretion and the subsequent downstream initiation of fibrosis [147]. In the aforementioned study, Jaffre et al. conclusively demonstrated a necessary interdependence between 5-HT_{2B} and AT_1 in regulating TGF-β1 secretion. Many of the cardiac-related studies into the molecular signaling pathways of the 5-HT_{2B} and AT_1 receptors have focused on the role of these GPCRs in ventricular fibroblasts.

We believe that similar signaling mechanisms may exist in modulating AVIC phenotype, and thus, directing the progression of CAVD. In support of this theory, the expression of AT_1 has been found to be significantly higher in excised diseased human AV leaflets compared to normal leaflets [237-238]; however, the role of this receptor in CAVD has not been extensively studied. In this study, we assessed potential co-dependence of 5-HT_{2B} and AT_1 in AVICs, and we determined the relative efficacy of antagonizing each of these GPCRs to prevent TGF-β1-induced myofibroblast activation. Interestingly, our results indicate that

while 5-HT_{2B} and AT_1 display functional co-dependence in AVICs, AT_1 antagonists are ineffective at preventing TGF-β1-mediated myofibroblast activation of AVICs. We believe that the results from this study will further elucidate signaling pathways that lead to pathologic differentiation of AVICs and identify druggable targets to control these pathways.

6.2. Methods

AVIC isolation and culture

AVICs were isolated from porcine valves obtained from a local abattoir by dissecting the valve cusps from the surrounding muscle and using collagenase to remove the fibroblasts from the ECM. Isolated fibroblasts were then cultured on T-75 tissue culture treated flasks in cell growth media consisting of DMEM supplemented with 10% fetal bovine serum (FBS), 1% penicillin/streptomycin antibiotic, and 1% amphotericin B antifungal. The cell culture flasks were kept in an incubator that is controlled at 37 ^{o}C and 5% CO_2. Cells will be grown to 60 - 80% confluence prior to further processing. Previous studies have shown that AVICs retain phenotypic integrity up to 10 passages after initial harvest [220]. However, we have observed phenotypic changes as early as 7 passages after harvest; therefore, we did not exceed this maximum limit.

Experimental treatments

All antagonist treatments were added 30 min prior to the addition of any agonist treatment. The antagonist treatments were as follows: 1 μM or 10 μM 5-HT_{2B} receptor (5-HT_{2B}) antagonist (SB 204741); 1 μM or 10 μM angiotensin II type 1 receptor (AT_1) antagonist (ZD 7155). After 30 min agonist treatments were added to the appropriate wells. The agonist treatments were as follows: 1 μM 5-HT_{2B} agonist (BW 723 c86); 1 μM AT_1 agonist (angiotensin II); 1 ng/ml TGF-β1. Following the addition of the agonist treatments, the samples were incubated for 1h for assays of signaling protein activation or 24 h for endpoint analyses.

Assay for extracellular TGF-β1

Extracellular media was collected after the experimental incubations listed above. Total TGF-β1 was quantified by activating all of the TGF-β1 by heating the media to 100 ^{o}C for 3 min. The active TGF-β1 within the media was then assayed using a PAI-I promoter firefly luciferase assay, as described previously [239]. Promega luciferase substrate was added to each sample and the subsequent luminescence was read using a Biotek Synergy plate reader.

Assay for AVIC activation

AVICs were lysed with mammalian cell lysis buffer and centrifuged to remove membrane components. The collected cell lysates were then frozen at -

80 ^{o}C for storage. Prior to probing for αSMA content, each frozen cell lysate was thawed and assayed for total protein content using a standard BCA Assay. An indirect ELISA was then used to detect αSMA as described previously [211]. Briefly, 100 µl of 5 µg/ml cell lysate solution was adsorbed onto the bottom of 96 well plates by overnight incubation in a carbonate/bicarbonate buffer (pH 9.6). The high pH buffer reduces inter-protein interactions to give an even distribution of proteins within the wells. Non-specific binding sites on the well were then blocked using a 5% solution of milk in phosphate-buffered saline (PBS) for at least 1.5 h at room temperature. Following this step, 100 µl of polyclonal antibody to αSMA (1:200 in blocking solution) was added to each well and allowed to incubate at room temperature for 1.5 h. After washing the wells 3 times with PBS, each plate was incubated for 1 h with a secondary antibody linked to a peroxidase enzyme. Subsequently, the plates were washed thoroughly with PBS to remove unbound secondary antibodies and each well received 100 µl of a detection substrate that reacts in the presence of peroxidase to give a product with a characteristic absorbance. The absorbance of each well was detected using a plate reader, and the αSMA content of each sample was compared to a standard curve created using αSMA peptide to calculate the concentration of αSMA in each sample.

Calcific nodule assay

To assay for calcific nodule formation, AVICs were cultured in BioFlex® culture plates as done previously [199]. After reaching confluence, AVICs were

treated with either 1 ng/ml TGF-β1 alone or in combination with SB204741 or ZD7155. Calcific nodules were identified using Alizarin red staining to assay for calcium phosphate deposition. After strain, AVICs were fixed in 3.7% formalin and 1 ml of Alizarin solution was added to each well for 30 min. The wells were then washed thoroughly with PBS and imaged with conventional microscopy.

Assays for TGF-β1 signaling

Samples to be analyzed for TGF-β1-induced activation of canonical and non-canonical signaling were lysed in RIPA buffer 1 h after AVICs were treated with the prescribed treatment. Lysate solutions were centrifuged to remove lipid components, and total protein concentration was determined using a BCA protein assay. All proteins were denatured by boiling the samples with β-mercaptoethanol, and gel electrophoresis was used to separate the proteins based upon size. Western blotting was then used to assay for Smad3 and p38 phosphorylation.

In addition to Smad3 phosphorylation, canonical TGF-β1 signaling was assayed via PAI-1 promoter activity after 24 h of treatment. To assay for this activity, we utilized a partial PAI-1 promoter (p3TP-lux) subcloned into a luciferase reporter plasmid [54]. This vector was introduced into AVICs via electroporation prior to the addition of GPCR antagonist or TGF-β1 treatments. Following electroporation, AVICs were seeded into 12-well plates and allowed to recover for 24 h. After 24 h of the prescribed treatment, AVICs were lysed using 200 µl reporter lysis buffer, and 20 µl of this lysate solution was added to a well

of a 96-well plate. Luciferase activity was detected by adding 100 µl luciferase substrate to each well and recording the luminescent product using a plate reader.

AVIC transfection

To transfect AVICs with the PAI-1 reporter plasmid or a plasmid for expression of mutated p38, AVICs were harvested via trypsinization and resuspended at 2 x 10^6 cells/ml in cytomix buffer supplemented with ATP and glutathione. This buffer is designed to mimic cytosolic composition in order to maintain cellular homeostasis during poration. This AVIC suspension was then loaded into 4 mm electroporation cuvettes along with 20 µg of the plasmid to be delivered. AVICs were then subjected to an exponential decay electroporation protocol using a capacitance of 500 µF and a peak voltage of 350 V. Following electroporation, the cuvettes were placed on ice for 10 min to allow the AVICs to recover. After this recovery incubation, AVICs were resuspended in culture media and reseeded onto the appropriate growth surface.

Statistical analyses

All data presented were calculated as the average of *at least* three independent experimental replications (n > 3). Statistical differences between groups were calculated by ANOVA, and pairwise differences were established

with post hoc testing using the most stringent pairwise Holm-Sidak test. Statistical significance was considered as $p < 0.05$.

6.3. Results

5-HT_{2B} and AT_1 are functionally co-dependent in AVICs

Previous studies have shown that agonism of 5-HT_{2B} or AT_1 lead to secretion of TGF-β1 in a variety of cell types including AVICs. Therefore, we used TGF-β1 secretion to assay the co-dependence of these two GPCRs in AVICs. AVICs treated with either the 5-HT_{2B} agonist BW723c86 or the AT_1 agonist Ang II exhibit increased secretion of TGF-β1 into the cell culture media (Fig. 6.1). For both agonists, this response is inhibited with an antagonist to either GPCR.

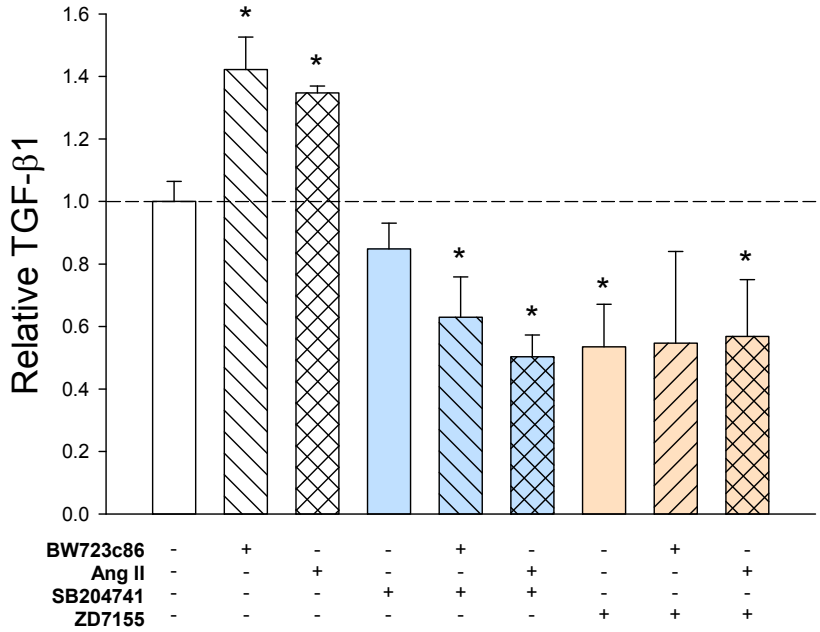

Fig. 6.1. TGF-β1 synthesis and signaling. (A) 5-HT_{2B} (hatched bar) and AT_1 agonists (double hatched bar) lead to increased TGF-β1 synthesis, while both antagonists prevent synthesis induced by either agonist treatment (blue and orangebars). * indicates significant difference ($p < 0.005$) versus control.

AT_1 antagonism does not prevent TGF-β1 activation of AVICs

We have previously shown that 5-HT_{2B} antagonism inhibits TGF-β1-induced activation of AVICs; therefore, we hypothesized that antagonism of AT_1, a GPCR similar to 5-HT_{2B}, may also be able to inhibit AVIC activation. To test this hypothesis, AVICs were treated with log doses of either 5-HT_{2B} antagonist (SB204741) or AT_1 antagonist (ZD7155) for 30 min prior to the addition of 1 ng/ml TGF-β1. AVICs exhibit significantly increased expression of αSMA following 24 h of the TGF-β1 treatment. Consistent with our previous findings, 1 and 10 μM treatments of SB204741 significantly inhibit TGF-β1-induced AVIC

activation in a dose dependent manner. However, ZD7155 treatment is less effective in mitigating the AVIC differentiation (Fig. 6.2).

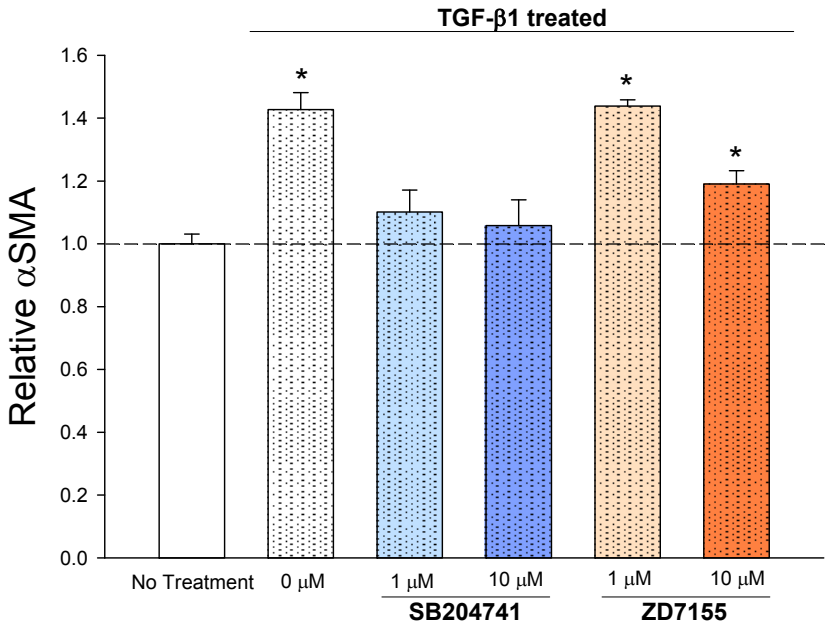

Fig. 6.2. 5-HT_{2B} and AT_1 antagonist effect on TGF-β1-induced activation of AVICs. AVICs treated 1 ng/ml TGF-β1 for 24 exhibit significantly increased αSMA expression. Both 1 and 10 μM 5-HT2B antagonist (SB204741) treatments blocked this activation. The AT_1 antagonist (ZD7155) treatments were less effective in inhibiting AVIC activation. * indicates significant difference ($p < 0.005$) versus control.

Treating AVICs with 1 μM ZD7155 has no effect on AVIC activation by TGF-β1, and while 10 μM ZD7155 significantly decreases increased αSMA expression due to TGF-β1 treatment, these AVICs still exhibit significantly higher αSMA than non-treated control samples. In addition to assaying for AVIC myofibroblast activation, we were also interested in assessing changes in a functional outcome indicative of CAVD—calcific nodule formation. Our lab has

recently developed an in vitro model system to study morphogenesis of dystrophic calcific nodules *in vitro* [199] that are formed due to an imbalance of forces between TGF-β1 treated contractile myofibroblastic AVICs and externally applied cyclic strain. To test the effects of the antagonist treatments on calcific nodule formation, AVICs were seeded in Bioflex culture plates and treated with either 1 μM or 10 μM of either antagonist for 30 min prior to the addition of 1 ng/ml TGF-β1 for 24 h. Following the 24 h incubation, 15% cyclic strain at 1 Hz was added to the cultured AVICs for an additional 24 h.

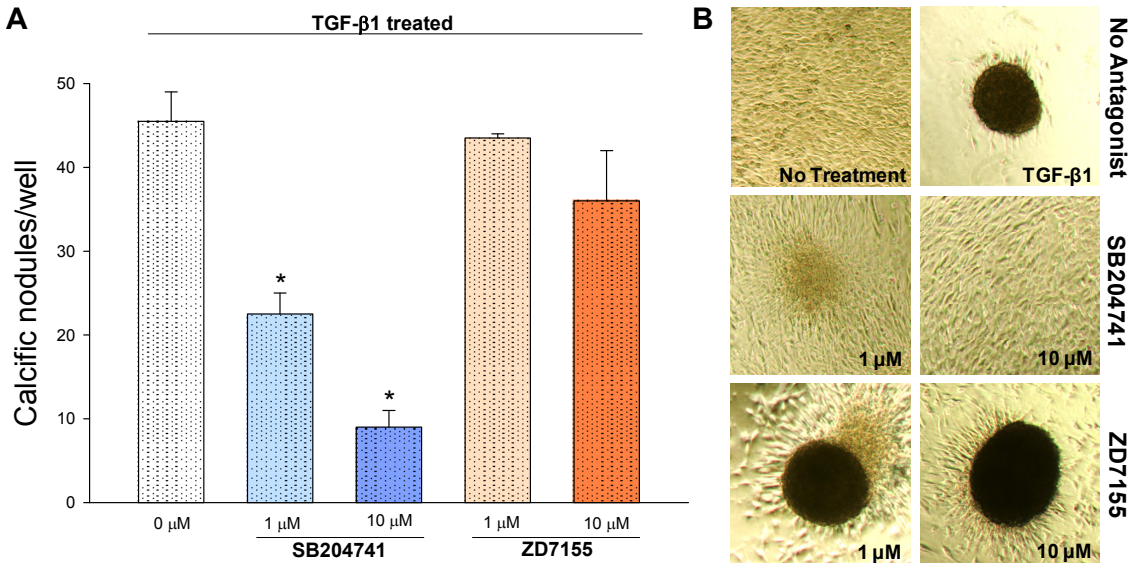

Fig. 6.3. 5-HT_{2B} and AT_1 antagonist effect on TGF-β1-induced calcific nodule formation. (A) AVICs treated 1 ng/ml TGF-β1 for 24 exhibit robust calcific nodule formation following 15% strain for 24 h. Both 1 and 10 μM 5-HT2B antagonist (SB204741) treatments significantly blocked this nodule formation; however, the AT_1 antagonist (ZD7155) treatments did not inhibit calcific nodule morphogenesis. (B) Alizarin red staining was used to identify nodules in all treatment groups. * indicates significant difference ($p < 0.005$) versus TGF-β1 treated control.

AVICs treated with TGF-β1 alone formed robust calcific nodules on the surface of the Bioflex plates (Fig. 6.3A). Similar to our previous findings, 5-HT_{2B} antagonism prevented formation of calcific nodules in a dose-dependent manner [211]; however, treating AVICs with ZD7155 did not significantly inhibit TGF-β1-induced calcific nodule formation as identified by Alizarin red staining (Fig. 6.3B).

AT_1 antagonism inhibits canonical, but not non-canonical, TGF-β1 signaling

Given the divergence of 5-HT_{2B} and AT_1 antagonism in inhibiting TGF-β1-induced activation of AVICs, we were next interested in understanding the effect of these antagonist treatments on TGF-β1 signaling. We have previously demonstrated that 5-HT_{2B} antagonism inhibits TGF-β1 induced phosphorylation of p38, but does not inhibit canonical Smad3 activation [211]. In this study, we assessed the phosphorylation state of both of these signaling proteins after 1 h of TGF-β1 treatment and treatment with each antagonist (Fig. 6.4A).

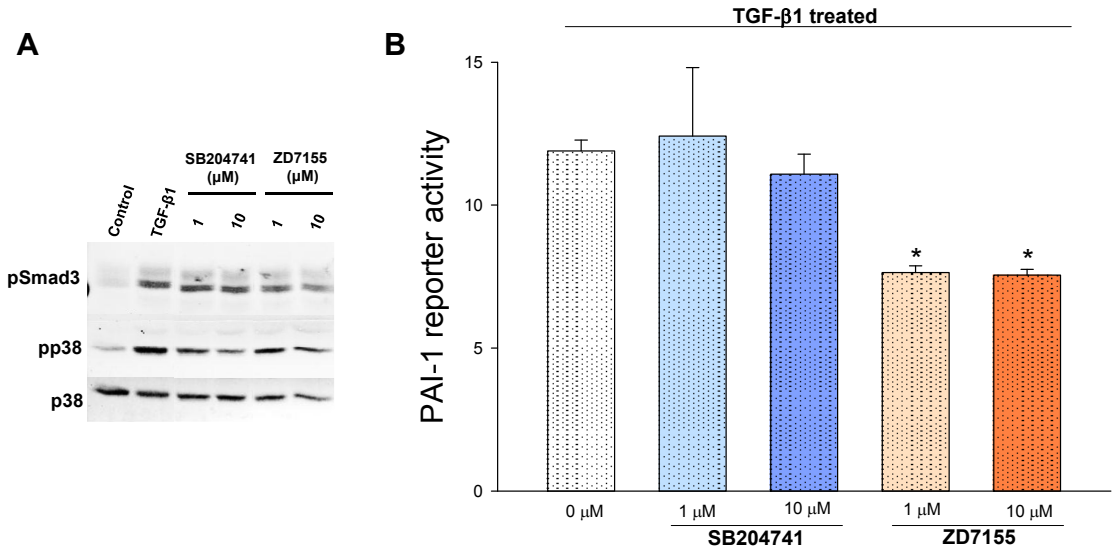

Fig. 6.4. 5-HT_{2B} and AT_1 antagonist effect on TGF-β1 canonical and non-canonical signaling. (A) AVICs treated 1 ng/ml TGF-β1 for 1h exhibit increased phosphorylation of both Smad3 (pSmad3) and p38 (pp38). The 5-HT_{2B} antagonist (SB204741) treatments does not effect pSmad3; however, pp38 was inhibits in a dose dependent manner. In contrast, AT1 antagonist treatment (ZD7155) significantly inhibits pSmad3, but does not significantly inhibit pp38. (B) A PAI-1 reporter plasmid supports the pSmad3 results as both ZD7155 treatments lead to decreased reporter activity. * indicates significant difference ($p < 0.005$) versus TGF-β1 treated control.

Consistent with our previous results, 5-HT_{2B} antagonism inhibits TGF-β1-mediated phosphorylation of p38 in a dose dependent manner; however, AT_1 antagonism does not prevent activation of this non-canonical pathway. Interestingly, however, AT_1 antagonism significantly inhibits TGF-β1-induced phosphorylation of Smad3. To further assess canonical TGF-β1 signaling activity AVICs were transfected to express a partial promoter sequence of PAI-1 (p3TP-lux), a common transcriptional target of activated Smad3, with a luciferase reporter gene. Similar to the Smad3 phosphorylation results, AT_1 antagonism significantly inhibits TGF-β1-induced PAI-1 promoter activity in a dose dependent manner with less activity observed at both 1 μM and 10 μM AT_1 antagonist treatment.

p38 MAPK signaling is required for TGF-β1 activation of AVICs

To further assess the importance of p38 phosphorylation in TGF-β1 signaling, AVICs were transfected with a plasmid to express a dominant negative form of p38 that was mutated to remove kinase activity and prevent subsequent downstream signaling. Control AVICs transfected with the plasmid backbone (i.e., missing the dominant negative p38 insert) display a normal two-fold increase in αSMA after treatment with 1 ng/ml TGF-β1 for 24 h; however, the introduction of dominant negative p38 significantly reduces TGF-β1-induced αSMA expression (Fig. 6.5).

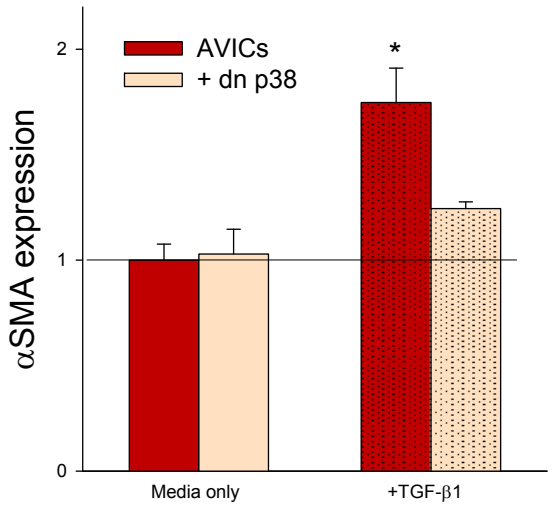

Fig. 6.5. Requirement for p38 phosphorylation in AVIC activation by TGF-β1. AVICs treated with TGF-β1 exhibit a significant increase in αSMA; however, AVICs transfected to express a dominant-negative form of p38 (dn p38) do not significantly increase αSMA expression following TGF-β1 treatment. * indicates significant difference ($p < 0.005$) versus non-treated control.

6.4. Discussion

In this study, we were interested in identifying potential therapeutic targets for CAVD by studying interactions between 5-HT_{2B}, AT_1, and TGF-β1 signaling. Our previous findings indicate that antagonism of 5-HT_{2B} leads to a physical arrest of non-canonical TGF-β1 signaling, thereby inhibiting TGF-β1-induced myofibroblast activation of AVICs [211]. We hypothesized that antagonism of a GPCR similar to 5-HT_{2B}, AT_1, may elicit a similar response in AVICs. Interestingly, though 5-HT_{2B} and AT_1 appear to be codependent in agonist-mediated TGF-β1 secretion from AVICs (Fig. 6.1), antagonism of AT_1 does not directly inhibit TGF-β1-induced myofibroblast activation of AVICs (Fig. 6.2), calcific nodule morphogenesis (Fig. 6.3), or non-canonical p38 signaling (Fig. 6.4A). In contrast, AT_1 antagonist treatment significantly inhibited canonical TGF-β1 signaling as indicated by Smad3 phosphorylation (Fig. 6.4A) and PAI-1 promoter activity (Fig. 6.4B). Finally, to determine the necessity of p38 signaling in TGF-β1-induced myofibroblast activation of AVICs, we transfected AVICs with a plasmid to express a dominant negative form of p38 that is unable to be phosphorylated by upstream kinases. These results further highlight the divergence of canonical and non-canonical TGF-β1 signaling in leading to AVIC myofibroblast activation.

Losartan, an FDA approved AT_1 antagonist, has been found to inhibit TGF-β1 signaling in those with Marfan's syndrome [17]. As such, AT_1 antagonists and other inhibitors to ang II signaling have been proposed to be promising candidates for CAVD therapy [240]. Here, we show that an AT_1 antagonist more

potent than losartan is less effective than 5-HT_{2B} antagonism in inhibiting non-canonical TGF-β1 signaling and ultimately AVIC activation and calcific nodule formation; however, AT_1 antagonists do inhibit canonical Smad signaling. Thus far the therapeutic potential of AT_1 antagonists for CAVD is unclear. Early epidemiological studies concluded that losartan, like statins, does not halt the progression of CAVD [234]. However, more recent studies have indicated positive cardiac outcomes including lower scores of AV remodeling for patients taking AT_1 antagonists for other indications [235].

The reason for the discrepancy could be one of timing. Our data indicate that AT_1 antagonism may be effective in preventing TGF-β1 synthesis and secretion from AVICs (Fig. 6.1). Therefore, if an AT_1 antagonist treatment is given prior to the onset of CAVD, this treatment may be effective in preventing increased TGF-β1 expression, thereby effectively preventing CAVD. Conversely, if the treatment is begun after the onset of CAVD, the AT_1 antagonism may not be able to inhibit ongoing TGF-β1-induced AVIC activation and pathological tissue alterations (Figs. 6.2 and 6.3). Alternatively, AT_1 antagonist inhibition of canonical TGF-β1 signaling may play an important role in preventing some of the tissue level changes observed in CAVD. These tissue level changes including differences in secretion of extracellular matrix components should be studied further. As we have previously suggested [241], an epidemiological study of patients taking approved 5-HT_{2B} antagonists should be conducted, and this type of study may also help delineate the relative importance of non-canonical versus canonical TGF-β1 signaling in leading to CAVD.

Chapter 7

Impact and Future Directions

7.1. Summary and impact of results

The overall goal of this research was to elucidate the mechanisms and characteristics of TGF-β1-induced myofibroblast activation in AVICs and assess the ability of 5-HT_{2B} and AT_1 antagonism in inhibiting this pathologic differentiation. We began addressing this goal in aim 1 by elucidating heretofore unknown characteristics of AVIC activation by TGF-β1, namely the increased expression of the atypical intercellular adhesion protein cadherin-11 through a pathway that is dependent upon non-canonical Erk1/2 phosphorylation. Our results indicate that expression of cadherin-11 and contractile proteins such as αSMA are both required for the build-up in intercellular tension that leads to formation of dystrophic calcific nodules *in vitro*. In addition to understanding the crucial role of cadherin-11 in calcific nodule morphogenesis, we believe that the identification of this marker of TGF-β1-induced activation of AVICs may have far-reaching implications. Currently, early cellular changes that lead to CAVD are difficult to detect; however, modern imaging techniques may be able to take advantage of the trans-membrane nature of cadherin-11 to detect pathologic differentiation of AVICs. These techniques may be used to inform physicians on timing of therapeutic intervention for CAVD.

After characterizing the important characteristics of TGF-β1-mediated activation of AVICs, in aim 2 we established the ability of antagonism of a specific serotonergic receptor, 5-HT_{2B}, to inhibit myofibroblast activation in AVICs. In doing so, we found that TGF-β1-induced expression of αSMA, the most common myofibroblast marker, is dependent upon non-canonical activation of the MAPK p38 rather than the canonical Smad pathway. Previous studies established that TGF-β1 activation of p38 is dependent upon phosphorylation of TβRII by Src tyrosine kinase, and our data indicate that antagonism of 5-HT_{2B} arrests this non-canonical signaling by physically restricting trafficking of Src within AVICs. We believe this physical sequestration of Src is due to receptor-mediated endocytosis, a process known to involve activated Src; therefore, we ended aim 2 by hypothesizing that other similar GPCRs may also be targeted to inhibit TGF-β1 effects. In aim 3 we tested this hypothesis by assessing the ability of an antagonist of AT_1 to inhibit TGF-β1-induced activation of AVICs. Interestingly, AT_1 antagonism is ineffective in substantially inhibiting AVIC activation and calcific nodule formation due to TGF-β1 treatment. The data indicate that AT_1 antagonism does not prevent TGF-β1-induced p38 phosphorylation but does significantly prevent activation of canonical TGF-β1 signaling as indicated by Smad3 phosphorylation and PAI-1 promoter activity.

These results further illustrate the divergence of canonical and non-canonical TGF-β1 signaling and their relative importance in leading to AVIC activation. The major impact of this work may lie in identifying methods to isolate divergent TGF-β1 pathways. To our knowledge, these studies are the first to

identify the roles of these MAPK (p38 and Erk1/2) pathways outside of canonical TGF-β1 signaling in altering AVIC phenotype. Decoupling these TGF-β1 signaling pathways may allow us to independently control TGF-β1-induced cellular outcomes and better understand how TGF-β1 leads to fibrotic diseases including CAVD. Fig 7.1 illustrates our current understanding of the molecular crosstalk considered in these studies and the proposed implications that may be linked with each AVIC output.

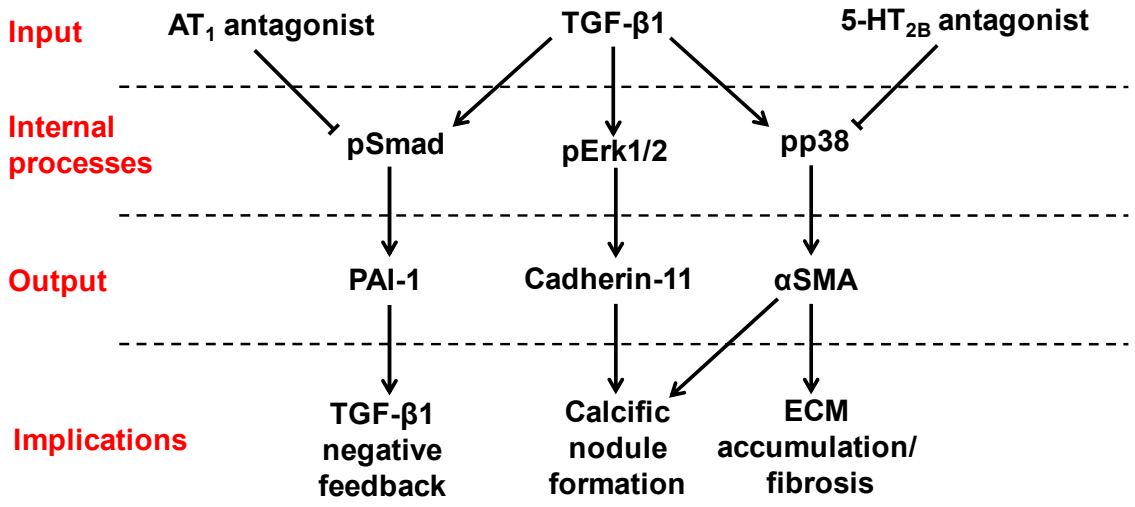

Fig. 7.1. Proposed schematic of mechanisms. Forward arrows indicate a positive regulation, and blunted arrows indicate a negative regulation.

Further, understanding methods to control each these molecular mechanisms may have impact in allowing researchers to better engineer tissues that recapitulate native function. Tissue engineering approaches are believed to be the ultimate therapeutic solution for pediatric patients born with congenital valve defects; however, ultimate success in designing a new AV that can replace a native AV and integrate with host tissues may depend on the ability to

manipulate cells within a tissue engineered scaffold [242]. A better understanding of the molecular processes that control AVIC phenotype are greatly beneficial toward achieving this goal. In conclusion, we believe that these studies shed new light on the molecular mechanisms that lead to CAVD and may aid in the discovery and design of CAVD therapeutics from both drugs to living tissues.

7.2. Future directions

We believe that the results presented in this dissertation provide new insight into the molecular mechanisms associated with pathologic AVIC differentiation and that this new knowledge may lead to novel therapeutic strategies for CAVD; however, much work remains before the identified mechanisms may be utilized clinically for CAVD therapy. Further *in vitro* and *ex vivo* studies should be conducted to better understand the interconnectivity of the various TGF-β1 and GPCR pathways and the associated AVIC outcomes. To begin, we have not fully explored the relationship between the antagonist treatments on TGF-β1-induced Erk1/2 phosphorylation and the ultimate expression of cadherin-11. These experiments should be conducted to complete our current understanding of the interaction between these signaling pathways.

In addition, the data indicate that AT_1 antagonism inhibits canonical signaling; however, the mechanism of this inhibition is not clear and other AT_1 antagonists should be tested to strengthen these data. Additionally, we have hypothesized that canonical Smad signaling may play an important role in a

negative feedback loop that prevents activation of latent TGF-β1. This theory is based upon the observation that increased canonical signaling is associated with activation of a partial promoter to PAI-1; however, to test this hypothesis, studies should be done to evaluate PAI-1 protein expression following increased activation of canonical signaling and assaying relative changes in TGF-β1 activation. Further, the tissue level implications of inhibiting non-canonical (via 5-HT_{2B} antagonism) versus canonical TGF-β1 signaling (via AT_1 antagonism) should be tested in an *ex vivo* model of CAVD similar to those used previously [10, 171]. These data may aid in the understanding of the relative importance of AVIC myofibroblast differentiation, cadherin-11 upregulation, and PAI-1 expression in ECM remodeling, and may point to a combination therapy approach to inhibit multiple pathways at once.

While the new level of *in vitro* and *ex vivo* understanding that is gained from the current and proposed studies is invaluable to the search for CAVD therapies, the ultimate impact will be determined by the ability to prevent the fibrotic and calcific tissue level changes that are characteristic of CAVD. Unfortunately, assessing these changes is not trivial as currently there is not a widely accepted animal model that recapitulates human CAVD. However, we hope that the mechanistic results of our study will further encourage research in both the few potential animal models that do exist and also epidemiological investigations on patients already taking approved 5-HT_{2B} antagonists for other diseases. Additionally, we believe that by better understanding the role of the

signaling pathways involved in CAVD, researchers may be able to identify and develop more appropriate animal models.

One path to begin an *in vivo* validation may lie in assessing the whether the signaling pathways identified with porcine AVICs in these studies are conserved in AVICs derived from human leaflets. Similarly, excised CAVD leaflets from human patients may be analyzed for expression of cadherin-11 to determine the validity of this protein as a biomarker for CAVD. Researchers may then be able to use information gathered from these human samples to verify similarities in promising animal models for CAVD. Once the similarities and differences between these models and the human pathologies are better understood, researchers may be better equipped to assess the validity of using these models as a reliable predictor of human CAVD outcomes.

A major strength that may expedite the clinical realization of antagonizing these GPCRs for CAVD therapy lies in the fact that many approved 5-HT_{2B} and AT_1 antagonists are already approved and used for other diseases. Previous epidemiological studies concluded that statins and AT_1 receptor antagonists [2, 234] have no effect in preventing surgical intervention due to CAVD; however, disappointing results from these studies may be due to the fact that participants were ~65 years of age and many may have already had advanced CAVD. Further, others have shown that *in vitro* treatments that are successful in preventing the progression of CAVD are not as efficacious in reversing the pathophysiological tissue changes characteristic of the disease [93, 218]. Furthermore, though 5-HT_{2B} antagonists have shown potential in preventing

fibrotic responses in other disease models [15], to our knowledge, no one has investigated the ability of 5-HT_{2B} antagonism to prevent CAVD. Therefore, we believe that the therapeutic potential of 5-HT_{2B} for CAVD should be explored.

REFERENCES

1. Roger, V.L., et al., *Heart disease and stroke statistics--2012 update: a report from the American Heart Association.* Circulation, 2012. **125**(1): p. e2-e220.
2. Stewart, R.A., *Clinical trials in heart valve disease.* Curr Opin Cardiol, 2009. **24**(4): p. 279-87.
3. Carabello, B.A. and W.J. Paulus, *Aortic stenosis.* Lancet, 2009. **373**(9667): p. 956-66.
4. Chrysohoou, C., D. Tsiachris, and C. Stefanadis, *Aortic stenosis in the elderly: Challenges in diagnosis and therapy.* Maturitas, 2011. **70**(4): p. 349-53.
5. Merryman, W.D., *Insights into (the interstitium of) degenerative aortic valve disease.* J Am Coll Cardiol, 2008. **51**(14): p. 1415; author reply 1416.
6. Olsson, M., M. Rosenqvist, and J. Nilsson, *Expression of HLA-DR antigen and smooth muscle cell differentiation markers by valvular fibroblasts in degenerative aortic stenosis.* J Am Coll Cardiol, 1994. **24**(7): p. 1664-71.
7. Rabkin-Aikawa, E., et al., *Dynamic and reversible changes of interstitial cell phenotype during remodeling of cardiac valves.* J Heart Valve Dis, 2004. **13**(5): p. 841-7.

8. Chalajour, F., et al., *Identification and characterization of cells with high angiogenic potential and transitional phenotype in calcific aortic valve.* Exp Cell Res, 2007. **313**(11): p. 2326-35.

9. Jian, B., et al., *Progression of aortic valve stenosis: TGF-beta1 is present in calcified aortic valve cusps and promotes aortic valve interstitial cell calcification via apoptosis.* Ann Thorac Surg, 2003. **75**(2): p. 457-65; discussion 465-6.

10. Merryman, W.D., et al., *Synergistic effects of cyclic tension and transforming growth factor-beta1 on the aortic valve myofibroblast.* Cardiovasc Pathol, 2007. **16**(5): p. 268-76.

11. Balachandran, K., et al., *Elevated cyclic stretch induces aortic valve calcification in a bone morphogenic protein-dependent manner.* Am J Pathol, 2010. **177**(1): p. 49-57.

12. Jian, B., et al., *Serotonin mechanisms in heart valve disease I: serotonin-induced up-regulation of transforming growth factor-beta1 via G-protein signal transduction in aortic valve interstitial cells.* Am J Pathol, 2002. **161**(6): p. 2111-21.

13. Jaffre, F., et al., *Serotonin and angiotensin receptors in cardiac fibroblasts coregulate adrenergic-dependent cardiac hypertrophy.* Circ Res, 2009. **104**(1): p. 113-23.

14. Ebrahimkhani, M.R., et al., *Stimulating healthy tissue regeneration by targeting the 5-HTB receptor in chronic liver disease.* Nat Med, 2011. **17**(12): p. 1668-73.

15. Fabre, A., et al., *Modulation of bleomycin-induced lung fibrosis by serotonin receptor antagonists in mice.* Eur Respir J, 2008. **32**(2): p. 426-36.

16. Olson, E.R., et al., *Inhibition of cardiac fibroblast proliferation and myofibroblast differentiation by resveratrol.* Am J Physiol Heart Circ Physiol, 2005. **288**(3): p. H1131-8.

17. Brooke, B.S., et al., *Angiotensin II blockade and aortic-root dilation in Marfan's syndrome.* N Engl J Med, 2008. **358**(26): p. 2787-95.

18. Sacks, M.S. and A.P. Yoganathan, *Heart valve function: a biomechanical perspective.* Philos Trans R Soc Lond B Biol Sci, 2007. **362**(1484): p. 1369-91.

19. Yoganathan, A.P., Z. He, and S. Casey Jones, *Fluid mechanics of heart valves.* Annu Rev Biomed Eng, 2004. **6**: p. 331-62.

20. Grashow, J.S., A.P. Yoganathan, and M.S. Sacks, *Biaixal stress-stretch behavior of the mitral valve anterior leaflet at physiologic strain rates.* Ann Biomed Eng, 2006. **34**(2): p. 315-25.

21. Schoen, F.J. and W.D. Edwards, *Valvular heart disease: general principles and stenosis*, in *Cardiovascular Pathology*, M.D. Silver, A.I. Gotlieb, and F.J. Schoen, Editors. 2001, Churchill Livingstone: New York, NY. p. 402-442.

22. Lloyd-Jones, D., et al., *Heart disease and stroke statistics--2009 update: a report from the American Heart Association Statistics Committee and Stroke Statistics Subcommittee.* Circulation, 2009. **119**(3): p. 480-6.

23. Merryman, W.D., et al., *Correlation between heart valve interstitial cell stiffness and transvalvular pressure: implications for collagen biosynthesis.* Am J Physiol Heart Circ Physiol, 2006. **290**(1): p. H224-31.

24. Filip, D.A., A. Radu, and M. Simionescu, *Interstitial cells of the heart valves possess characteristics similar to smooth muscle cells.* Circ Res, 1986. **59**(3): p. 310-20.

25. Hochmuth, R.M., *Micropipette aspiration of living cells.* J Biomech, 2000. **33**(1): p. 15-22.

26. Sato, M., et al., *Application of the micropipette technique to the measurement of cultured porcine aortic endothelial cell viscoelastic properties.* J Biomech Eng, 1990. **112**(3): p. 263-8.

27. Banasik, J.L., *Pathophysiology*. 3 ed. 2005, Philadelphia, PA: Elsevier Saunders.

28. Thurbrikar, M., *The Aortic Valve*. 1990, Boca Raton, FL: CRC.

29. Schoen, F., *Aortic valve structure-function correlations: Role of elastic fibers no longer a stretch of the imagination.* J Heart Valve Dis, 1997. **6**: p. 1-6.

30. Schoen, F.J., *Evolving concepts of cardiac valve dynamics: the continuum of development, functional structure, pathobiology, and tissue engineering.* Circulation, 2008. **118**(18): p. 1864-80.

31. Thubrikar, M., *The Aortic Valve*. 1990, Boca Raton: CRC. 221.

32. Vesely, I. and R. Noseworthy, *Micromechanics of the fibrosa and the ventricularis in aortic valve leaflets.* J Biomech, 1992. **25**(1): p. 101-13.

33. Kershaw, J.D., et al., *Specific regional and directional contractile responses of aortic cusp tissue.* J Heart Valve Dis, 2004. **13**(5): p. 798-803.

34. Stamatas, G.N. and L.V. McIntire, *Rapid flow-induced responses in endothelial cells.* Biotechnol Prog, 2001. **17**(3): p. 383-402.

35. Butcher, J.T., et al., *Unique morphology and focal adhesion development of valvular endothelial cells in static and fluid flow environments.* Arterioscler Thromb Vasc Biol, 2004. **24**(8): p. 1429-34.

36. Cucina, A., et al., *Shear stress induces changes in the morphology and cytoskeleton organisation of arterial endothelial cells.* Eur J Vasc Endovasc Surg, 1995. **9**(1): p. 86-92.

37. Simmons, C.A., et al., *Spatial heterogeneity of endothelial phenotypes correlates with side-specific vulnerability to calcification in normal porcine aortic valves.* Circ Res, 2005. **96**(7): p. 792-9.

38. Butcher, J.T. and R.M. Nerem, *Valvular endothelial cells regulate the phenotype of interstitial cells in co-culture: effects of steady shear stress.* Tissue Eng, 2006. **12**(4): p. 905-15.

39. Butcher, J.T. and R.M. Nerem, *Valvular endothelial cells and the mechanoregulation of valvular pathology.* Philos Trans R Soc Lond B Biol Sci, 2007. **362**(1484): p. 1445-57.

40. El-Hamamsy, I., et al., *Endothelium-dependent regulation of the mechanical properties of aortic valve cusps.* J Am Coll Cardiol, 2009. **53**(16): p. 1448-55.

41. Simmons, C.A., *Aortic valve mechanics: an emerging role for the endothelium.* J Am Coll Cardiol, 2009. **53**(16): p. 1456-8.

42. Merryman, W.D., *Mechanobiology of the aortic valve interstitial cell*, in *Bioengineering*. 2007, University of Pittsburgh: Doctoral Dissertation. p. 172.

43. Chester, A.H. and P.M. Taylor, *Molecular and functional characteristics of heart-valve interstitial cells.* Philos Trans R Soc Lond B Biol Sci, 2007. **362**(1484): p. 1437-43.

44. Hinz, B., et al., *The myofibroblast: one function, multiple origins.* Am J Pathol, 2007. **170**(6): p. 1807-16.

45. Desmouliere, A., *Factors influencing myofibroblast differentiation during wound healing and fibrosis.* Cell Biol Int, 1995. **19**(5): p. 471-6.

46. Desmouliere, A., et al., *Transforming growth factor-beta 1 induces alpha-smooth muscle actin expression in granulation tissue myofibroblasts and in quiescent and growing cultured fibroblasts.* J Cell Biol, 1993. **122**(1): p. 103-11.

47. Grinnell, F. and C.H. Ho, *Transforming growth factor beta stimulates fibroblast-collagen matrix contraction by different mechanisms in mechanically loaded and unloaded matrices.* Exp Cell Res, 2002. **273**(2): p. 248-55.

48. Walker, G.A., et al., *Valvular myofibroblast activation by transforming growth factor-beta: implications for pathological extracellular matrix remodeling in heart valve disease.* Circ Res, 2004. **95**(3): p. 253-60.

49. Waltenberger, J., et al., *Involvement of transforming growth factor-beta in the formation of fibrotic lesions in carcinoid heart disease.* Am J Pathol, 1993. **142**(1): p. 71-8.

50. Wipff, P.J., et al., *Myofibroblast contraction activates latent TGF-beta1 from the extracellular matrix.* J Cell Biol, 2007. **179**(6): p. 1311-23.

51. Jenkins, G., *The role of proteases in transforming growth factor-beta activation.* Int J Biochem Cell Biol, 2008. **40**(6-7): p. 1068-78.

52. Attisano, L. and J.L. Wrana, *Signal transduction by the TGF-beta superfamily.* Science, 2002. **296**(5573): p. 1646-7.

53. Howe, P.H., *Transforming growth factor Beta*, in *The Cytokine Handbook*, A.W. Thomson and M.T. Lotze, Editors. 2003, Elsevier Science: London. p. 1119-1141.

54. Wrana, J.L., et al., *TGF beta signals through a heteromeric protein kinase receptor complex.* Cell, 1992. **71**(6): p. 1003-14.

55. Olieslagers, S., et al., *TGF-beta1/ALK5-induced monocyte migration involves PI3K and p38 pathways and is not negatively affected by diabetes mellitus.* Cardiovasc Res, 2011. **91**(3): p. 510-8.

56. You, J., et al., *Osteopontin gene regulation by oscillatory fluid flow via intracellular calcium mobilization and activation of mitogen-activated protein kinase in MC3T3-E1 osteoblasts.* J Biol Chem, 2001. **276**(16): p. 13365-71.

57. Compton, L.A., et al., *Transforming growth factor-beta induces loss of epithelial character and smooth muscle cell differentiation in epicardial cells.* Dev Dyn, 2006. **235**(1): p. 82-93.

58. Galliher, A.J. and W.P. Schiemann, *Src phosphorylates Tyr284 in TGF-beta type II receptor and regulates TGF-beta stimulation of p38 MAPK during breast cancer cell proliferation and invasion.* Cancer Res, 2007. **67**(8): p. 3752-8.

59. Kim, W., et al., *The integrin-coupled signaling adaptor p130Cas suppresses Smad3 function in transforming growth factor-beta signaling.* Mol Biol Cell, 2008. **19**(5): p. 2135-46.

60. Rocnik, E.F., et al., *Functional linkage between the endoplasmic reticulum protein Hsp47 and procollagen expression in human vascular smooth muscle cells.* J Biol Chem, 2002. **277**(41): p. 38571-8.

61. Tasab, M., M.R. Batten, and N.J. Bulleid, *Hsp47: a molecular chaperone that interacts with and stabilizes correctly-folded procollagen.* Embo J, 2000. **19**(10): p. 2204-11.

62. Sauk, J.J., N. Nikitakis, and H. Siavash, *Hsp47 a novel collagen binding serpin chaperone, autoantigen and therapeutic target.* Front Biosci, 2005. **10**: p. 107-18.

63. Follonier Castella, L., et al., *Regulation of myofibroblast activities: calcium pulls some strings behind the scene.* Exp Cell Res, 2010. **316**(15): p. 2390-401.

64. Merryman, W.D., et al., *The effects of cellular contraction on aortic valve leaflet flexural stiffness.* J Biomech, 2006. **39**(1): p. 88-96.

65. Ferdous, Z., H. Jo, and R.M. Nerem, *Differences in valvular and vascular cell responses to strain in osteogenic media.* Biomaterials, 2011. **32**(11): p. 2885-93.

66. Huang, H.Y., J. Liao, and M.S. Sacks, *In-situ deformation of the aortic valve interstitial cell nucleus under diastolic loading.* J Biomech Eng, 2007. **129**(6): p. 880-89.

67. Lemasters, J.J., et al., *Mitochondrial calcium and the permeability transition in cell death.* Biochim Biophys Acta, 2009. **1787**(11): p. 1395-401.

68. Osman, L., et al., *Role of human valve interstitial cells in valve calcification and their response to atorvastatin.* Circulation, 2006. **114**(1 Suppl): p. I547-52.

69. Yip, C.Y., et al., *Calcification by Valve Interstitial Cells Is Regulated by the Stiffness of the Extracellular Matrix.* Arterioscler Thromb Vasc Biol, 2009.

70. Zayzafoon, M., *Calcium/calmodulin signaling controls osteoblast growth and differentiation.* J Cell Biochem, 2006. **97**(1): p. 56-70.

71. Charras, G.T., et al., *Estimating the sensitivity of mechanosensitive ion channels to membrane strain and tension.* Biophys J, 2004. **87**(4): p. 2870-84.

72. Geddes-Klein, D.M., K.B. Schiffman, and D.F. Meaney, *Mechanisms and consequences of neuronal stretch injury in vitro differ with the model of trauma.* J Neurotrauma, 2006. **23**(2): p. 193-204.

73. Erxleben, C., *Stretch-activated current through single ion channels in the abdominal stretch receptor organ of the crayfish.* J Gen Physiol, 1989. **94**(6): p. 1071-83.

74. Robicsek, F., M.J. Thubrikar, and A.A. Fokin, *Cause of degenerative disease of the trileaflet aortic valve: review of subject and presentation of a new theory.* Ann Thorac Surg, 2002. **73**(4): p. 1346-54.

75. Otto, C.M., *Valvular Heart Disease*. 2004, Philadelphia, PA: Saunders.

76. Shun, C.T., et al., *Activation of Human Valve Interstitial Cells by a Viridians Streptococci Modulin Induces Chemotaxis of Mononuclear Cells.* J Infect Dis, 2009. **199**(10): p. 1488-1496.

77. Fedak, P.W., et al., *Bicuspid aortic valve disease: recent insights in pathophysiology and treatment.* Expert Rev Cardiovasc Ther, 2005. **3**(2): p. 295-308.

78. Fedak, P.W., et al., *Vascular matrix remodeling in patients with bicuspid aortic valve malformations: implications for aortic dilatation.* J Thorac Cardiovasc Surg, 2003. **126**(3): p. 797-806.

79. Aicher, D., et al., *Endothelial nitric oxide synthase in bicuspid aortic valve disease.* Ann Thorac Surg, 2007. **83**(4): p. 1290-4.

80. Schoen, F.J., *Cardiac valves and valvular pathology: update on function, disease, repair, and replacement.* Cardiovasc Pathol, 2005. **14**(4): p. 189-94.

81. Rabkin, E., et al., *Activated interstitial myofibroblasts express catabolic enzymes and mediate matrix remodeling in myxomatous heart valves.* Circulation, 2001. **104**(21): p. 2525-32.

82. Taylor, P.M., et al., *The cardiac valve interstitial cell.* Int J Biochem Cell Biol, 2003. **35**(2): p. 113-8.

83. Berk, B.C., K. Fujiwara, and S. Lehoux, *ECM remodeling in hypertensive heart disease.* J Clin Invest, 2007. **117**(3): p. 568-75.

84. Merryman, W.D., *Insights into (the interstitium of) degenerative aortic valve disease.* J Am Coll Cardiol, 2008. **51**(14): p. 1415.

85. Barakat, A.I. and P.F. Davies, *Mechanisms of shear stress transmission and transduction in endothelial cells.* Chest, 1998. **114**(1 Suppl): p. 58S-63S.

86. Davies, P.F. and S.C. Tripathi, *Mechanical stress mechanisms and the cell. An endothelial paradigm.* Circ Res, 1993. **72**(2): p. 239-45.

87. Ingber, D.E., *Mechanobiology and diseases of mechanotransduction.* Ann Med, 2003. **35**(8): p. 564-77.

88. Jaalouk, D.E. and J. Lammerding, *Mechanotransduction gone awry.* Nat Rev Mol Cell Biol, 2009. **10**(1): p. 63-73.

89. Stewart, B.F., et al., *Clinical factors associated with calcific aortic valve disease. Cardiovascular Health Study.* J Am Coll Cardiol, 1997. **29**(3): p. 630-4.

90. Merryman, W.D., et al., *Defining biomechanical endpoints for tissue engineered heart valve leaflets from native leaflet properties.* Prog Pediat Cardiol, 2006. **21**(2): p. 153-60.

91. Rajamannan, N.M., W.D. Edwards, and T.C. Spelsberg, *Hypercholesterolemic aortic-valve disease.* N Engl J Med, 2003. **349**(7): p. 717-8.

92. Rajamannan, N.M., et al., *Atorvastatin inhibits hypercholesterolemia-induced cellular proliferation and bone matrix production in the rabbit aortic valve.* Circulation, 2002. **105**(22): p. 2660-5.

93. Benton, J.A., et al., *Statins block calcific nodule formation of valvular interstitial cells by inhibiting alpha-smooth muscle actin expression.* Arterioscler Thromb Vasc Biol, 2009. **29**(11): p. 1950-7.

94. Aronow, W.S., et al., *Association of coronary risk factors and use of statins with progression of mild valvular aortic stenosis in older persons.* Am J Cardiol, 2001. **88**(6): p. 693-5.

95. Novaro, G.M., et al., *Effect of hydroxymethylglutaryl coenzyme a reductase inhibitors on the progression of calcific aortic stenosis.* Circulation, 2001. **104**(18): p. 2205-9.

96. Cowell, S.J., et al., *A randomized trial of intensive lipid-lowering therapy in calcific aortic stenosis.* N Engl J Med, 2005. **352**(23): p. 2389-97.

97. Rossebo, A.B., et al., *Intensive lipid lowering with simvastatin and ezetimibe in aortic stenosis.* N Engl J Med, 2008. **359**(13): p. 1343-56.

98. Rapport, M.M., A.A. Green, and I.H. Page, *Serum vasoconstrictor, serotonin; isolation and characterization.* J Biol Chem, 1948. **176**(3): p. 1243-51.

99. Erspamer, V. and B. Asero, *Identification of enteramine, the specific hormone of the enterochromaffin cell system, as 5-hydroxytryptamine.* Nature, 1952. **169**(4306): p. 800-1.

100. Roth, B.L., et al., *5-Hydroxytryptamine2-family receptors (5-hydroxytryptamine2A, 5-hydroxytryptamine2B, 5-hydroxytryptamine2C): where structure meets function.* Pharmacol Ther, 1998. **79**(3): p. 231-57.

101. Edited by Roth, B.L., *The Serotonin Receptors: From Molecular Pharmacology to Human Therapeutics*. 2006: Humana Press.

102. Berger, M., J.A. Gray, and B.L. Roth, *The expanded biology of serotonin.* Annu Rev Med, 2009. **60**: p. 355-66.

103. Guyton, A.C. and J.E. Hall, *Textbook of Medical Physiology*. 9th ed. 1996, Philadelphia: W.B. Saunders Company.

104. Maricq, A.V., et al., *Primary structure and functional expression of the 5HT3 receptor, a serotonin-gated ion channel.* Science, 1991. **254**(5030): p. 432-7.

105. Kroeze, W.K., D.J. Sheffler, and B.L. Roth, *G-protein-coupled receptors at a glance.* J Cell Sci, 2003. **116**(Pt 24): p. 4867-9.

106. Kroeze, W.K., K. Kristiansen, and B.L. Roth, *Molecular biology of serotonin receptors structure and function at the molecular level.* Curr Top Med Chem, 2002. **2**(6): p. 507-28.

107. Armbruster, B.N. and B.L. Roth, *Mining the receptorome.* J Biol Chem, 2005. **280**(7): p. 5129-32.

108. Allen, J.A. and B.L. Roth, *Strategies to Discover Unexpected Targets for Drugs Active at G Protein-Coupled Receptors.* Annu Rev Pharmacol Toxicol, 2010.

109. Raymond, J.R., et al., *Multiplicity of mechanisms of serotonin receptor signal transduction.* Pharmacol Ther, 2001. **92**(2-3): p. 179-212.

110. Roth, B.L., et al., *Binding of typical and atypical antipsychotic agents to 5-hydroxytryptamine-6 and 5-hydroxytryptamine-7 receptors.* J Pharmacol Exp Ther, 1994. **268**(3): p. 1403-10.

111. Abbas, A.I., et al., *Amisulpride is a potent 5-HT7 antagonist: relevance for antidepressant actions in vivo.* Psychopharmacology (Berl), 2009. **205**(1): p. 119-28.

112. Roth, B.L. and Z. Xia, *Molecular and cellular mechanisms for the polarized sorting of serotonin receptors: relevance for genesis and treatment of psychosis.* Crit Rev Neurobiol, 2004. **16**(4): p. 229-36.

113. Dumuis, A., M. Sebben, and J. Bockaert, *The gastrointestinal prokinetic benzamide derivatives are agonists at the non-classical 5-HT receptor (5-HT4) positively coupled to adenylate cyclase in neurons.* Naunyn Schmiedebergs Arch Pharmacol, 1989. **340**(4): p. 403-10.

114. Kaumann, A.J. and L. Sanders, *5-Hydroxytryptamine causes rate-dependent arrhythmias through 5-HT4 receptors in human atrium: facilitation by chronic beta-adrenoceptor blockade.* Naunyn Schmiedebergs Arch Pharmacol, 1994. **349**(4): p. 331-7.

115. Lindner, M.D., et al., *An assessment of the effects of serotonin 6 (5-HT6) receptor antagonists in rodent models of learning.* J Pharmacol Exp Ther, 2003. **307**(2): p. 682-91.

116. Kursar, J.D., et al., *Molecular cloning, functional expression, and mRNA tissue distribution of the human 5-hydroxytryptamine2B receptor.* Mol Pharmacol, 1994. **46**(2): p. 227-34.

117. Conn, P.J. and E. Sanders-Bush, *Selective 5HT-2 antagonists inhibit serotonin stimulated phosphatidylinositol metabolism in cerebral cortex.* Neuropharmacology, 1984. **23**(8): p. 993-6.

118. Roth, B.L., et al., *Aortic recognition sites for serotonin (5HT) are coupled to phospholipase C and modulate phosphatidylinositol turnover.* Neuropharmacology, 1984. **23**(10): p. 1223-5.

119. Meltzer, H.Y., S. Matsubara, and J.C. Lee, *Classification of typical and atypical antipsychotic drugs on the basis of dopamine D-1, D-2 and serotonin2 pKi values.* J Pharmacol Exp Ther, 1989. **251**(1): p. 238-46.

120. Weiner, D.M., et al., *5-hydroxytryptamine2A receptor inverse agonists as antipsychotics.* J Pharmacol Exp Ther, 2001. **299**(1): p. 268-76.

121. Kozikowski, A.P., et al., *HTS and rational drug design to generate a class of 5-HT(2C)-selective ligands for possible use in schizophrenia.* ChemMedChem, 2010. **5**(8): p. 1221-5.

122. Pazos, A., R. Cortes, and J.M. Palacios, *Quantitative autoradiographic mapping of serotonin receptors in the rat brain. II. Serotonin-2 receptors.* Brain Res, 1985. **346**(2): p. 231-49.

123. Abramowski, D., et al., *Localization of the 5-hydroxytryptamine2C receptor protein in human and rat brain using specific antisera.* Neuropharmacology, 1995. **34**(12): p. 1635-45.

124. Doly, S., et al., *Role of serotonin via 5-HT2B receptors in the reinforcing effects of MDMA in mice.* PLoS One, 2009. **4**(11): p. e7952.

125. Doly, S., et al., *Serotonin 5-HT2B receptors are required for 3,4-methylenedioxymethamphetamine-induced hyperlocomotion and 5-HT release in vivo and in vitro.* J Neurosci, 2008. **28**(11): p. 2933-40.

126. Banas, S.M., et al., *Deconstructing Antiobesity Compound Action: Requirement of Serotonin 5-HT(2B) Receptors for Dexfenfluramine Anorectic Effects.* Neuropsychopharmacology, 2010.

127. Barnes, N.M. and T. Sharp, *A review of central 5-HT receptors and their function.* Neuropharmacology, 1999. **38**(8): p. 1083-152.

128. Pytliak, M., et al., *Serotonin receptors - from molecular biology to clinical applications.* Physiol Res, 2010.

129. Vane, J.R., *The relative activities of some tryptamine analogues on the isolated rat stomach strip preparation.* Br J Pharmacol Chemother, 1959. **14**(1): p. 87-98.

130. Kaumann, A.J. and F.O. Levy, *5-hydroxytryptamine receptors in the human cardiovascular system.* Pharmacol Ther, 2006. **111**(3): p. 674-706.

131. Choi, D.S. and L. Maroteaux, *Immunohistochemical localisation of the serotonin 5-HT2B receptor in mouse gut, cardiovascular system, and brain.* FEBS Lett, 1996. **391**(1-2): p. 45-51.

132. Ullmer, C., et al., *Expression of serotonin receptor mRNAs in blood vessels.* FEBS Lett, 1995. **370**(3): p. 215-21.

133. Fitzgerald, L.W., et al., *Possible role of valvular serotonin 5-HT(2B) receptors in the cardiopathy associated with fenfluramine.* Mol Pharmacol, 2000. **57**(1): p. 75-81.

134. Manivet, P., et al., *The serotonin binding site of human and murine 5-HT2B receptors: molecular modeling and site-directed mutagenesis.* J Biol Chem, 2002. **277**(19): p. 17170-8.

135. Kellermann, O., et al., *Sequential onset of three 5-HT receptors during the 5-hydroxytryptaminergic differentiation of the murine 1C11 cell line.* Br J Pharmacol, 1996. **118**(5): p. 1161-70.

136. Tournois, C., et al., *Cross-talk between 5-hydroxytryptamine receptors in a serotonergic cell line. Involvement of arachidonic acid metabolism.* J Biol Chem, 1998. **273**(28): p. 17498-503.

137. Manivet, P., et al., *PDZ-dependent activation of nitric-oxide synthases by the serotonin 2B receptor.* J Biol Chem, 2000. **275**(13): p. 9324-31.

138. Nebigil, C.G., et al., *Serotonin 2B receptor is required for heart development.* Proc Natl Acad Sci U S A, 2000. **97**(17): p. 9508-13.

139. Nebigil, C.G., et al., *5-hydroxytryptamine 2B receptor regulates cell-cycle progression: cross-talk with tyrosine kinase pathways.* Proc Natl Acad Sci U S A, 2000. **97**(6): p. 2591-6.

140. Setola, V., et al., *3,4-methylenedioxymethamphetamine (MDMA, "Ecstasy") induces fenfluramine-like proliferative actions on human cardiac valvular interstitial cells in vitro.* Mol Pharmacol, 2003. **63**(6): p. 1223-9.

141. Hafizi, S., et al., *Mitogenic and secretory responses of human valve interstitial cells to vasoactive agents.* J Heart Valve Dis, 2000. **9**(3): p. 454-8.

142. Nebigil, C.G., et al., *Overexpression of the serotonin 5-HT2B receptor in heart leads to abnormal mitochondrial function and cardiac hypertrophy.* Circulation, 2003. **107**(25): p. 3223-9.

143. Jaffre, F., et al., *Involvement of the serotonin 5-HT2B receptor in cardiac hypertrophy linked to sympathetic stimulation: control of interleukin-6, interleukin-1beta, and tumor necrosis factor-alpha cytokine production by ventricular fibroblasts.* Circulation, 2004. **110**(8): p. 969-74.

144. Launay, J.M., et al., *Ras involvement in signal transduction by the serotonin 5-HT2B receptor.* J Biol Chem, 1996. **271**(6): p. 3141-7.

145. Li, B., et al., *Fluoxetine-mediated 5-HT2B receptor stimulation in astrocytes causes EGF receptor transactivation and ERK phosphorylation.* Psychopharmacology (Berl), 2008. **201**(3): p. 443-58.

146. Hsu, C.Y., et al., *Kinetic analysis of the inhibition of the epidermal growth factor receptor tyrosine kinase by Lavendustin-A and its analogue.* J Biol Chem, 1991. **266**(31): p. 21105-12.

147. Rosenkranz, S., *TGF-beta1 and angiotensin networking in cardiac remodeling.* Cardiovasc Res, 2004. **63**(3): p. 423-32.

148. Liang, Y.J., et al., *Mechanical stress enhances serotonin 2B receptor modulating brain natriuretic peptide through nuclear factor-kappaB in cardiomyocytes.* Cardiovasc Res, 2006. **72**(2): p. 303-12.

149. Gustafsson, B.I., et al., *Carcinoid heart disease.* Int J Cardiol, 2008.

150. Weintraub, M., et al., *A double-blind clinical trial in weight control. Use of fenfluramine and phentermine alone and in combination.* Arch Intern Med, 1984. **144**(6): p. 1143-8.

151. Connolly, H.M., et al., *Valvular heart disease associated with fenfluramine-phentermine.* N Engl J Med, 1997. **337**(9): p. 581-8.

152. Khan, M.A., et al., *The prevalence of cardiac valvular insufficiency assessed by transthoracic echocardiography in obese patients treated with appetite-suppressant drugs.* N Engl J Med, 1998. **339**(11): p. 713-8.

153. Mason, J.W., M.E. Billingham, and J.P. Friedman, *Methysergide-induced heart disease: a case of multivalvular and myocardial fibrosis.* Circulation, 1977. **56**(5): p. 889-90.

154. Graham, J.R., et al., *Fibrotic disorders associated with methysergide therapy for headache.* N Engl J Med, 1966. **274**(7): p. 359-68.

155. Graham, J.R., *Cardiac and pulmonary fibrosis during methysergide therapy for headache.* Am J Med Sci, 1967. **254**(1): p. 1-12.

156. Redfield, M.M., et al., *Valve disease associated with ergot alkaloid use: echocardiographic and pathologic correlations.* Ann Intern Med, 1992. **117**(1): p. 50-2.

157. Rothman, R.B., et al., *Evidence for possible involvement of 5-HT(2B) receptors in the cardiac valvulopathy associated with fenfluramine and other serotonergic medications.* Circulation, 2000. **102**(23): p. 2836-41.

158. Newman-Tancredi, A., et al., *Differential actions of antiparkinson agents at multiple classes of monoaminergic receptor. III. Agonist and antagonist properties at serotonin, 5-HT(1) and 5-HT(2), receptor subtypes.* J Pharmacol Exp Ther, 2002. **303**(2): p. 815-22.

159. Schade, R., et al., *Dopamine agonists and the risk of cardiac-valve regurgitation.* N Engl J Med, 2007. **356**(1): p. 29-38.

160. Zanettini, R., et al., *Valvular heart disease and the use of dopamine agonists for Parkinson's disease.* N Engl J Med, 2007. **356**(1): p. 39-46.

161. Pritchett, A.M., et al., *Valvular heart disease in patients taking pergolide.* Mayo Clin Proc, 2002. **77**(12): p. 1280-6.

162. Huang, X.P., et al., *Parallel functional activity profiling reveals valvulopathogens are potent 5-hydroxytryptamine(2B) receptor agonists:*

implications for drug safety assessment. Mol Pharmacol, 2009. **76**(4): p. 710-22.

163. Roth, B.L., *Drugs and valvular heart disease.* N Engl J Med, 2007. **356**(1): p. 6-9.

164. Setola, V., et al., *Molecular determinants for the interaction of the valvulopathic anorexigen norfenfluramine with the 5-HT2B receptor.* Mol Pharmacol, 2005. **68**(1): p. 20-33.

165. Parissis, D., A. Papachristodoulou, and A. Dimitriadis, *Inflammatory aneurysm of the abdominal aorta in a patient treated with ropinirole.* J Neurol, 2010. **257**(9): p. 1582-4.

166. Droogmans, S., et al., *Possible association between 3,4-methylenedioxymethamphetamine abuse and valvular heart disease.* Am J Cardiol, 2007. **100**(9): p. 1442-5.

167. Young, R., et al., *Pizotyline effectively attenuates the stimulus effects of N-methyl-3,4-methylenedioxyamphetamine (MDMA).* Pharmacol Biochem Behav, 2005. **82**(2): p. 404-10.

168. Droogmans, S., et al., *Dose dependency and reversibility of serotonin-induced valvular heart disease in rats.* Cardiovasc Toxicol, 2009. **9**(3): p. 134-41.

169. Rabkin, E., et al., *Evolution of cell phenotype and extracellular matrix in tissue-engineered heart valves during in-vitro maturation and in-vivo remodeling.* J Heart Valve Dis, 2002. **11**(3): p. 308-14; discussion 314.

170. Aikawa, E., et al., *Human semilunar cardiac valve remodeling by activated cells from fetus to adult: implications for postnatal adaptation, pathology, and tissue engineering.* Circulation, 2006. **113**(10): p. 1344-52.

171. Balachandran, K., et al., *An ex vivo study of the biological properties of porcine aortic valves in response to circumferential cyclic stretch.* Ann Biomed Eng, 2006. **34**(11): p. 1655-65.

172. Balachandran, K., et al., *Elevated cyclic stretch alters matrix remodeling in aortic valve cusps: implications for degenerative aortic valve disease.* Am J Physiol Heart Circ Physiol, 2009. **296**(3): p. H756-64.

173. Porvasnik, S.L., et al., *PRX-08066, a novel 5-hydroxytryptamine receptor 2B antagonist, reduces monocrotaline-induced pulmonary arterial hypertension and right ventricular hypertrophy in rats.* J Pharmacol Exp Ther, 2010. **334**(2): p. 364-72.

174. Monassier, L., et al., *Serotonin 5-HT(2B) receptor blockade prevents reactive oxygen species-induced cardiac hypertrophy in mice.* Hypertension, 2008. **52**(2): p. 301-7.

175. Esteve, J.M., et al., *Functions of serotonin in hypoxic pulmonary vascular remodeling.* Cell Biochem Biophys, 2007. **47**(1): p. 33-44.

176. Nebigil, C.G., et al., *Ablation of serotonin 5-HT(2B) receptors in mice leads to abnormal cardiac structure and function.* Circulation, 2001. **103**(24): p. 2973-9.

177. Hauso, O., et al., *Long-term serotonin effects in the rat are prevented by terguride.* Regul Pept, 2007. **143**(1-3): p. 39-46.

178. Skhirtladze, C., et al., *Src kinases in systemic sclerosis: central roles in fibroblast activation and in skin fibrosis.* Arthritis Rheum, 2008. **58**(5): p. 1475-84.

179. Mishra, R., et al., *TGF-beta-regulated collagen type I accumulation: role of Src-based signals.* Am J Physiol Cell Physiol, 2007. **292**(4): p. C1361-9.

180. Samarakoon, R., et al., *TGF-beta1-induced plasminogen activator inhibitor-1 expression in vascular smooth muscle cells requires pp60(c-src)/EGFR(Y845) and Rho/ROCK signaling.* J Mol Cell Cardiol, 2008. **44**(3): p. 527-38.

181. Xu, J., et al., *Serotonin mechanisms in heart valve disease II: the 5-HT2 receptor and its signaling pathway in aortic valve interstitial cells.* Am J Pathol, 2002. **161**(6): p. 2209-18.

182. Pechkovsky, D.V., et al., *Transforming growth factor beta1 induces alphavbeta3 integrin expression in human lung fibroblasts via a beta3 integrin-, c-Src-, and p38 MAPK-dependent pathway.* J Biol Chem, 2008. **283**(19): p. 12898-908.

183. Cohn, R.D., et al., *Angiotensin II type 1 receptor blockade attenuates TGF-beta-induced failure of muscle regeneration in multiple myopathic states.* Nat Med, 2007. **13**(2): p. 204-10.

184. Habashi, J.P., et al., *Losartan, an AT1 antagonist, prevents aortic aneurysm in a mouse model of Marfan syndrome.* Science, 2006. **312**(5770): p. 117-21.

185. Hofmann, C., et al., *Lisuride, a dopamine receptor agonist with 5-HT2B receptor antagonist properties: absence of cardiac valvulopathy adverse drug reaction reports supports the concept of a crucial role for 5-HT2B receptor agonism in cardiac valvular fibrosis.* Clin Neuropharmacol, 2006. **29**(2): p. 80-6.

186. Hinz, B., *Formation and function of the myofibroblast during tissue repair.* J Invest Dermatol, 2007. **127**(3): p. 526-37.

187. Tomasek, J.J., et al., *Myofibroblasts and mechano-regulation of connective tissue remodelling.* Nat Rev Mol Cell Biol, 2002. **3**(5): p. 349-63.

188. Hinz, B., *The myofibroblast: paradigm for a mechanically active cell.* J Biomech, 2010. **43**(1): p. 146-55.

189. Serini, G. and G. Gabbiani, *Mechanisms of myofibroblast activity and phenotypic modulation.* Exp Cell Res, 1999. **250**(2): p. 273-83.

190. Goldbarg, S.H., et al., *Insights into degenerative aortic valve disease.* J Am Coll Cardiol, 2007. **50**(13): p. 1205-13.

191. Freeman, R.V. and C.M. Otto, *Spectrum of calcific aortic valve disease: pathogenesis, disease progression, and treatment strategies.* Circulation, 2005. **111**(24): p. 3316-26.

192. Helske, S., et al., *Aortic valve stenosis: an active atheroinflammatory process.* Curr Opin Lipidol, 2007. **18**(5): p. 483-91.

193. Mohler, E.R., 3rd, et al., *Identification and characterization of calcifying valve cells from human and canine aortic valves.* J Heart Valve Dis, 1999. **8**(3): p. 254-60.

194. Rajamannan, N.M., *Calcific aortic valve disease: cellular origins of valve calcification.* Arterioscler Thromb Vasc Biol, 2011. **31**(12): p. 2777-8.

195. Rajamannan, N.M., et al., *Calcific aortic valve disease: not simply a degenerative process: A review and agenda for research from the National Heart and Lung and Blood Institute Aortic Stenosis Working Group. Executive summary: Calcific aortic valve disease-2011 update.* Circulation, 2011. **124**(16): p. 1783-91.

196. Chen, J.H., et al., *beta-catenin mediates mechanically regulated, transforming growth factor-beta1-induced myofibroblast differentiation of aortic valve interstitial cells.* Arterioscler Thromb Vasc Biol, 2011. **31**(3): p. 590-7.

197. Cushing, M.C., J.T. Liao, and K.S. Anseth, *Activation of valvular interstitial cells is mediated by transforming growth factor-beta1 interactions with matrix molecules.* Matrix Biol, 2005. **24**(6): p. 428-37.

198. Balachandran, K., et al., *Elevated cyclic stretch induces aortic valve calcification in a bone morphogenic protein-dependent manner.* Am J Pathol. **177**(1): p. 49-57.

199. Fisher, C.I., J. Chen, and W.D. Merryman, *Calcific nodule morphogenesis by heart valve interstitial cells is strain dependent.* Biomech Model Mechanobiol, 2012.

200. Yip, C.Y., et al., *Calcification by valve interstitial cells is regulated by the stiffness of the extracellular matrix.* Arterioscler Thromb Vasc Biol, 2009. **29**(6): p. 936-42.

201. Chen, J.H., et al., *Identification and characterization of aortic valve mesenchymal progenitor cells with robust osteogenic calcification potential.* Am J Pathol, 2009. **174**(3): p. 1109-19.

202. Mohler, E.R., 3rd, et al., *Bone formation and inflammation in cardiac valves.* Circulation, 2001. **103**(11): p. 1522-8.

203. Benton, J.A., H.B. Kern, and K.S. Anseth, *Substrate properties influence calcification in valvular interstitial cell culture.* J Heart Valve Dis, 2008. **17**(6): p. 689-99.

204. Cushing, M.C., et al., *Fibroblast growth factor represses Smad-mediated myofibroblast activation in aortic valvular interstitial cells.* FASEB J, 2008. **22**(6): p. 1769-77.

205. Gu, X. and K.S. Masters, *Role of the MAPK/ERK pathway in valvular interstitial cell calcification.* Am J Physiol Heart Circ Physiol, 2009. **296**(6): p. H1748-57.

206. Hinz, B., et al., *Myofibroblast development is characterized by specific cell-cell adherens junctions.* Mol Biol Cell, 2004. **15**(9): p. 4310-20.

207. Lee, D.M., et al., *Cadherin-11 in synovial lining formation and pathology in arthritis.* Science, 2007. **315**(5814): p. 1006-10.

208. Schneider, D.J., et al., *Cadherin-11 contributes to pulmonary fibrosis: potential role in TGF-beta production and epithelial to mesenchymal transition.* FASEB J, 2012. **26**(2): p. 503-12.

209. Merryman, W.D., et al., *Differences in tissue-remodeling potential of aortic and pulmonary heart valve interstitial cells.* Tissue Eng, 2007. **13**(9): p. 2281-9.

210. Heupel, W.M., et al., *Different Ca2+ affinities and functional implications of the two synaptic adhesion molecules cadherin-11 and N-cadherin.* Mol Cell Neurosci, 2008. **37**(3): p. 548-58.

211. Hutcheson, J.D., et al., *5-HT2B antagonism arrests non-canonical TGF-β1-induced valvular myofibroblast differentiation.* J Mol Cell Cardiol, 2012. **In press**.

212. Pittet, P., et al., *Fibrogenic fibroblasts increase intercellular adhesion strength by reinforcing individual OB-cadherin bonds.* J Cell Sci, 2008. **121**(Pt 6): p. 877-86.

213. Samarakoon, R. and P.J. Higgins, *Integration of non-SMAD and SMAD signaling in TGF-beta1-induced plasminogen activator inhibitor type-1 gene expression in vascular smooth muscle cells.* Thromb Haemost, 2008. **100**(6): p. 976-83.

214. Li, J., et al., *MEK/ERK and p38 MAPK regulate chondrogenesis of rat bone marrow mesenchymal stem cells through delicate interaction with TGF-beta1/Smads pathway.* Cell Prolif, 2010. **43**(4): p. 333-43.

215. Jiang, W., et al., *Role of cross-talk between the Smad2 and MAPK pathways in TGF-beta1-induced collagen IV expression in mesangial cells.* Int J Mol Med, 2010. **26**(4): p. 571-6.

216. Greenberg, R.S., et al., *FAK-dependent regulation of myofibroblast differentiation.* FASEB J, 2006. **20**(7): p. 1006-8.

217. Bertipaglia, B., et al., *Cell characterization of porcine aortic valve and decellularized leaflets repopulated with aortic valve interstitial cells: the VESALIO Project (Vitalitate Exornatum Succedaneum Aorticum Labore Ingenioso Obtenibitur).* Ann Thorac Surg, 2003. **75**(4): p. 1274-82.

218. Akat, K., M. Borggrefe, and J.J. Kaden, *Aortic valve calcification: basic science to clinical practice.* Heart, 2009. **95**(8): p. 616-23.

219. Levy, R.J., *Serotonin transporter mechanisms and cardiac disease.* Circulation, 2006. **113**(1): p. 2-4.

220. Maish, M.S., et al., *Tricuspid valve biopsy: a potential source of cardiac myofibroblast cells for tissue-engineered cardiac valves.* J Heart Valve Dis, 2003. **12**(2): p. 264-9.

221. Forbes, I.T., et al., *N-(1-methyl-5-indolyl)-N'-(3-methyl-5-isothiazolyl)urea: a novel, high-affinity 5-HT2B receptor antagonist.* J Med Chem, 1995. **38**(6): p. 855-7.

222. Bromidge, S.M., et al., *Biarylcarbamoylindolines are novel and selective 5-HT(2C) receptor inverse agonists: identification of 5-methyl-1-[[2-[(2-methyl-3-pyridyl)oxy]- 5-pyridyl]carbamoyl]-6-trifluoromethylindoline (SB-*

243213) as a potential antidepressant/anxiolytic agent. J Med Chem, 2000. **43**(6): p. 1123-34.

223. Qiu, P., X.H. Feng, and L. Li, *Interaction of Smad3 and SRF-associated complex mediates TGF-beta1 signals to regulate SM22 transcription during myofibroblast differentiation.* J Mol Cell Cardiol, 2003. **35**(12): p. 1407-20.

224. Solway, J., et al., *Structure and expression of a smooth muscle cell-specific gene, SM22 alpha.* J Biol Chem, 1995. **270**(22): p. 13460-9.

225. Brabek, J., et al., *CAS promotes invasiveness of Src-transformed cells.* Oncogene, 2004. **23**(44): p. 7406-15.

226. Wendt, M.K. and W.P. Schiemann, *Therapeutic targeting of the focal adhesion complex prevents oncogenic TGF-beta signaling and metastasis.* Breast Cancer Res, 2009. **11**(5): p. R68.

227. Yu, L., M.C. Hebert, and Y.E. Zhang, *TGF-beta receptor-activated p38 MAP kinase mediates Smad-independent TGF-beta responses.* EMBO J, 2002. **21**(14): p. 3749-59.

228. Fonseca, P.M., et al., *Regulation and localization of CAS substrate domain tyrosine phosphorylation.* Cell Signal, 2004. **16**(5): p. 621-9.

229. Sandilands, E. and M.C. Frame, *Endosomal trafficking of Src tyrosine kinase.* Trends Cell Biol, 2008. **18**(7): p. 322-9.

230. Pedroja, B.S., et al., *Plasminogen activator inhibitor-1 regulates integrin alphavbeta3 expression and autocrine transforming growth factor beta signaling.* J Biol Chem, 2009. **284**(31): p. 20708-17.

231. Magalhaes, A.C., H. Dunn, and S.S. Ferguson, *Regulation of G Protein-Coupled Receptor Activity, Trafficking and Localization by Gpcr-Interacting Proteins.* Br J Pharmacol, 2011.

232. Mariggio, S., et al., *Tyrosine phosphorylation of G-protein-coupled-receptor kinase 2 (GRK2) by c-Src modulates its interaction with Galphaq.* Cell Signal, 2006. **18**(11): p. 2004-12.

233. Gong, H., et al., *G protein subunit Galpha13 binds to integrin alphaIIbbeta3 and mediates integrin "outside-in" signaling.* Science, 2010. **327**(5963): p. 340-3.

234. Olsen, M.H., et al., *Effect of losartan versus atenolol on aortic valve sclerosis (a LIFE substudy).* Am J Cardiol, 2004. **94**(8): p. 1076-80.

235. Cote, N., et al., *Angiotensin receptor blockers are associated with a lower remodelling score of stenotic aortic valves.* Eur J Clin Invest, 2011. **41**(11): p. 1172-9.

236. Nadir, M.A., et al., *Impact of renin-angiotensin system blockade therapy on outcome in aortic stenosis.* J Am Coll Cardiol, 2011. **58**(6): p. 570-6.

237. Helske, S., et al., *Induction of local angiotensin II-producing systems in stenotic aortic valves.* J Am Coll Cardiol, 2004. **44**(9): p. 1859-66.

238. O'Brien, K.D., et al., *Association of angiotensin-converting enzyme with low-density lipoprotein in aortic valvular lesions and in human plasma.* Circulation, 2002. **106**(17): p. 2224-30.

239. Abe, M., et al., *An assay for transforming growth factor-beta using cells transfected with a plasminogen activator inhibitor-1 promoter-luciferase construct.* Anal Biochem, 1994. **216**(2): p. 276-84.

240. Bashore, T.M. and T.J. Gardner, *Valvular heart disease.* J Am Coll Cardiol, 2003. **42**(2): p. 388-90.

241. Hutcheson, J.D., et al., *Serotonin receptors and heart valve disease--it was meant 2B.* Pharmacol Ther, 2011. **132**(2): p. 146-57.

242. Mendelson, K. and F.J. Schoen, *Heart valve tissue engineering: concepts, approaches, progress, and challenges.* Ann Biomed Eng, 2006. **34**(12): p. 1799-819.